THE PROCEEDINGS OF
THE PHYSICAL SOCIETY
Section B

VOL. 65, PART 1 1 January 1952 No. 385 B

EDITORIAL

Fellows of the Physical Society will realize that during the last few years the size of the *Proceedings* has significantly increased. The Papers Committee and Council have had to decide that this continued expansion must now be checked, both because of increases in the cost of paper, of printing and of the other services ancillary to publishing, and also because of the increasing difficulty of obtaining, for example, sufficiently large allocations of paper.

In the matter of actual presentation of papers assistance can be given by the way in which diagrams and mathematics are prepared. Diagrams should be displayed in such a way as to take a minimum of space, e.g. a shallow, wide diagram is preferable to a long, narrow diagram, and individual single curves can often be superposed in one framework. In general no elementary mathematical steps should be included in a paper and every effort should be made to reduce tables to a minimum, and to replace any series of values, wherever possible, by the mean and a standard deviation. The co-operation of Fellows of the Society can materially assist in procuring these small but necessary economies.

Papers are still sometimes written in an unduly verbose style. If the referees of such a paper have made no objections and the paper is accepted, its undue length makes inroads into the publication space available. If the referees do object, the typing of referees' reports and additional communications to authors and referees places an extra burden on the secretarial staff. If authors ensured that their papers were written in a concise style, considerable advantage would result : submitting a manuscript to a critical colleague can be a useful check.

Recently an increasing tendency has been noticed for authors, both individual and in research establishments, to submit for publication papers which contain interim experimental results, or tentative conclusions from their work. It is felt that the value of such articles would be greatly increased if their publication were withheld until more final results and conclusions were established. Moreover, much valuable time on the part of the referees of the papers, and of the office staff, could be saved if authors would consider this point more seriously before submitting papers for publication.

H. H. HOPKINS,
Honorary Papers Secretary.

Water Bells*

By F. L. HOPWOOD
St. Bartholomew's Hospital, London E.C.1

MS. received 31*st May* 1951

ABSTRACT. The author shows that when water is discharged through an annular slit above a plane water surface, the sealed ' water bells ' thus formed exhibit some novel and remarkable properties not hitherto described. The primitive water bell is a dome-shaped bubble whose dimensions increase with increased rates of flow. If this is perforated with a finger the maximum diameter of the bell suddenly doubles itself. On continuously reducing the flow the expanded bubble contracts and assumes an alternating sequence of stable and semi-stable forms of great beauty. All these, when perforated, *contract* slightly. The semi-stable forms have the general appearance of a hyperboloid surmounted by a saucer-shaped depression with the annular slit at the bottom. On inflating an expanded bubble by a slow stream of small air bubbles, semi-stable forms similar to the above are produced, but possessing an additional inflection in their contours. During these changes the maximum differences of pressure do not exceed one-tenth of a millimetre of water above or below atmospheric pressure. The author shows how the apparatus can easily be modified to produce enclosing water bells. It may also be adapted to produce sonic and ultrasonic underwater vibrations.

OVER a century ago F. Savart, in two classical memoirs (1833, 1834), described the appearance and behaviour of the liquid films and columns produced when a downward vertical jet of water impinged on a horizontal circular metal disc, or on an identical coaxial jet projected vertically upwards. Under certain conditions the resulting liquid films assumed approximately hemispherical forms which later investigators have called 'water bells'. Measurements of the dimensions of liquid bells for different rates of flow by Buchwald and Koenig (1935, 1936), by Bond (1935), and Puls (1936), have yielded values for the surface tensions of freshly formed surfaces of water and other liquids.

It is the purpose of the present communication to describe a new and more convenient method of producing water bells, and to give an account of some of their beautiful and rather surprising properties which do not appear to have been previously published.

The apparatus (fig. 1) consists of a thin-walled brass tube about 10 cm long and 2·1 cm external diameter, provided with an axial screw-threaded rod soldered into a plug closing one end of the tube. At the other end, the tube is nearly closed by a stout metal cylinder or nut, which is movable along the rod and controls an annular slit whose width may be varied from about 0·4 mm to 1·4 mm. The apparatus is connected to the water mains through a side tube and the flow of water regulated by a suitable stopcock. With the flow directed downwards in the tube, all the forms described by Savart are easily obtainable. They will not be further described here.

For the present purpose the tube is mounted in a water bath and the flow directed upwards towards the slit. The height is so adjusted that the water bell formed by the sheet of water issuing from the slit constitutes a sealed enclosure bounded by the surface of the water in the bath (fig. 2).

---

* Demonstration at the Conversazione of the Physical Society, 6th April 1951.

When first established in the above way, the water bell resembles a dome-shaped bubble. Increasing the rate of flow of water causes a general increase in its dimensions. The circular line of contact with the water in the bath is, in effect, the base of a miniature cataract which is fringed internally and externally with a rim of small effervescing bubbles. This fringe of bubbles is due to the entrainment of air by the descending sheet of water. On inserting a finger to equalize the internal and external pressures, the bell suddenly *expands* in an astonishing manner to about double diameter, and assumes a more flattened shape. If now the rate of flow of water is very gradually reduced, the bell contracts and assumes in succession a series of stable forms alternating with semi-stable forms of great beauty and interest.

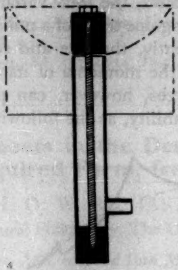

Fig. 1. Tube for production of water bells.

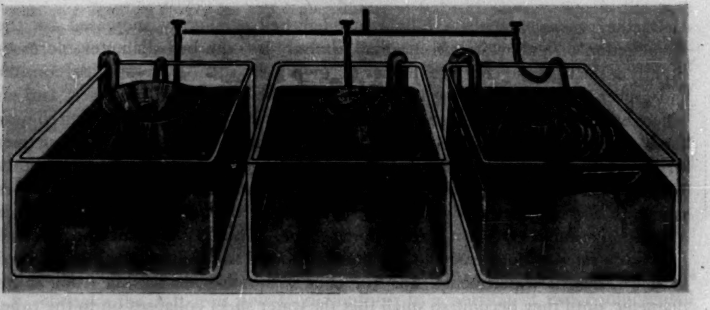

Fig. 3. Fig. 2. Fig. 4.
Water bells.

The stable forms change in appearance from the spherical cap of the extended bell to a truncated cone having a saucer shaped upper surface (fig. 2). Suitable adjustment of the rate of flow, or a slight alteration in the height of the slit effected by means of a lever, causes the conical wall of the bell to rise and produce a remarkably sharp edge, almost a knife edge, to the now more pronounced saucer-like upper surface. In this somewhat unstable state cusps frequently appear in the rim of the saucer, and sprays of droplets are projected outwards over it.

At the same time the conical wall of the bell tends to become more like a hyperboloid (fig. 3). Further reduction in flow causes the bell to repeat the above sequence of stable and unstable forms several times as it shrinks in size.

A limiting form of bell assumed at low rates of flow is shown in fig. 4. Here the shape is that of a vertical cylinder closed by an upper horizontal cap which is covered with a pattern of stationary concentric capillary waves, whose crests are less than 1 cm apart. The ripples are presumably due to disturbances originating at the edge of the cap which travel upstream with the velocity of the outward moving water. Generating lines of the cylinder are also seen.

In contrast to the behaviour of the bells produced as the rate of flow is increasing, those formed when the flow is being reduced, *collapse* slightly when perforated by a finger. It is a matter for surprise that throughout all the changes of size and form described above, the total variation of air pressure inside the bells is of an order not exceeding one tenth of a millimetre of water above or below atmospheric pressure. Evidently, the size and form of a stable water bell is controlled almost entirely by the momenta of its elements, surface tension and gravity. Relatively small forces, however, can produce considerable changes in water bells verging on instability, as the following experiments also show.

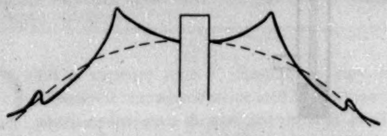

Fig. 5. - - - Cross section of stable expanded water bell.
—— Cross section of inflated water bell.

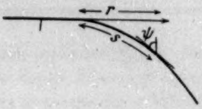

Fig. 6.

If the pressure inside a fully expanded bell is slightly increased by the introduction of a slow stream of small air bubbles, the bell diameter increases slightly at the base and contracts higher up, giving rise to the hyperboloidal contour and saucer cap mentioned earlier. Gradually the rim of the cap rises, and an inflection develops on the descending sheet of water to form a moat or ditch near the base of the bell (fig. 5). At the same time the previously circular base assumes an indented character. Finally, when the rim of the saucer cap has risen to a height of 1·5 to 2 cm above the slit, and the excess pressure in the bell approaches one tenth of a millimetre of water, air escapes under the base and the bell shrinks a little in size and reverts to its earlier dome shape. This sequence may be repeated for steady rates of flow less than the maximum of 5 to 10 litres per minute used in this series of experiments, and for bells with bases decreasing from 35 cm diameter, until they become so small that the water sheet collapses on to the tube.

The mathematical formulation of the relationship between the parameters defining the unstable forms of water bells has not yet been achieved. For the dome shaped stable forms Boussinesq (1869) has derived such a relation which may be written

$$T=\frac{Q}{4\pi}\,\frac{-\Delta(v\sin\psi)}{\Delta s-\Delta(r\sin\psi)}, \qquad \ldots\ldots(1)$$

where T is the surface tension, Q the volume of water issuing per second, v the particle velocity, and r, s, ψ, coordinates shown in fig. 6. The particle velocity v is derived from the equation of continuity $v=Q/2\pi rh\rho$ where h is the thickness of the film and ρ its density. Equation (1) is that employed by Buchwald and Koenig for their determinations of the surface tensions of water and other liquids.

It is possible to produce a small water bell inside a larger one, by mounting on the same axial rod two slotted tubes with independent water supplies.

In most of the experiments described above the solid metal cylinder which was used to regulate the width of the slit had the same external diameter as the tube. When this cylinder was replaced by a thin metal disc of larger diameter, and the whole apparatus submerged, underwater sonic and ultrasonic vibrations were produced in the bath by appropriate regulation of the flow of water through the slit.

REFERENCES

BOND, W. N., 1935, *Proc. Phys. Soc.*, **47**, 549.
BOUSSINESQ, J., 1869, *C. R. Acad. Sci., Paris*, **69**, 45, 128.
BUCHWALD, E., and KOENIG, H., 1935, *Ann. Phys., Lpz.*, **23**, 557; 1936, *Ibid.*, **26**, 659.
PULS, H. O., 1936, *Phil. Mag.*, **22**, 970.
SAVART, F., 1833, *Ann. Chim. Phys.*, **54**, 55; 1834, *Ibid.*, **55**, 257.

The Use of Current Sheets in the Design of Magnets to give Bounded Fields of Required Form, free from Edge Distortion

BY H. O. W. RICHARDSON
Department of Natural Philosophy, The University, Edinburgh

Communicated by N. Feather; MS. received 16*th March* 1951, *and in revised form* 20*th August* 1951

ABSTRACT. The use of current sheets to produce static magnetic fields of required form, with freedom from edge or fringing distortion and with no stray flux, is discussed. Two types of magnet winding are considered. The first, or field-terminating type, encloses a tube of force and serves as a sharp boundary to the field. The second, or iron-shrouded type, is wound against the inner surface of an iron shroud and, with a suitable distribution of turns, can generate any required shape of field in the iron enclosure. In both types stray field can be avoided if the iron return-path is infinitely permeable, or if it is covered with an 'anti-reluctance' winding.

A discussion is given of (*a*) the uniform field, (*b*) the field whose lines of force are coaxial circles, (*c*) the synchrotron field, and (*d*) the prolate spheroidal field, whose lines are confocal ellipses.

§ 1. INTRODUCTION

In designing a magnet to produce a field of given shape, a common method is to make the soft-iron pole-faces conform to a portion of two equipotential surfaces derived from theory. These surfaces usually extend to infinity so that the pole-faces deviate sharply from them at the edges. This deviation is the source of a distortion of the field which is propagated inwards into the gap as what might be called a fringing perturbation. In conventional designs the perturbation is kept small inside a limited region between the poles, either by encircling this region with a wide 'guard-ring' zone of outer pole-face, or by building up a peripheral ridge around each pole-face to introduce a second perturbation of opposite sign.

In this note we discuss certain dispositions of the magnetizing windings by which these fringing distortions can be avoided. The underlying principles have long been known in the 'astatic' inductance (see §4(i)) but they have, apparently, been little used in making magnets, perhaps because the winding in each case must form current sheets flowing round the region containing the desired field, which is thus made rather inaccessible.

By the use of the method here advocated, the field can be made zero outside the winding, and the resulting absence of stray flux and edge distortion makes 'guard-ring' zones and peripheral ridges redundant and so permits a large saving in iron. In a calculated case (a spheroidal field β-spectrometer) the saving exceeds 95%.

A second application of current sheets is discussed, in which the field emerges perpendicularly from the winding to enter an encasing iron shroud. Arrangements of this sort can be used to generate fields of a general kind inside an iron enclosure, but coil-winding difficulties would be serious except for the axially symmetric type of field enclosed in a hollow cylinder with iron end-plates.

The theory gives the distribution of turns needed in a thin winding on the inner surface of the shroud in order to generate the required field. This distribution is also a first approximation in the less elementary boundary-value problem of a thick winding.

§2. THE CURRENT SHEET WHICH TERMINATES A FIELD

Consider a current sheet of infinitesimal thickness but of finite strength denoted by $\mathbf{k}$, a vector along the current flow, of magnitude equal to the current (in e.m.u.) per centimetre crossing a line in the sheet normal to the flow.

The well-known magnetic boundary conditions are, at a point P in the sheet: (i) The normal component of induction $\mathbf{B}$ is continuous:

$$B_1 \cos\theta_1 = B_2 \cos\theta_2 \quad \text{or} \quad \mathbf{n}\cdot\mathbf{B}_1 = \mathbf{n}\cdot\mathbf{B}_2. \qquad \ldots\ldots(1)$$

Here θ_1 and θ_2 are the angles at P between the outward-drawn normal unit-vector $\mathbf{n}$ and the line of induction pointing along $\mathbf{B}_1$ and $\mathbf{B}_2$ on the inner and outer sides of the sheet. In some practical cases the sheet may serve as a boundary between two isotropic media of permeabilities μ_1 and μ_2. (ii) The tangential component of field strength $\mathbf{H}$ is discontinuous and receives an increment $\mathbf{H}_T$ in traversing the sheet, having a direction normal to the current flow $\mathbf{k}$, of magnitude $4\pi k$.

In vector form, $\mathbf{H}_T$, $\mathbf{k}$ and $\mathbf{n}$ form a right-handed triad shown in fig. 1. Thus, in the case of uniform permeability ($\mu_1 = \mu_2$),

$$\mathbf{H}_2 - \mathbf{H}_1 = \mathbf{H}_T = 4\pi(\mathbf{k}\times\mathbf{n}). \qquad \ldots\ldots(2)$$

An important particular case of (2) arises when $\mathbf{H}_1 = -\mathbf{H}_T$ so that $\mathbf{H}_2 = 0$ and, at P,

$$\mathbf{H}_1 = -4\pi(\mathbf{k}\times\mathbf{n}). \qquad \ldots\ldots(3)$$

If (3) can be satisfied over the inner surface of the current sheet, we see that, since $\mathbf{H}_2 = 0$, the field $\mathbf{H}_1$ is terminated discontinuously by the sheet. $\mathbf{H}_1$ is everywhere tangential to the inner surface, which no flux crosses. Hence we can always design a field-terminating sheet of this type by choosing a tube of force of the field $\mathbf{H}_1$ and winding a current sheet round the tube which satisfies (3). The lines of current flow along $\mathbf{k}$, according to (3), are normal to $\mathbf{H}_1$ and hence lie in its equipotential surfaces. The closed curve in which an equipotential intersects the chosen tube of force is thus a stream line of the current flow.

To construct such a current sheet, a practical method would be to wind closely a coil of wire on a former having the shape of the tube of force, making each turn lie as well as possible in an equipotential surface. This would only be approximately possible because of the spiralling of the winding.

With wire of rectangular cross section, closely packed, the current flow may be resolved into a closed circulation round the tube of force and a small longitudinal component. The magnetic effect of this small component could be much reduced by winding on a second layer, in which the spiralling was in the opposite sense. An alternative, suggested to the writer by Professor Feather, would be to arrange a series of parallel return paths for the current, distributed evenly round the winding, to generate a field opposite to that of the longitudinal component.

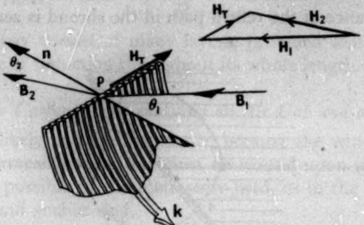

Fig. 1. Angular relations between the current sheet strength **k** and the field vectors **B** and **H**.

From (3), at every point P of the sheet, $|\mathbf{H}_1| = 4\pi k$, so that the number of turns per centimetre is proportional to the potential gradient, and the current provides just the right magneto-motive force (m.m.f.) to maintain the field.

§ 3. THE IRON-SHROUDED CURRENT SHEET

The second particular case of (2) is that in which the outer field $\mathbf{H}_2$ is normal to the sheet. The tangential component of $\mathbf{H}_1$ is thus annihilated by the sheet, but its normal component, according to (1), is unchanged, if $\mu_1 = \mu_2$.

The normal emergence of $\mathbf{H}_2$ means that the outer surface of the sheet is an equipotential. This condition can always be satisfied by enclosing the sheet in a close-fitting shroud of infinite permeability whose surface is therefore an equipotential, on which the lines of force must be incident normally.

In order to be properly oriented for annihilation, the tangential component of $\mathbf{H}_1$ must be normal to the current flow **k**, and of magnitude $4\pi k$. Thus the conditions are

$$H_1 \sin\theta_1 = -4\pi k, \qquad H_1 \cos\theta_1 = H_2. \qquad \ldots\ldots(4)$$

These may be combined in a vector equation

$$[\mathbf{n}\times\mathbf{H}_1] = -4\pi\mathbf{k}. \qquad \ldots\ldots(5)$$

This follows from (2) on forming the vector triple product

$$[\mathbf{n}\times(\mathbf{H}_2-\mathbf{H}_1)] = 4\pi\{(\mathbf{n}\,.\,\mathbf{n})\mathbf{k}-(\mathbf{n}\,.\,\mathbf{k})\mathbf{n}\} = 4\pi\mathbf{k}.$$

This reduces to (5) if $\mathbf{H}_2$ is normal to the sheet.

The conditions (4) and (5) are easily satisfied for a given field $\mathbf{H}_1$ having axial symmetry, if the sheet is a figure of revolution, on which the current stream lines are circles about the axis. The lines of force of $\mathbf{H}_1$ must be in the meridional planes and their angle of incidence θ_1 on the sheet will be constant round each turn of the winding. The turn-density must be arranged to satisfy (4).

Take a unit north pole round a closed circuit (in a meridional plane) which intersects the sheet at 1 and 2 in fig. 2. Denoting the magnetic scalar potential by M, the work done is $W=4\pi\int_1^2 k\,dl=\oint \mathbf{H}\,.\,d\mathbf{s}=M_2-M_1+M_4-M_3$.

The points 3 and 4 are on the equipotential surface of the permeable shroud, so that $M_3=M_4$, and, from (4)

$$M_2-M_1=\int_1^2 -\mathbf{H}\,.\,d\mathbf{s}=\int_1^2 -H_1\sin\theta_1\,dl=4\pi\int_1^2 k\,dl. \qquad \ldots\ldots(6)$$

Thus $\mathbf{H}_1$ requires no other source of m.m.f. than that provided by the current sheet, if the reluctance of the return path in the shroud is zero.

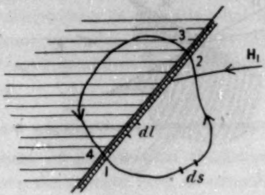

Fig. 2.

Eqn. (6) can be generalized into a simple rule relating the ampere-turns in a current sheet to the potential M on its inner surface. The sheet need not possess axial symmetry but it must terminate the internal field either with or without the assistance of a permeable shroud. Because there is no external field, no work is done in taking unit pole along that part of any closed path, linked with the winding, which lies outside the sheet. Hence if we take a pole along a path s lying on the inner surface of the sheet, the work done between two points 1 and 2 is equal to 4π times the total current flowing across s in the sheet between the points 1 and 2. Thus

$$M_2-M_1=4\pi NC/10, \qquad \ldots\ldots(7)$$

where NC is the number of ampere-turns in the winding between 1 and 2. This equation makes it possible to calculate the distribution of turns inside an iron enclosure which will generate a chosen source-free and curl-free portion of an arbitrary magnetic field for which the expression for the potential M is known.

§4. EXAMPLES OF THE FIELD-TERMINATING CURRENT SHEET

(i) *The Toroidal Winding*

This well-known winding, if uniform, with each turn lying in a meridional plane, generates an internal field with circular lines of force. No flux penetrates the winding, in which each layer encloses a complete ring-shaped tube of force. The absence of stray field was utilized by Fortescue (1915) in the astatic inductance.

(ii) *A Sheet enclosing a General Tube of Induction in an Inhomogeneous Medium*

Suppose we know a theoretical solution of a magnetostatic problem, such as that of the field of a circular current in a homogeneous medium. We then choose a particular tube of force and wind round it a complete tubular current sheet in which each turn lies nearly in an equipotential surface of the field. If the strength **k** is adjusted so that $4\pi k = H$ over the surface, (3) is satisfied, and on removing the source of the original field, H falls to zero everywhere except inside the sheet, where it is preserved unchanged.

This can be generalized to a sheet enclosing a tube of induction in an isotropic medium in which μ varies with position. The turns must again follow the intersection of the equipotential surfaces with the tube and we must have, at every point of the sheet,

$$4\pi k = H = B/\mu. \qquad \ldots\ldots(8)$$

The winding may consist of many layers, provided that each layer follows one particular tube of induction throughout its whole length.

(iii) *A Complete Current Sheet enclosing an Air Gap and a Permeable Core*

Case (ii) is unlikely to arise in practice because the winding can hardly be embedded in a permeable solid, but must be wound upon it as a core. If μ is uniform, it is still possible to eliminate stray field, as in the well-known case of the uniformly wound anchor ring.

Burrows (1909) proposed to eliminate leakage flux from a more complex magnetic circuit by bringing its surface to a constant magnetic potential M by the use of a special winding. This was designed to distribute the m.m.f. along the circuit so that it matched the magnetic reluctance at every point in accordance with (8). He attributed the idea to Rosa. However, his experiments on the magnetic circuits of permeameters, and later work such as, for example, that of Hughes (1926) and Webb and Ford (1929), have shown the difficulty of entirely avoiding leakage. This is partly because, apart from the anchor ring, the circuits used have not fitted known solutions of a field problem. Leakage has originated from corners and from abrupt changes in the area of the core and of its windings.

In the important practical case (iii) we may expect a small leakage, associated with a slight distortion of the field, to arise at the discontinuity at the pole-faces, which are formed by the two ends of the iron core. Suppose the air gap is surrounded by a thick winding of many layers to give a strong field. Then since each layer cannot be continued along its appropriate tube of induction inside the iron, some of these tubes will diverge outwards on entering the pole-pieces. A part of their inclination θ_2 to the inside normal will be transmitted to the air-gap side of the pole-face, in accordance with the usual law of refraction, $\tan\theta_1 = (\tan\theta_2)/\mu$. Thus the pole-faces may not be perfectly equipotential, unless μ is very large, or unless θ_2 is made small by suitably shaping the return path in the iron.

§5. THE USE OF IRON POLE-FACES TO CLOSE THE ENDS OF A CURRENT-SHEET

If μ is large the value of the surface current **k** needed to bring the iron part of the circuit to uniform potential M will be small, and in practice may often be taken as zero, without ill-effect. We then only need to make the shape of that part of a pole-face which closes an end of the winding conform to the known equipotentials of the field, so that the lines of force can enter the iron normally without distortion. The surface of the rest of the iron can have any economical shape giving a short return-path and not too high a flux density. Some realizable cases are:

(*a*) ***The uniform field*** (fig. 3). This can be obtained between parallel plane pole-faces which are joined by a yoke and which close the ends of a uniform winding. The field will be nearly free from inhomogeneity and will not stray outside the winding.

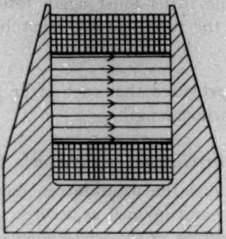

Fig. 3. Production of a uniform field. A section through the soft iron and the winding.

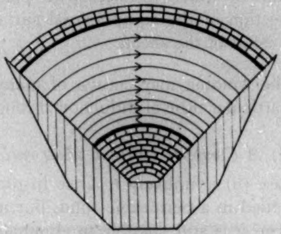

Fig. 4. A circular field inside a sector of a toroidal winding between inclined plane pole-faces.

(*b*) *The circular field* $H = H_0 r^{-1}$ (fig. 4). The winding is merely a sector of the toroidal coil of § 4 (i) placed between two iron pole-faces constituting meridional planes of the toroid. Any convenient shape may be chosen for the meridional section of the winding.

(*c*) *The synchrotron field* $H = H_0 r^{-2/3}$. This field is required in a ring-shaped region of large radius *r*, over which the percentage change in *r* is so small that the theoretical equipotentials are nearly parallel planes. In the usual procedure, the fringing perturbation is counteracted by peripheral ridges.

The alternative method using multi-layered field-terminating current sheets would have a rather similar magnet with a nearly parallel air-gap, devoid of ridges, whose meridional section would resemble fig. 3, the field lines being parallel to the ring-axis, which would lie below the diagram. The current would flow in opposite senses in the inner and outer ring-shaped sheets.

This method would permit a saving in iron because the waste flux is eliminated and, by bringing the undistorted part of the field into contact with the pole-faces, it would make possible a reduction in the width of the gap and hence in the m.m.f. However, the outer winding contributes nothing to the m.m.f., so that unless the vacuum chamber could be fitted into a gap of less than half the original height there would be no saving in copper.

(*d*) *The prolate spheroidal field.* A conventional method of producing this field in a limited region near the axis is shown in fig. 5 (*a*), in which the pole-pieces are approximate hyperboloids of revolution bounded by peripheral ridges A A, and the magnetizing coils B are placed round some part of the iron circuit. The return path must be distant from the axis in order to avoid distortion.

The alternative method is also shown in which the field is terminated radially by a current sheet C enclosing a prolate spheroidal tube of force. If the winding is thick each layer of turns should lie on a particular member of the confocal family of spheroids $\eta = \text{constant}$. The number of turns per centimetre will be proportional to H, where $H = H_0/\{(1-\xi^2)(\eta^2-\xi^2)\}^{1/2}$.

Here η and ξ are prolate spheroidal coordinates defined by $\eta = (r_1 + r_2)/2a$ and $\xi = (r_1 - r_2)/2a$; r_1 and r_2 are the distances from the two common foci of the conicoids and the foci are $2a$ apart.

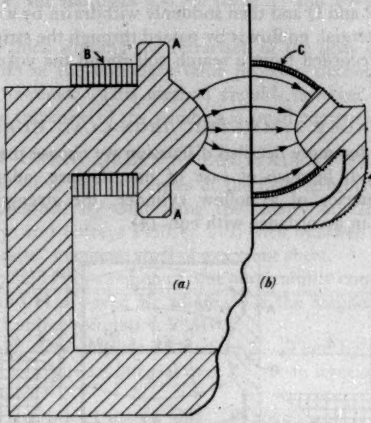

Fig. 5. (*a*) A conventional way of producing a prolate spheroidal field. (*b*) A method using a spheroidal winding C. The section passes through both foci of the spheroids and bisects the magnet yoke. D indicates schematically a Burrows-type winding, to bring the iron to a uniform potential.

If infinitely permeable, the iron is all at the same potential and its shape outside the winding does not affect the field inside. Thus the hyperboloidal pole-faces may be terminated near the boundary of the current sheet and the return path may be shortened with much saving in iron. There would be little saving in copper because the number of ampere-turns is unchanged and the mean diameter of the alternative winding is fairly large.

§6. THE NEUTRALIZATION OF THE RELUCTANCE OF THE IRON

Unless specially annealed and purified iron is used we must expect an appreciable potential gradient in any return path due to its magnetic reluctance. If the path is formed by a single yoke, as in fig. 5 (*a*), its leakage flux may cause an undesirable deviation of such a field from axial symmetry.

This can be countered by arranging several similar return paths symmetrically around the axis, or even by adopting complete axial symmetry, as discussed in the next section. An alternative general method, applicable to all the cases of figs. 3, 4 and 5, would be to neutralize the potential gradient in the return path by the method of Burrows (1909) by enclosing it in an 'anti-reluctance' winding giving a distributed m.m.f., with the current adjusted to bring all the iron to the same potential. Such a winding is indicated in fig. 5 (*b*).

In practice the permeability μ changes rapidly with $\mathbf{B}$ so that the neutralizing current will not be a constant fraction of that in the main winding C. The correct value of neutralizing current might be found experimentally by adjusting it until no magnetic potential difference could be detected between two points P and Q of the iron.

In this connection a suitably sensitive method of detection might be that of Hughes (1926) in which the ends of a highly permeable strip of stalloy are brought into contact with P and Q and then suddenly withdrawn by a spring. If P and Q are at the same potential, no flux is by-passed through the strip, and no deflection of a fluxmeter is recorded from a search coil round the yoke, when the strip is withdrawn sharply.

§7. THE AXIALLY SYMMETRIC IRON-CLAD CURRENT SHEET

As an example for more detailed discussion we choose the case of the prolate spheroidal field and, because of ease of manufacture, adopt a current sheet wound on the interior of a hollow cylinder, the strength being given by $-k=H_1 \sin\theta_1/4\pi$, in accordance with eqn. (4).

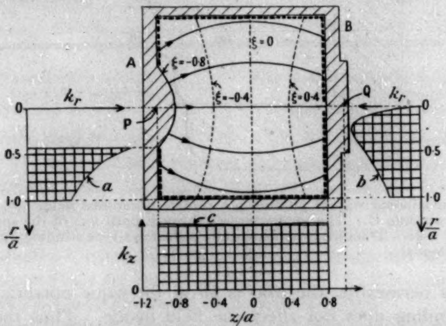

Fig. 6. An iron-shrouded current sheet generating a prolate spheroidal field, shown in axial section. Curves *a*, *b* and *c* give the variation of k_r and k_z, the ampere turns per mm over the end-plates A and B and over the inner wall of the cylinder, respectively. A and B show alternative modes of construction.

Two alternatives are available for the disc windings on the ends of the cylinder, as shown in fig. 6. In the form A, each winding has an axial hole which encircles an inward hyperboloidal bulge on the iron disc which closes the cylindrical shroud. In the form B, the windings spiral right in to the axis, where k is zero. The iron end-plates are now plane on their inner faces, which must lie between the foci of the conicoids at P and Q, in order to avoid an infinity in k on the axis.

For the spheroidal field, the potential M is

$$M=H_0 a \tanh^{-1}\xi. \qquad \ldots\ldots(9)$$

We choose $M=0$ over the mid-plane $\xi=0$. H_0 is the intensity at the origin at the centre of the field. Using radial and axial cylindrical coordinates, r and z, we have from (4) that the strength k_z of the winding on the outer cylinder is $k_z=(1/4\pi)\partial M/\partial z$ and on the end-discs it is k_r, where $k_r=(1/4\pi)\partial M/\partial r$.

Differentiating (9)

$$k_z = \frac{H_0 a}{8\pi}\left\{\frac{1+z/a}{r_1} + \frac{1-z/a}{r_2}\right\}\left\{1-\left(\frac{r_1-r_2}{2a}\right)^2\right\}^{-1},$$

$$k_r = \frac{H_0 r}{8\pi}\left\{\frac{1}{r_1} - \frac{1}{r_2}\right\}\left\{1-\left(\frac{r_1-r_2}{2a}\right)^2\right\}^{-1}.$$

Here $r_1=\{r^2+(a+z)^2\}^{1/2}$ and $r_2=\{r^2+(a-z)^2\}^{1/2}$; k_z has been plotted for the cylinder $r=a$, and k_r for the discs $z=-a$ (case A) and $z=+0{\cdot}8a$ (case B) in fig. 6.

In the case of a thick winding the refraction of the lines of force is gradual and an exact solution of the boundary-value problem cannot be found by the present elementary method. This method should, however, give a good first approximation if the thickness of the winding is small compared with the air gap.

§8. A PROOF USING GREEN'S 'EQUIVALENT STRATUM'

An alternative proof of the properties of the field-terminating and iron-clad windings can be obtained by combining the theory of Green's 'equivalent stratum' (see Jeffreys and Jeffreys 1950, p. 219) with Maxwell's treatment (1873, §648) of the 'composite' magnetic shell of a current sheet.

Consider a static field $\mathbf{H}$ in a region of unit permeability containing no current, so that curl $\mathbf{H}=0$ and $\mathbf{H}=-\operatorname{grad} M$, where M is the magnetic scalar potential and is a solution of Laplace's equation $\nabla^2 M=0$.

Inside this region, draw any closed surface Σ. Then by Green's theorems, M can be expressed as a surface integral over Σ. At an interior point P inside Σ, we have $M=M_{\mathrm{P}}$ where

$$M_{\mathrm{P}} = \frac{1}{4\pi}\int_{\Sigma}\left\{\frac{1}{R}\frac{\partial M}{\partial n} - \frac{M\cos\theta}{R^2}\right\}d\Sigma.$$

$\partial/\partial n$ denotes differentiation along $\mathbf{n}$, the outward-drawn normal to $d\Sigma$, and θ is the angle between $\mathbf{n}$ and the radius vector $\mathbf{R}$, drawn from $d\Sigma$ to P.

The first term in the integral equals the potential at P due to a layer of pole on Σ, of density I poles/cm² where $I=(1/4\pi)\partial M/\partial n$. The second term equals that due to an outward-pointing dipole layer or magnetic shell on Σ of strength $M/4\pi$.

Suppose now that these two layers, which constitute Green's 'equivalent stratum', form a physically real part of some magnetic structure enclosing Σ. This real stratum terminates the field and has just the properties of the two kinds of current sheet, for the following reasons. First, the layer of pole generates a discontinuity equal to $4\pi I$ in $\partial M/\partial n$, the normal component of the field, which is thus annihilated on the exterior of the surface. Second, the dipole layer reduces M to zero everywhere outside the closed surface, because the well-known discontinuity of $4\pi\Phi$ on the two sides of a magnetic shell of strength Φ is just equal to M.

The requisite surface layer of pole may be produced by induction on the inner surface of our magnetic structure, which must provide a return path of zero reluctance for the flux in order to make $M=0$ outside Σ. Thus one part of the real stratum must be an infinitely permeable shroud which is only needed on those areas of Σ over which $\partial M/\partial n$ is not zero. The remaining part is a means of imposing the requisite magnetic shell of strength $-M/4\pi$ on the inner surface of Σ.

To generate the shell, consider a current sheet whose circulation is in closed stream lines on the inner surface of Σ. The flow along **k** may be defined by Φ, the stream function of Maxwell, related to k by $\Phi = \int k\,ds$ where ds is an element of a line drawn in Σ normally to **k**. Φ is the current crossing any line drawn in Σ from a fixed point p to another point q. Consider a current sheet such as that in fig. 7, and place p on its right-hand edge, which is thus identified as the stream line $\Phi = 0$. If q is moved along a path such as s it will eventually reach the left-hand edge at the stream line $\Phi = i$, where i is the total current.

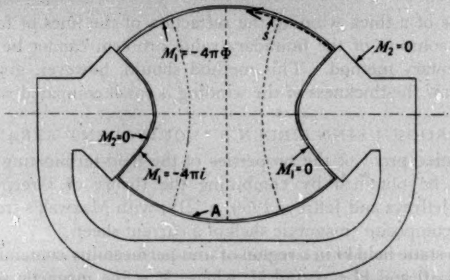

Fig. 7. **The doublet layer associated with a prolate spheroidal field-terminating current sheet, A. A 'schematic' axial section through the pole-pieces of an infinitely permeable magnet. The strength of the doublet layer is zero over the right-hand pole-face.**

The current $d\Phi$, between the stream lines Φ and $\Phi + d\Phi$, is the boundary of an equivalent magnetic shell of strength $d\Phi$, whose shape is arbitrary and hence may be assigned to lie in the surface Σ to the left of its generating current $d\Phi$. On moving to the left from p, the strength of the composite shell due to all the currents $d\Phi$ will equal Φ and will reach the maximum value i, over the left-hand pole-face.

The potential due to the composite shell at any point not in the infinitesimal thickness of the dipole layer is

$$M = \int_\Sigma \frac{\Phi \cos\theta}{R^2}\, d\Sigma.$$

This gives the familiar relation between the potentials at two neighbouring points a and b just inside and just outside the closed surface Σ: $M_b = M_a + 4\pi\Phi$. The permeable shroud makes $M_b = 0$ so that $M_a = -4\pi\Phi = -4\pi NC/10$.

This forms an alternative proof of equation (7) and has the same form if we put $M_a = M_1$, and $M_2 = 0$, so that the point 2 lies on $\Phi = 0$.

ACKNOWLEDGMENTS

It is a pleasure to thank Professor N. Feather and Dr. R. Schlapp for many helpful suggestions.

REFERENCES

Burrows, C. W., 1909, *Bull. Nat. Bur. Stand., Wash.*, **6**, 31.

Fortescue, C., 1915, *Trans. Amer. Inst. Elect. Engrs.*, **34**, 1199.

Hughes, E., 1926, *Phil. Mag.*, **2**, 163.

Jeffreys, H., and Jeffreys, B. S., 1950, *Mathematical Physics*, 2nd edition (Cambridge : University Press).

Maxwell, J. C., 1873, *Electricity and Magnetism* (Oxford : Clarendon Press).

Webb, C. E., and Ford, L. H., 1929, *J. Instn. Elect. Engrs.*, **67**, 1302.

The Extension of the Electrolytic Tank Method to the Study of Magnetic Fields due to Iron-clad Current Sheets in Three Dimensions

By H. O. W. RICHARDSON
Department of Natural Philosophy, The University, Edinburgh

Communicated by N. Feather; *MS. received* 16*th March* 1951, *and in revised form* 20*th August* 1951

ABSTRACT. An application of the electrolytic tank method to plot the magnetic fields of a current sheet is described. In general, three-dimensional fields due to currents can be plotted, provided that the current is close to the surface of a piece of permeable iron.

§ 1. INTRODUCTION

THE electrolytic tank method may be used to plot three-dimensional magnetic fields due to currents which are everywhere in close proximity to an iron surface. When the currents flow in a thin layer of closely wound turns of wire the arrangement can be treated with good accuracy as an iron-clad current sheet whose field is that of a single 'composite' magnetic shell. The shell can be represented in the tank by its electrostatic analogue. The tank method is not, in general, applicable to currents in thicker types of winding, except in the two-dimensional case, when the method of Pérès and Malavard (1938) and of Peierls (1946) may be used. A radially restricted zone of an axially symmetric field may be plotted by the method of Peierls and Skyrme (1949).

The conditions under which the electric equipotentials in the tank can represent the scalar magnetic equipotentials, $M=\text{constant}$, of a static field $\mathbf{H}$ in a homogeneous space are as follows (Liebmann 1950, p. 115): (*a*) M must be known over the boundaries of the space and (*b*) no magnetizing current must be included inside the boundaries.

These conditions are satisfied inside any space bounded by an infinitely permeable iron shroud, free from apertures, carrying a current sheet on part or all of its inner surface. Condition (*a*) is fulfilled because we can assign a value of M to every point of the inner surface, if the distribution of ampere-turns is known, by using the relation given in the preceding paper (Richardson 1952),

$$M=-4\pi\Phi=-4\pi NC/10. \qquad \ldots\ldots(1)$$

Φ is the stream function at the point and equals one-tenth of the ampere-turns NC lying between it and the right-hand reference end of the current sheet. Viewed from that end, the current flow is assumed to be clockwise.

Thus, in the case of an iron enclosure, we can use the tank to find the shape of field in the interior by applying to the inner surface electric potentials V everywhere proportional to Φ. Alternatively, it may happen that some particular shape of interior field $\mathbf{H}$ is required. We may then vary the boundary values of V on electrodes lining the inner surface until the plotted potentials have the desired form in the electrolyte. By using (1) the current distribution of ampere-turns to generate $\mathbf{H}$ can be read off from the observed set of boundary values of V.

The procedure can easily be extended to the case in which the iron does not form an enclosure. Minor difficulties arise for an unsymmetrical arrangement with more than one aperture. This case is discussed in § 3.

§2. THE REPRESENTATION OF A CURRENT SHEET BY A GRID OF ELECTRODES

The desired values of V may be imposed upon the boundary by applying them to the elements of a grid of electrodes in the tank, shaped to delineate the inner surface of the iron enclosure. The grid spacing should be small, and each element should follow a stream line $\Phi = \text{constant}$ of the magnetizing current, because these lines are the equipotential contours of M on the boundary. The current-free parts of the iron can be represented by the usual continuous conductors because they have no tangential field component.

A grid of electrodes has been used to represent a current sheet by Braid and Richardson (1951) in order to predict the equipotentials of the magnet shown in fig. 1. The pole-pieces A and the windings W have cylindrical symmetry about the axis DD. The return path is completed by twelve flat similar iron plates C, arranged uniformly round the dodecagonal end-plates B.

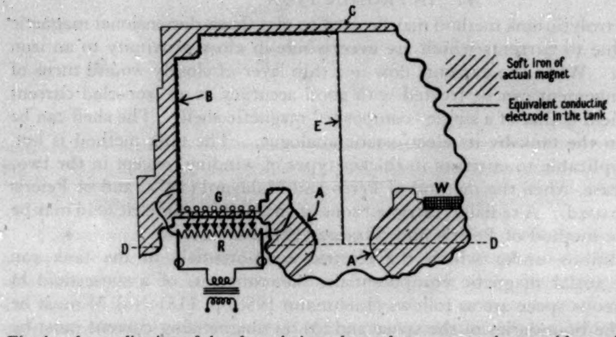
C
Soft iron of actual magnet
Equivalent conducting electrode in the tank
B
E
G
A
W
R
D
D
A

Fig. 1. An application of the electrolytic tank to solve a current sheet problem. The winding W (shown only on the right) was represented approximately by the grid G.

A 30° sector of the field was explored with the glass bottom of the tank, tilted at that angle, emerging from the water surface along the axis DD. The following instantaneous potentials were applied from a transformer: (1) $V=0$ on the inner surfaces of B and C, and on the mid-plane of symmetry E; (2) $V = \text{constant}$ on the pole-face A; (3) eight intermediate potentials on the parallel elements of the grid G which were fed from the potential-divider R, adjusted to give a uniform tangential gradient of V, parallel to DD, to represent the uniform winding W on the left-hand pole. The grid was made of thick wires, bent into circular arcs along the stream lines of the magnetizing current.

In this application, high accuracy was required only in the region between the poles, at some distance from W, so that a rough representation of the current was adequate. The thickness of the actual winding is about one-sixth of its diameter and is small compared with the air gap, so that each coil may be treated as a thin current sheet on a re-entrant part of an iron shroud. A coarse grid with only nine potential steps between A and B could be used because there was sufficient space for the resulting unevenness of the field to die away.

§ 3. CURRENT SHEETS IN AN IRON SHROUD WITH APERTURES

In iron-clad β-spectrometers and magnetic lenses apertures in the iron are usually present. In the majority of such cases the tank method may still be used to predict the field if the winding can be represented with sufficient accuracy as a thin current sheet. The method is exact if an equipotential surface of known shape exists over which the composite magnetic shell due to the sheet may be completed.

If we assign $M=0$ to the known surface we can, in the tank method, place upon it an electric double layer, equivalent to the magnetic shell, having $V=0$ on one side and V proportional to the ampere-turns on the other. The side with $V=0$ does not need to be represented by an electrode, except on diaphragms such as W′ in fig. 2 (*c*), in which both sides of the layer contribute to the field.

Three different ways of completing the shell may arise, depending on the geometry of the system.

Case (*a*). It may be possible to complete the shell entirely over the surface of the iron. This can be done if there are no apertures in the surface on one side of the current sheet. An electrode system representing a magnet of this class is shown in fig. 2 (*a*), for an axially symmetric case. The water surface may be level with the axis, and the walls and bottom of the tank must be distant from the electrodes, to avoid distortion of the remoter equipotentials. To satisfy div $\mathbf{B}=0$ no net current should flow to the walls, which should preferably be non-conducting.

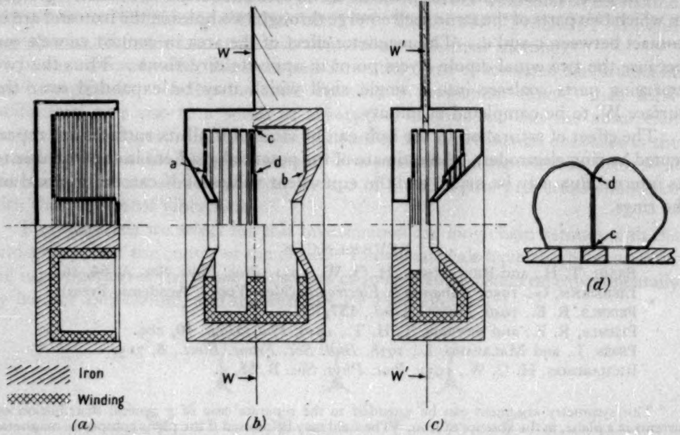

Fig. 2. (*a*), (*b*) and (*c*) give examples of the three classes of iron-clad winding with apertures, shown in axial section. The equivalent systems of tank electrodes are drawn above the axis. (*d*) shows a magnetic shell emerging through two holes in an iron shroud.

Case (*b*). The shell can be completed over an existing plane of symmetry, normal to the lines of force. This plane will be an equipotential and must exist in any symmetrical shrouded lens such as that in fig. 2 (*b*). Each symmetrical half of the winding can be supposed to generate its own composite shell, starting at a or b. The two shells join at c and pass together over the mid-plane.

The symmetry allows a rigorous treatment of the contribution of the parts of the two sheets between c and d, although they are not in contact with the iron. The field between these two parts must be normal to the mid-plane so that each sheet refracts the lines of force as though it was actually in contact with an iron plane.* The symmetry makes it unnecessary to model the right half of the lens, and the plane W may be formed by an earthed conducting wall of the tank. The potentials imposed on the ring electrodes would start with $V=0$ at a, and increase in proportion to the ampere-turns to a maximum on the central disc.

Case (*c*). No equipotential of known shape may exist. Only an approximate solution is now possible, by a method such as is shown in fig. 2(*c*), in which we guess the shape of the equipotential W′ and then use it to carry the shell away from the iron to be completed over an effectively infinitely distant boundary. The inner part of the shell starts in the current sheet and passes through the aperture over the surface of the iron to W′. In this way the uncertainty in the field due to errors in the shape of W′ originates in a remote region of weak field and has a minimum value in the important region near the axis. The shell on W′ must be represented by a partition in the tank with $V=0$ on one side and V proportional to the ampere-turns on the other.

The case of many apertures presents no further difficulty. Consider fig. 2(*d*), in which two parts of the same shell emerge through two holes in the iron and are in contact between c and d. The magnetic effect of the area in contact cancels out because the two equal dipole layers point in opposite directions. Thus the two emerging parts coalesce into a single shell which may be expanded over the surface W′ to be completed at infinity.

The effect of saturation in the iron can be studied if all its surfaces are represented by ring electrodes. An estimate of the potential gradient in the iron due to its internal flux may be made, and the equivalent values of V can be imposed on the rings.

REFERENCES

Braid, T. H., and Richardson, H. O. W., 1951, *Proc. Phys. Soc.* A, **64,** 163.
Liebmann, G., 1950, *Advances in Electronics* (New York : Academic Press).
Peierls, R. E., 1946, *Nature, Lond.*, **157,** 831.
Peierls, R. E., and Skyrme, T. H. T., 1949, *Phil. Mag.*, **40,** 269.
Pérès, J., and Malavard, L., 1938, *Bull. Soc. Franç. Elect.*, **8,** 715.
Richardson, H. O. W., 1952, *Proc. Phys. Soc.* B, **65,** 5.

---

* This symmetry argument can be extended to the separate case of a general distribution of currents in a plane, in the absence of iron. The field may be plotted if the plane composite magnetic shell is represented by plane electrodes.

On the Torsional Vibrations of Long Chain Molecules*

By B. SZIGETI
Department of Theoretical Physics, University of Liverpool

Communicated by H. Fröhlich; *MS. received* 8*th June* 1951, *and in amended form* 22*nd August* 1951

ABSTRACT. Simplified models are discussed for long chain molecules in which all units are equal except for one which is heavier than the others. Certain general conclusions are reached for the vibrations of such molecules. The results will be applied to the out-of-plane or torsional vibrations of long chain ketones in a following paper.

§1. INTRODUCTION

The twisting of long chain molecules is of considerable importance in connection with many of their properties. It is fairly certain, for instance, that this twist is responsible for the order–disorder transition of crystalline hydrocarbons (Oldham and Ubbelohde 1939, Müller 1940, Fröhlich 1944), and may also be of major importance in connection with their melting.

In the ordered solid, the twist sets in in the form of torsional oscillations of small amplitude. If the molecule contains a permanent dipole, then these oscillations give rise to a series of absorption frequencies, but the absorption spectra have not yet been measured because of the experimental obstacles in the frequency region in which they occur. The present work represents a theoretical treatment of the absorption spectrum and of the dielectric properties connected with these torsional vibrations.

The materials we select for this investigation are long chain ketones with the keto-group near the centre of the chain. These materials have also been used for the investigation of the phase transitions of long chain substances, experimentally by Müller and Daniel, and theoretically by Fröhlich.

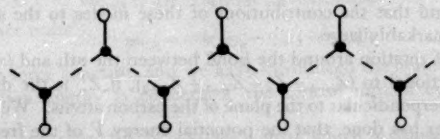

Fig. 1. A portion of a long chain hydrocarbon. The filled circles are carbon atoms while each empty circle represents two hydrogens, one of which is above and one below the plane of the C atoms.

Fig. 1 shows a long chain hydrocarbon in its configuration of lowest energy. All the carbon atoms are in the same plane. It is usual, in a first approximation, to divide the vibrations of such a molecule into two groups, one comprising the vibrations of the hydrogens with respect to the carbon skeleton while the other group contains the skeletal vibrations in the course of which the CH_2 groups vibrate as rigid units with respect to each other. If the skeletal vibrations are of small amplitude, then the vibrations of the bond lengths and bond angles involve displacements of the C atoms in the carbon plane, while rotations around C—C bonds are connected with vibrations of the carbons perpendicular to this plane. The former modes have been treated by Kirkwood (1939) and others, the latter, the 'out-of-plane' vibrations, by Pitzer (1940).

---

* This paper is based on *E.R.A. Report*, Ref. L/T 266.

In the course of the out-of-plane vibrations the C—C bonds are, in general, not exactly parallel to the plane of the figure; since all the bond angles are preserved, a consideration of fig. 1 will show that, even when these vibrations take place with the smallest amplitude, the motion of the CH_2 groups consists, in general, in a translation perpendicular to the molecular plane and a simultaneous rotation around the molecular axis. These vibrations thus lead to a torsion of the molecule.

However, in a long chain hydrocarbon the C—H bonds are so arranged that the total dipole moment of the molecule vanishes. This can be proved not only for the equilibrium configuration represented in fig. 1, but also for all other configurations in which the bond angles are unaltered (cf. for instance Fröhlich 1949). In the case of hydrocarbons, therefore, the out-of-plane or torsional vibrations have no effect on the dielectric properties.

On the other hand, if we replace one of the CH_2 groups by CO we obtain a ketone which has a permanent dipole moment. The oxygen is in the carbon plane and the C=O bond is perpendicular to the chain axis. In the course of the out-of-plane vibrations the motion of the CO group is similar to that of the CH_2 group and it also consists of a simultaneous translation and rotation.

It then follows from the previous argument that if either in equilibrium position or in any displacement arising in the course of the out-of-plane vibrations of a ketone the oxygen were replaced by H_2 in such a way that the CH_2 group pointed in the same direction as the CO group did, then the total dipole moment of the ketone would vanish. Therefore, the dipole moment of the ketone is $\mu_{\mathrm{CO}}-\mu_{\mathrm{CH_2}}$ if μ_{CO} and $\mu_{\mathrm{CH_2}}$ are the dipole moments of the respective groups, and this dipole moment points in the direction of the C=O bond. We shall see that about half of the torsional modes involve a change in the direction of the C=O bond, and these vibrations must therefore contribute to the absorption spectrum and to the dielectric constant. Since some of the frequencies are very low, we shall find that the contributions of these modes to the static dielectric constant are remarkably large.

The angle of rotation around the bond between the nth and $(n+1)$th carbon atoms is proportional to $(Z_{n-1}-Z_n-Z_{n+1}+Z_{n+2})$, if Z_n is the displacement of the nth carbon perpendicular to the plane of the carbon atoms. We shall therefore assume, as Pitzer has done, that the potential energy V of the free hydrocarbon molecule in the course of the out-of-plane vibrations is

$$V=\tfrac{1}{2}k\sum_{n}(Z_{n-1}-Z_n-Z_{n+1}+Z_{n+2})^2. \qquad \ldots\ldots(1)$$

Although the potential energy for rotation around the two bonds adjacent to the CO group is probably lower than that around the others, we shall neglect this difference and assume that eqn. (1) is also valid for ketones. However, we shall deviate from Pitzer's approximation in that we shall take into account the spatial extension of the CH_2 and CO groups and their rotation around the chain axis, since this is essential for our problem. We shall also take account of the fact that the CO group is heavier than the CH_2 groups.

The latter condition together with the potential energy given by eqn. (1) makes an exact solution of the normal modes very complicated. We shall therefore discuss simplified models each consisting of a chain in which one unit is heavier than the others, but from the point of view of interaction energy the heavy unit is equivalent to the other units of the chain. The units of some of these models are capable of rotational, those of others of translational vibration only, and only nearest neighbours interact. We shall discuss the modes of vibration of these models in some detail and this will enable us to draw certain conclusions with respect to the vibrations of similar chains whose interaction energy is, however, not restricted to nearest neighbours. These conclusions, which are summarized in §5, will first be valid for one-dimensional translation or rotation only; in a later paper we shall apply them to the out-of-plane vibrations of the ketone molecule, taking into account that these consist of a simultaneous translation and rotation. Finally we shall consider how these vibrations and the dielectric properties connected with them are modified by the intermolecular forces in the crystal.

This method will also be applicable to other substituted hydrocarbons.

§2. DIFFERENT UNIT IN THE CENTRE OF THE CHAIN

One of the models we shall discuss is a linear chain of N rigid units which are capable of rotational vibration around the chain axis. The moment of inertia of the units around this axis is m, except for one unit for which it is m'. In the first instance we shall assume that this different unit is in the central position; this implies that N must be odd, but otherwise N may have any value larger than one. We shall denote the central unit by 0, those on its right by $1, 2, \ldots (N-1)/2$ and those on its left by $-1, -2, \ldots -(N-1)/2$. Assuming a first-order force between nearest neighbours and denoting the angle of rotation of the nth unit by η_n, the equation of motion of the central unit is

$$m'\ddot{\eta}_0 = -k(2\eta_0 - \eta_1 - \eta_{-1}), \qquad \ldots\ldots(2)$$

while, in the case of free ends, the equations for the two end units are

$$\left.\begin{aligned} m\ddot{\eta}_{(N-1)/2} &= -k[\eta_{(N-1)/2} - \eta_{(N-3)/2}] \\ m\ddot{\eta}_{-(N-1)/2} &= -k[\eta_{-(N-1)/2} - \eta_{-(N-3)/2}] \end{aligned}\right\} \qquad \ldots\ldots(3)$$

and for all other units

$$m\ddot{\eta}_n = -k(2\eta_n - \eta_{n-1} - \eta_{n+1}), \qquad \ldots\ldots(4)$$

where k is the force constant, and we have introduced the condition that, as far as the interaction energy is concerned, the central unit is equivalent to the others.

Simultaneously we shall also consider a chain which is similar to the previous one, except that its units are only capable of translational vibration in one direction. If we now number the units in the same way as before, but denote the linear displacement by η, the mass of the central unit by m' and that of the others by m, then eqns. (2) to (4) also represent the equations of motion of this chain. The solution of the problem represented by eqns. (2) to (4) will therefore give the vibrations of both models, except that m, m' and the η's have different meanings in the two cases.

If m' were equal to m, then eqns. (2) to (4) would represent the equations of motion for the one-dimensional vibration of a linear monatomic chain with free ends. The solution for this case has been given by Born and von Kármán (cf. Born 1942) and is, in our notation

$$\eta_n = A \sin \omega t \cos (n + \tfrac{1}{2}N)\sigma. \qquad \ldots\ldots(5)$$

In order to satisfy eqns. (4), ω and σ must be connected by

$$\omega^2 = (4k/m) \sin^2 \tfrac{1}{2}\sigma \qquad \ldots\ldots(6)$$

and the values of σ which satisfy eqns. (3) are given by

$$\sigma = l\pi/N, \qquad l = 1, 2, \ldots (N-1). \qquad \ldots\ldots(7)$$

Non-integral values of l do not satisfy eqns. (3), while integral values other than those enumerated above do not represent physically new solutions.

The solutions (5) are standing waves and l represents the number of half waves contained in a length equivalent to N nearest neighbour distances. Hence $N/2$ nearest neighbour distances contain an odd or even number of quarter waves according as l is odd or even. For odd values of l eqn. (5) can therefore also be written

$$\eta_n = A' \sin \omega t \sin n\sigma \qquad \ldots\ldots(5')$$

and for even values of l,

$$\eta_n = A' \sin \omega t \cos n\sigma, \qquad \ldots\ldots(5'')$$

where $A' = A$ for some values of l and $A' = -A$ for others. Eqn.(5′) represents solutions where $\eta_n = -\eta_{-n}$, while for (5″) $\eta_n = \eta_{-n}$.

In our case, when $m' \neq m$, the odd solutions (5′) still satisfy the equations of motion because $\eta_0 = 0$ so that eqn. (2) is identically satisfied. These solutions are of little interest to us since they do not involve a displacement of that unit which differs from the others. The even solutions (5″), on the other hand, do not satisfy eqn. (2) and have to be replaced by

$$\eta_n = B \sin \omega t \cos (|n|\sigma + \delta). \qquad \ldots\ldots(8)$$

Inserting this into eqn. (4) the same connection is obtained between ω and σ as before, viz.

$$\omega^2 = (4k/m) \sin^2 \tfrac{1}{2}\sigma. \qquad \ldots\ldots(9)$$

When we insert the last two equations into eqn. (2) we find that

$$\tan \delta = \{(m' - m)/m\} \tan \tfrac{1}{2}\sigma \qquad \ldots\ldots(10)$$

and the eqns. (3) require that σ must satisfy the relation

$$\sigma = l\pi/N - 2\delta/N, \qquad l = 2, 4, 6, \ldots . \qquad \ldots\ldots(11)$$

The difference between the solutions (5″) and (8) is illustrated in fig. 2 for $N = 11$ and $l = 4$. The figure shows the space factor $\cos (|n|\sigma + \delta)$ as a continuous function of n; the values for integral n, which alone are of physical interest, are marked by circles. It is seen that for $m' \neq m$ the two halves of the curve, corresponding to positive and negative values of n, experience a phase shift with respect to each other and form a cusp at $n = 0$, and the amplitude of the central unit is smaller than when $m' = m$. In addition, the wavelength and therefore the frequency are also somewhat different in the two cases.

(i) *Counting the Independent Modes*

For a given σ, the various values of δ satisfying eqn. (10) only differ by integral multiples of π and therefore represent the same solution, since increasing δ by an integral multiple of π either leaves all the η's unchanged or multiplies them all by -1. Without loss of generality we can therefore make δ a unique function of σ by restricting it to the range

$$-\tfrac{1}{2}\pi<\delta<\tfrac{1}{2}\pi. \qquad \ldots\ldots(12)$$

Moreover, if $\sigma=\sigma_1$ is a solution, then changing it by integral multiples of 2π or replacing it by $\sigma=2\pi-\sigma_1$ leads to the same solution. In the first case δ remains unchanged, while in the latter it is multiplied by -1, but for integral values of n eqn. (8) remains unaltered in either case. Similarly to the Born–Kármán solutions, we can therefore restrict σ to the range

$$0>\sigma>\pi. \qquad \ldots\ldots(13)$$

$\sigma=0$ and $\sigma=\pi$ do not represent vibrations; $\sigma=0$ corresponds to uniform displacement of the whole chain while if $\sigma=\pi$ all the displacements vanish identically.

Inserting eqn. (10) into (11) and solving for l we get

$$l=\frac{N\sigma}{\pi}+\frac{2}{\pi}\arctan\left(\frac{m'-m}{m}\tan\tfrac{1}{2}\sigma\right), \qquad l=2,4,6,\ldots. \qquad \ldots\ldots(14)$$

where, in view of eqn. (12), the arc tan is between $-\pi/2$ and $\pi/2$. We can find all the allowed solutions if we plot the right-hand side of eqn. (14) as a function of σ in the range between 0 to π, and select those values for which l is an even integer. Eqn. (9) shows that all these modes have different frequencies and must therefore represent independent solutions. They are also clearly independent of the odd solutions (5′) because they have different symmetry.

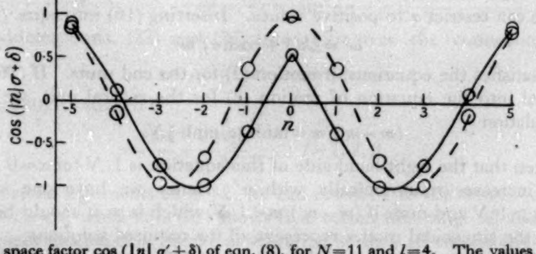

Fig. 2. The space factor $\cos(|n|\sigma'+\delta)$ of eqn. (8), for $N=11$ and $l=4$. The values for integral n are marked by circles. Full line: $m'/m=3{\cdot}76$; broken line: $m'=m$; in this case eqn. (8) becomes identical with (5″).

As a chain of N units has $N-1$ modes of vibration and equation (5′) represents $(N-1)/2$ odd solutions, there must also be $(N-1)/2$ even solutions. We shall now count our even solutions to see whether we have found all the modes of the chain.

(*a*) $m'>m$. If $m'>m$, the right-hand side of eqn. (14) increases monotonically with σ and $l\to N+1$ as $\sigma\to\pi$. Therefore all even values of l less than $N+1$ represent physically independent solutions, and as there are $(N-1)/2$ such values, we have found all the normal modes.

(*b*) $m'<m$. The case when $m'<m$ is somewhat more complicated. Although this case is of no direct interest for ketones or other substituted hydrocarbons,

nevertheless a short discussion will help us to understand the effect of m' on the vibrations of the chain.

In this case, for $\sigma \to \pi$, $l \to N-1$, while differentiating eqn. (14) with respect to σ we get

$$\frac{dl}{d\sigma} = \frac{1}{\pi}\left[N - \frac{(m-m')/m}{\cos^2 \frac{1}{2}\sigma + \{(m-m')/m\}^2 \sin^2 \frac{1}{2}\sigma}\right]. \qquad \ldots\ldots(15)$$

If $(m-m')/m > 1/N$, $dl/d\sigma$ is positive for all values of σ and in that case l increases monotonically with σ. Therefore all even values of l less than $N-1$ represent allowed solutions, but l equal to $N-1$ does not; in this case eqns. (8) to (11) only represent $\frac{1}{2}(N-1)-1$ modes, and one solution is still missing.

On the other hand, eqn. (15) shows that if $(m-m')/m < 1/N$ then $dl/d\sigma$ becomes negative before σ reaches π; and hence in this case (14) has a maximum for a value of $\sigma < \pi$ and, since $l = N-1$ for $\sigma = \pi$, there must be a value of σ less than π which also gives $l = N-1$. In this case $l = N-1$ represents a solution and we have found all the $(N-1)/2$ even modes. A further consideration shows that although eqn. (14) now has a maximum there is only one value of $\sigma < \pi$ for each of the $N-1$ allowed values of l. This clearly must be so since otherwise we should have more solutions than is compatible with our problem.

(ii) *The Hyperbolic Solution*

We have found that if $(m-m')/m > 1/N$, then the number of sinusoidal solutions (8) is one less than required. The missing solution is

$$\eta_n = (A/\alpha)(-1)^n \sinh[(\tfrac{1}{2}N - |n|)\alpha] \sin \omega t \qquad \ldots\ldots(16)$$

where α is real. Moreover, since all the η's remain unchanged if α is replaced by $-\alpha$, we can restrict α to positive values. Inserting (16) into eqns. (4) we find

$$\omega^2 = 2k(1 + \cosh \alpha)/m. \qquad \ldots\ldots(17)$$

This also satisfies the equations of motion (3) for the end units. If (16) and (17) are inserted into the equation of motion (2) for the central unit, we find after some calculation

$$(m-m')/m = \tanh \tfrac{1}{2}\alpha / \tanh \tfrac{1}{2}N\alpha. \qquad \ldots\ldots(18)$$

It is seen that the right-hand side of this equation is $1/N$ for $\alpha = 0$ and, since $N > 1$, it increases monotonically with α. Hence we have one solution if $(m-m')/m \geqslant 1/N$ and none if $(m-m')/m < 1/N$, which is as it should be as in the latter case the sinusoidal modes represent all the required solutions.

If $(m-m')/m = 1/N$, then $\alpha = 0$ but the eqns. (16) tend to well-defined limits and represent a solution. This was our reason for including the factor $1/\alpha$ in eqn. (16).

Eqn. (16) represents a solution where the displacements of neighbouring units have opposite signs and their absolute values decrease exponentially from the centre of the chain. Eqn. (17) shows that as $(m-m')/m$ increases from zero to unity, α increases from zero to infinity. Hence if $(m-m')/m$ is not much larger than $1/N$, α is not very different from zero and the exponential solution (16) is not very different from the sinusoidal solutions. But if $m' \ll m$, then α is very large and only η_0 has appreciable values while all the other η's are much smaller. This is what one would expect: if $m' \ll m$, there must be a mode of vibration in the course of which only the light unit vibrates and all the others remain stationary.

§ 3. DIFFERENT UNIT AT THE END OF THE CHAIN

We are also interested in cases where the unit whose mass or moment of inertia differs from the others is not exactly in the centre of the chain. In order to get an idea how our solutions are affected by the position of the different unit, we shall now solve for the vibrations of the two chains discussed in the previous section for the other extreme case, namely for the case when the different unit is at the end of the chain.

We now number the units 0, 1, 2, . . . $N-1$ where the unit which differs from the others is the zeroth. N the number of units in the chain can be any integer larger than one, odd or even. The equation of motion for the zeroth unit is

$$m'\ddot{\eta}_0 = -k(\eta_0 - \eta_1), \qquad \ldots\ldots(19)$$

for the unit at the other end

$$m\ddot{\eta}_{N-1} = -k(\eta_{N-1} - \eta_{N-2}) \qquad \ldots\ldots(20)$$

and for all others

$$m\ddot{\eta}_n = -k(2\eta_n - \eta_{n-1} - \eta_{n+1}). \qquad \ldots\ldots(21)$$

If $m' = m$ the solutions are given by eqn. (5); that equation, with our present numbering of units, is

$$\eta_n = A \sin \omega t \cos (n + \tfrac{1}{2})\sigma, \qquad \sigma = l\pi/N. \qquad \ldots\ldots(5\,a)$$

Eqn. (5 *a*) shows that if $m' = m$ the amplitude of the end units is never zero, whether l is odd or even. Therefore, in contrast to the chains discussed in § 2, in the present case if $m' \neq m$ all the solutions are affected, not only the ones with even l. We find that if $m' \neq m$ the equations of motion (19) to (21) can be solved with

$$\eta_n = A \sin \omega t \cos (n\sigma + \epsilon). \qquad \ldots\ldots(22)$$

Inserting this into eqn. (21) we find the same connection between ω and σ as before:

$$\omega^2 = (4k/m) \sin^2 \tfrac{1}{2}\sigma \qquad \ldots\ldots(23)$$

and introducing eqns. (22) and (23) into (19) gives the connection between ϵ and σ:

$$\tan \epsilon = \{(2m' - m)/m\} \tan \tfrac{1}{2}\sigma \qquad \ldots\ldots(24)$$

while eqn. (20) is satisfied if

$$\sigma = \frac{l\pi}{N} - \frac{\epsilon - \tfrac{1}{2}\sigma}{N}, \qquad l = 1, 2, 3, \ldots . \qquad \ldots\ldots(25)$$

Using the same arguments as in § 2, we can restrict ϵ to the range $-\tfrac{1}{2}\pi < \epsilon < \tfrac{1}{2}\pi$, and σ to $0 < \sigma < \pi$, while eqn. (23) shows that within this range all allowed values of σ represent independent modes of vibration as they all correspond to different frequencies.

Inserting (24) into (25) and solving for l gives

$$l = \frac{2N-1}{2\pi}\sigma + \frac{1}{\pi} \arctan \left(\frac{2m' - m}{m} \tan \tfrac{1}{2}\sigma \right) \qquad l = 1, 2, 3, \ldots . \qquad \ldots\ldots(26)$$

We can again find all the allowed solutions by plotting the right-hand side of eqn. (26) for all values of σ between 0 and π and selecting those which correspond to an integral l.

Because of the restriction that $\epsilon = \arctan [\{(2m' - m)/m\} \tan \tfrac{1}{2}\sigma]$ is between $-\pi/2$ and $+\pi/2$, the right-hand side is a single-valued function of σ. If $2m' > m$ the right-hand side increases monotonically with σ and when $\sigma \to \pi$ then $l \to N$. Hence there is a solution for all integral values of l less than N, and eqns. (22) to (25) thus represent all the $N-1$ solutions which we can have.

If $2m' < m$ the situation is rather similar to that in §2 for eqn. (14) when $m' < m$. By arguments similar to those used there, it can be shown that as long as $(m-2m')/m < 1/(2N-1)$ all the solutions are of the type (22), while if $(m-2m')/m > 1/(2N-1)$ then there are only $N-1$ sinusoidal solutions and one hyperbolic solution rather similar to eqn. (16). We shall not discuss this in detail as only the case when $m' > m$ is of direct interest for substituted hydrocarbons.

§4. GENERAL RELATIONS BETWEEN THE PROPERTIES OF THE SUBSTITUTED AND UNSUBSTITUTED CHAIN

We now wish to extend some of our results to other linear chains where the interaction energy is not restricted to nearest neighbours but can have any form. We shall still assume that the units of our chains are capable of rotation or translation in one direction only. We shall call a 'substituted chain' one where the mass or moment of inertia of one of the units m' differs from all the others, which we shall denote by m as before, and all the units obey the same law of interaction, while the corresponding 'unsubstituted chain' will be one which has the same number of units and obeys the same law of interaction, but the mass or moment of inertia of all its units is m.

Among the results obtained in §§2 and 3 we shall now select some which appear independent of the particular form of the interaction energy. This will make it possible to establish general connections between the properties of the substituted and the corresponding unsubstituted chain. We shall restrict ourselves to the case when $m' > m$.

(i) *All the Modes are Extended Over the Whole Chain*

The first interesting result for the substituted chain which should be generally valid is that if $m' > m$ all the modes of vibration extend over the whole chain; there is no mode which is particularly characteristic of the unit with mass or moment m'. Only if $m' < m$ is one mode localized in the neighbourhood of this different unit.

The situation would be somewhat changed if the 'different unit' differed from the others not only with respect to its mass or moment of inertia but also with respect to its interaction energy.

(ii) *Effect of the Position of the Heavy Unit*

We showed in the Introduction that the dielectric properties connected with the torsional vibrations of ketones are determined by the displacement of the CO group. We are therefore interested in the amplitude of vibration of the heavy unit as well as in the frequencies.

We have found in §§2 and 3 that if m' is in the centre of the chain, the frequencies of only half of the modes are altered and only these modes involve a displacement of the heavy unit; while if m' is at the end, all the frequencies are affected and all the modes involve a displacement of the heavy unit. This clearly follows from reasons of symmetry and should be true for any form of interaction energy.

Obviously, the behaviour of a chain whose heavy unit is between the centre and the end will be intermediate between the two extreme cases. As we have found in §§2 and 3 that these two extreme cases do not differ excessively, we expect that, if the number of units is fairly large, a change in the position of the heavy unit by a few nearest neighbour distances does not have a large effect on the properties of the chain. Therefore, while we are, in general, interested in chains whose heavy unit is near the centre, we expect that such chains behave similarly to a chain whose heavy unit is exactly in the centre and we shall derive the properties of the latter only.

(iii) *The Frequency Shift*

In the case discussed in § 2 with the heavy unit in the centre, let ω_l' denote the frequency connected with a particular value of l, and ω_l the corresponding frequency of the unsubstituted chain. Let the values of σ for the two chains be similarly denoted by σ_l' and σ_l, respectively. $\omega_l' = \omega_l$ for odd values of l, while for even l comparison of eqns. (6) and (9) gives

$$\omega_l'/\omega_l = \sin\tfrac{1}{2}\sigma_l'/\sin\tfrac{1}{2}\sigma_l \qquad \ldots\ldots(27)$$

where σ_l' is given by eqn. (11) and σ_l by (7). Inserting the value of σ_l from (7) into (11) and using (10) gives

$$\left.\begin{aligned} \tfrac{1}{2}\sigma_l &= \tfrac{1}{2}\sigma_l' + \delta/N \\ \delta &= \arctan\left[\{(m'-m)/m\}\tan\tfrac{1}{2}\sigma_l'\right]. \end{aligned}\right\} \qquad \ldots\ldots(28)$$

Let us treat eqns. (10), (11), (27) and (28) as if l were a continuously varying quantity. Inserting (28) into (27), a first order expansion in σ' gives for small values of l/N

$$\frac{\omega_l'}{\omega_l} = \frac{\frac{1}{2}\sigma_l'}{\frac{1}{2}\sigma_l'\{1+(m'-m)/Nm\}} = \frac{Nm}{(N-1)m+m'} = \frac{M}{M'}, \qquad \ldots\ldots(29)$$

where $M = Nm$ denotes the total mass or moment of inertia of the unsubstituted chain and $M' = (N-1)m + m'$ is the corresponding quantity for the substituted chain.

For $l = N$, σ is π and σ' nearly π. Therefore, as $l \rightarrow N$, ω_l'/ω_l becomes very near to unity but actually does not quite reach it. Since, further, it can be proved (cf. Appendix I) that ω_l'/ω_l increases monotonically with l we have

$$M/M' < \omega_l'/\omega_l < 1 \qquad \ldots\ldots(30)$$

where ω_l'/ω_l increases from the lower to the upper limit as l increases from 0 to N; but it must be remembered that only even integer values of l correspond to vibrations. If N is large, the allowed values of l/N are densely spaced and ω_l'/ω_l for the lowest and highest frequencies is practically equal to the lower or higher limit, respectively, in (30).

It is proved in Appendix II that the same conclusions also hold for the chain discussed in § 3 with the heavy unit at the end, except that in that case l may, of course, be odd or even.

It seems to us that these results are independent of the particular form of the interaction energy and that the latter only determines the details of how ω_l'/ω_l increases between the two limiting values. In particular, we shall assume for chains with the heavy unit in the centre that, whatever the interaction, for the odd modes $\omega_l' = \omega_l$ while for the even modes ω_l'/ω_l is between the limits indicated by (30) and, between these limits, increases with increasing ω.

If N is very large, the total mass or inertia is not altered appreciably by the substitution, $M/M' \simeq 1$ and (30) shows that in that case $\omega_l'/\omega_l \simeq 1$ for all modes of vibration. This result may be somewhat surprising, as one might perhaps have expected that there should be one frequency which is characteristic for the heavy unit and which depends on m/m' rather than on M/M'. We have found, however, that all the modes of vibration extend over the whole chain, and this explains the present result.

In the case of those ketones in which we shall be interested M/M' will range between about 0·98 and 0·75.

(iv) *The Amplitude of the Heavy Unit*

We are also interested in the mean square amplitude of vibration of the heavy unit, which will be of importance for the dielectric properties of ketones. For the centrally substituted chain of § 2 let η_{0l}' denote the displacement of the heavy unit in the course of the lth normal vibration. Only even values of l are of interest, because η_{0l}' is always zero if l is odd. It follows from the theory of normal vibrations that the various modes can be considered independently from each other. The potential energy V_l for the lth mode is

$$V_l = \tfrac{1}{2}\omega_l'^2 \sum_n m_n \eta_{nl}'^2 \qquad \ldots\ldots(31)$$

where m_n is the mass or moment of inertia of the nth unit and η_{nl}' its displacement in the course of the lth vibration. The ratios of displacements η_{nl}'/η_{0l}' are constant; from eqn. (8) we have $\eta_{nl}' = \{\cos(|n|\sigma_l' + \delta_l)/\cos\delta_l\}\eta_{0l}'$, and we shall put

$$S_l' = \sum_n m_n \cos^2(|n|\sigma_l' + \delta_l) = (m' - m)\cos^2\delta_l + m\sum_n \cos^2(|n|\sigma_l' + \delta_l) \qquad \ldots\ldots(32)$$

where the second equality holds because $m_n = m$ for all units except for the zeroth, for which it is m'. Eqn. (31) can now be written

$$V_l = \tfrac{1}{2}\omega_l'^2 \eta_{0l}'^2 S_l'/\cos^2\delta_l. \qquad \ldots\ldots(33)$$

As the frequencies of the torsional vibrations of ketones are low we shall assume that classical physics applies. In that case the time average of V_l is $\tfrac{1}{2}\boldsymbol{k}T$, and if we average over eqn. (33) we get

$$\overline{\eta_{0l}'^2} = (\boldsymbol{k}T/\omega_l'^2 S_l)\cos^2\delta_l, \qquad \ldots\ldots(34)$$

where $\overline{\eta_{0l}'^2}$ is the time average of $\eta_{0l}'^2$.

All this is clearly also valid for the unsubstituted chain if we replace m' by m. Let ω_l, σ_l, S_l and η_{0l} without primes denote the quantities referring to the unsubstituted chain; η_{0l} is the displacement of the central unit in the course of the lth vibration; $\cos\delta = 1$ if $m' = m$, and from eqn. (32) we then have

$$S_l = m\Sigma_n \cos^2 n\sigma_l \quad \text{or} \quad S_l = \tfrac{1}{2}Nm \qquad \ldots\ldots(35)$$

because the vibrational modes of the unsubstituted chain consist of an integral number of half waves so that $\cos^2 n\sigma$ averaged over all units is $\tfrac{1}{2}$. With these values eqn. (34) becomes for the unsubstituted chain

$$\overline{\eta_{0l}^2} = 2\boldsymbol{k}T/\omega_l^2 Nm \qquad \ldots\ldots(36)$$

while for the substituted chain we can write

$$\overline{\eta_{0l}'^2} = \overline{\eta_{0l}^2}\cos^2\delta_l\,\omega_l^2 S_l/\omega_l'^2 S_l' \qquad \ldots\ldots(37)$$

if $\overline{\eta_{0l}'^2}$ and $\overline{\eta_{0l}^2}$ are values for the same temperature.

We have found that, for small l/N, $\omega_l/\omega_l' \simeq M'/M$ and $\cos\delta_l \simeq 1$, while it is shown in Appendix III that $S_l/S_l' \simeq M/M'$ in this case. Therefore, for small values of l/N we have, from eqn. (37), $\overline{\eta_{0l}'^2}/\overline{\eta_{0l}^2} \simeq M'/M$. Eqn. (30) shows that if M'/M is of order unity, ω_l/ω_l' is of order unity for all l, and clearly this is also the case for S_l/S_l'. For a given N and m'/m, the variation of $\overline{\eta_{0l}'^2}/\overline{\eta_{0l}^2}$ with l is therefore mainly determined by $\cos\delta_l$. Eqns. (10) and (11) show that for a given N and l, $\cos\delta_l$ is the smaller the larger m'/m, while, for a given N and m'/m, $\cos\delta_l$ decreases from 1 to 0 as l increases from 0 to N. Therefore

$$M'/M>\overline{\eta_{0l}'^2}/\overline{\eta_{0l}^2}>0 \qquad \ldots\ldots(38)$$

and between these limits $\overline{\eta_{0l}'^2}/\overline{\eta_{0l}^2}$ decreases with increasing l, i.e. with increasing ω. It seems reasonable to assume that (38) holds independently of the particular form of the potential and that the latter only determines the details of how $\overline{\eta_{0l}'^2}/\overline{\eta_{0l}^2}$ decreases with increasing ω between the two limits.

Comparison of (38) and (30) shows that the substitution changes the amplitude of the central unit much more than it changes the frequency. If N is fairly large, the values of $\overline{\eta_{0l}'^2}/\overline{\eta_{0l}^2}$ for the lowest and highest frequencies are near to the lower or upper limit, respectively, in (38). Thus for the lowest frequencies the amplitude of the central unit is increased slightly by the substitution, while for the highest frequencies it is diminished by a large factor.

(v) *Born–Kármán Boundary Conditions*

As mentioned before, in a following paper we shall generalize our results for ω_l'/ω_l and $\overline{\eta_{0l}'^2}/\overline{\eta_{0l}^2}$ so as to make them applicable to ketones. This will make it possible to calculate approximate values for the ω_l' and $\overline{\eta_{0l}'^2}$, if the ω_l and $\overline{\eta_{0l}^2}$ are known for the unsubstituted chain. The exact calculation of the latter for the potential given by eqn. (1) is difficult if the ends of the chain are free; we shall therefore follow Pitzer and calculate the normal modes of the unsubstituted hydrocarbons by applying the Born–Kármán boundary conditions. It is clear that if N is large enough the Born–Kármán method reproduces the frequencies fairly well, but it may be worth showing that it also represents a good approximation for $\overline{\eta_{0l}^2}$.

We shall show this for a chain where the interaction is restricted to nearest neighbours. The normal modes of such a chain with free ends are represented by eqns. (5′) and (5″), while, if the Born–Kármán boundary condition is imposed, which is

$$\eta_{n+N}=\eta_n, \qquad \ldots\ldots(39)$$

then the normal modes can be written in the form

$$\eta_n=A\sin\omega t\sin n\sigma \qquad \ldots\ldots(40')$$

and

$$\eta_n=A\sin\omega t\cos n\sigma \qquad \ldots\ldots(40'')$$

with

$$\omega^2=(4k/m)\sin^2\tfrac{1}{2}\sigma \qquad \ldots\ldots(41)$$

and the values of σ which satisfy the boundary condition are

$$\sigma=l2\pi/N, \qquad l=1, 2, 3, \ldots (N-1)/2. \qquad \ldots\ldots(42)$$

It is seen that the solutions (40″) are identical with (5″), while (40′) is slightly different from (5′). But neither (5′) nor (40′) involves a displacement of the central unit; hence the Born–Kármán method gives the amplitude of the central unit exactly.

But the other units are displaced in the course of the modes represented by (5′) and (40′). Since (40′) and (5′) differ, the Born–Kármán method is not exact for the amplitudes of the units other than the central. For the amplitudes of the units near the two ends the discrepancy becomes quite considerable.

For a more complicated potential, in general, none of the Born–Kármán solutions coincides exactly with the solutions for free ends. But the central unit should be least affected by the boundary conditions and, from analogy with the simple case just discussed, we may expect that if N is large enough the Born–Kármán method represents a good approximation not only for the frequency but also for the mean square amplitude of the central unit $\overline{\eta_{0l}^2}$.

§ 5. SUMMARY OF CONCLUSIONS

We have considered linear chains of N rigid units which can execute either translational vibrations in one direction or rotational vibrations around the chain axis. The interaction energy need not be restricted to nearest neighbours.

We call a 'substituted chain' one all the units of which are equal except for one unit which is heavier. From the point of view of interaction energy the heavy unit is equivalent to the others. For a chain whose vibration is translational we denote by m' the mass of the heavy unit and by m the mass of the others; while if the vibration is rotational, m' and m denote the moments of inertia of the two kinds of units around the chain axis.

The corresponding 'unsubstituted chain' has the same number of units and the same interaction energy, but all the units are equal. In the case of translational vibration their mass and in the case of rotational vibration their moment is m.

(i) If N is odd and the central unit of the substituted chain is the heavy one, the following conclusions hold: (*a*) All the vibrational modes extend over the whole chain: none is localized around the heavy unit. (*b*) There is a one-to-one correspondence between the modes of the substituted and the unsubstituted chain. We denote by $\overline{\eta_{0l}'^2}$ the mean square amplitude of the central unit and by ω_l' the frequency for the lth mode of the substituted chain, and by $\overline{\eta_{0l}^2}$ and ω_l the same quantities for the corresponding mode of the unsubstituted chain. $\overline{\eta_{0l}'^2}$ and $\overline{\eta_{0l}^2}$ are values for the same temperature. For half of the modes the central unit is stationary, i.e. $\overline{\eta_{0l}'^2}=\overline{\eta_{0l}^2}=0$, and $\omega_l'=\omega_l$, while for the other modes

$$Nm/\{(N-1)m+m'\}<\omega_l'/\omega_l<1$$

and
$$\{(N-1)m+m'\}/Nm>\overline{\eta_{0l}'^2}/\overline{\eta_{0l}^2}>0$$

and between these limits, for any particular set of N, m and m', ω_l'/ω_l increases and $\overline{\eta_{0l}'^2}/\overline{\eta_{0l}^2}$ decreases with increasing ω_l. It is seen that for translation $(N-1)m+m'$ and Nm represent the total masses of the two chains, while in the case of rotation they represent the total moments of inertia. The ω_l' and $\overline{\eta_{0l}'^2}$ can thus be calculated approximately if the ω_l and $\overline{\eta_{0l}^2}$ are known. (*c*) If N is large, the application of the Born–Kármán boundary condition to the unsubstituted chain provides a good approximation not only for the ω_l but also for the $\overline{\eta_{0l}^2}$.

(ii) If the heavy unit of the substituted chain is not in the central position, with N odd or even, some of the foregoing conclusions still hold. They all hold approximately if N is large and the heavy unit is near the centre, provided that $\overline{\eta_{0l}'^2}$ always refers to the amplitude of the heavy unit and $\overline{\eta_{0l}^2}$ to the amplitude of the corresponding unit in the unsubstituted chain.

(iii) We have also briefly considered substituted chains with $m' < m$, although this is of no interest in connection with substituted hydrocarbons. In this case one mode of vibration is different from the others; if $m' \ll m$, then in the course of this mode only the one light unit vibrates and the rest of the chain remains stationary.

APPENDIX I

In connection with eqns. (27) and (28), we wish to prove that ω_l'/ω_l increases monotonically with l in the range $0 < l < N$. Introducing the value of $\frac{1}{2}\sigma$ from (28) into (27) we get, dropping the suffix l,

$$\frac{\omega'}{\omega} = \frac{\sin \frac{1}{2}\sigma'}{\sin \frac{1}{2}\sigma' \cos \delta/N + \cos \frac{1}{2}\sigma' \sin \delta/N}.$$

Using eqn. (10) this can be written

$$\frac{\omega'}{\omega} = \frac{1}{\cos \delta/N + \{(m'-m)/m\}(\sin \delta/N)/\tan \delta}.$$

On the right-hand side of this last equation, the first term in the denominator clearly decreases with δ. So does the second term, because $m' > m$, $N > 1$ and $0 < \delta < \frac{1}{2}\pi$. Thus the denominator decreases and ω'/ω increases with δ. As δ increases with σ' and therefore with l, we have proved that ω_l'/ω_l increases monotonically with l in the entire range.

APPENDIX II

We shall now consider the frequencies of the chain discussed in § 3, with the heavy unit at the end. The symbols with primes will now refer to this chain, while those without primes refer to the corresponding unsubstituted chain as before. Comparison of eqns. (23) and (6) again gives

$$\omega_l'/\omega_l = \sin \tfrac{1}{2}\sigma' / \sin \tfrac{1}{2}\sigma \qquad \ldots\ldots \text{(A 1)}$$

and introducing the fact that $\frac{1}{2}\sigma = l\pi/2N$ into eqn. (25) and solving for $\frac{1}{2}\sigma$ we get, using (24)

$$\tfrac{1}{2}\sigma = \tfrac{1}{2}\sigma' + \tau \qquad \ldots\ldots \text{(A 2)}$$

$$\tau = \frac{1}{2N}\left[\arctan\left(\frac{2m'-m}{m}\tan \tfrac{1}{2}\sigma'\right) - \tfrac{1}{2}\sigma'\right]. \qquad \ldots\ldots \text{(A 3)}$$

We shall now prove that the results obtained for ω_l'/ω_l for the centrally substituted chain also hold when the substitution is at the end, i.e. that $M/M' < \omega_l'/\omega_l < 1$ and that within these two limits ω_l'/ω_l increases with increasing ω_l. In the present case only integral values of l have a physical meaning, but it will again be convenient to treat eqns. (A 1) to (A 3) as if they were valid for all values of l between 0 and N; we can then calculate the values of ω_l'/ω_l for $l=0$ and $l=N$, and prove that between these two limits ω_l'/ω_l increases monotonically with l and therefore with ω_l.

We have shown in § 3 that for $l=N$, $\sigma'=\pi$. As σ is also equal to π in this case, eqn. (A 1) shows that, omitting the suffix l, $\omega'/\omega = 1$ if $l=N$. To calculate ω'/ω for the lower limit, i.e. for small values of l and σ', we insert (A 2) and (A 3) into (A 1) and expand in powers of σ'. Maintaining terms of first order only, we get

$$\frac{\omega'}{\omega}=\frac{\frac{1}{2}\sigma'}{\{1-1/2N+(2m'-m)/2Nm\}\frac{1}{2}\sigma'}=\frac{Nm}{(N-1)m+m'}=\frac{M}{M'}.$$

In other words we get the same limits for ω'/ω as in (30).

We still have to prove that ω'/ω increases with l in the entire range. Introducing the value of $\frac{1}{2}\sigma$ from (A 2) into (A 1) we can write

$$\frac{\omega'}{\omega}=\frac{1}{\cos\tau+\sin\tau/\tan\frac{1}{2}\sigma'}. \qquad \ldots\ldots(\text{A}\,4)$$

As $m'>m$ and $0<\frac{1}{2}\sigma'<\frac{1}{2}\pi$, eqn. (A 3) shows that τ increases and therefore $\cos\tau$ decreases with increasing σ'. If τ were proportional to σ' then $\sin\tau/\tan\frac{1}{2}\sigma'$ would certainly also decrease with σ'. Actually τ increases more slowly than proportional to σ' and therefore *a fortiori* $\sin\tau/\tan\frac{1}{2}\sigma'$ decreases with σ'. Eqn. (A 4) thus shows that ω'/ω increases monotonically with σ' and therefore with l in the entire range.

APPENDIX III

To prove the statement following eqn. (37), we wish to calculate S_l/S_l' for small values of l/N. We shall consider a chain with large N, because the larger N, the smaller values of l/N are allowed.

For small l/N, $\sigma'\ll 1$ and the sum in eqn. (32) can be replaced by an integration. As the slope of $\cos^2(|n|\sigma'+\delta)$ has a discontinuity at $n=0$, we integrate from 0 to $+\frac{1}{2}N$ and multiply by 2 in order to take account of the negative values of n. Omitting the suffix l, we then have

$$\begin{aligned}\sum_n\cos^2(|n|\sigma'+\delta)&=2\int_0^{N/2}\cos^2(n\sigma'+\delta)\,dn\\&=\frac{1}{\sigma'}[n\sigma'+\delta+\sin(n\sigma'+\delta)\cos(n\sigma'+\delta)]_{n=0}^{n=N/2}\\&=\frac{1}{\sigma'}(\tfrac{1}{2}N\sigma'-\sin\delta\cos\delta) \qquad \ldots\ldots(\text{A}\,5)\end{aligned}$$

because, from eqn. (11), $\sin(\frac{1}{2}N\sigma'+\delta)=0$. Inserting eqn. (A 5) into (32) we have

$$S_l'=\tfrac{1}{2}Nm-(m/\sigma')\sin\delta\cos\delta+(m'-m)\cos\delta. \qquad \ldots\ldots(\text{A}\,6)$$

As $\sigma'\ll 1$, we can express $\sin\delta$ and $\cos\delta$ as a power series in σ'. From eqn. (10) we have, up to first order in σ', $\sin\delta=\{(m'-m)/2m\}\sigma'$; $\cos\delta=1$. Inserting these values into eqn. (A 6) and comparing with (35) we get

$$\frac{S_l}{S_l'}=\frac{\frac{1}{2}Nm}{\frac{1}{2}(N-1)m+m'}=\frac{M}{M'}\quad\text{for}\quad l/N\ll 1.$$

REFERENCES

Born, M., 1942, *Proc. Phys. Soc.*, **54**, 362.

Fröhlich, H., 1944, *Trans. Faraday Soc.*, **40**, 498; 1949, *Theory of Dielectrics* (Oxford; Clarendon Press), p. 113.

Kirkwood, J. G., 1939, *J. Chem. Phys.*, **7**, 506.

Müller A., 1940, *Proc. Roy. Soc.* A, **174**, 137.

Oldham, J. W. H., and Ubbelohde, A. R., 1939, *Trans. Faraday Soc.*, **35**, 328.

Pitzer, K. S., 1940, *J. Chem. Phys.* **8**, 711.

Fluorescence of Dyestuff Solutions: Viscosity and Temperature Effects

By N. R. TAWDE and N. RAMANATHAN*
Spectroscopic Laboratories, The Institute of Science, Bombay

MS. received 11th June 1951

ABSTRACT. The effect of viscosity and temperature of the medium on the polarization of the fluorescent light emitted by some dyestuff solutions when excited by linearly polarized monochromatic light is investigated by the visual and photoelectric methods. The variations in the polarization caused by temperature are found to depend on the concentration and molecular weight of the dyestuff.

§ 1. INTRODUCTION

AVAILABLE literature on the various branches of the fluorescence of liquids and solutions reveals that the aspects of the study of fluorescence dealing particularly with the polarization and lifetime of the excited states of fluorescent molecules have not received systematic attention on a wide scale. By the work of Weigert (1921), Wawilow and Lewshin (1923), Perrin (1929), Mitra (1939), Choudhuri (1944) and others it has been established that the fluorescent light emitted by dyestuffs in solution is partially polarized and that the degree of polarization depends on the viscosity and temperature of the medium and the wavelength of the exciting radiations, besides other factors. In the previous work, however, there appears to be some amount of apparently conflicting material in the different experimental results on the one hand and in the experimental results and theory on the other. Moreover, it was felt that almost all the study has been confined to practically the same compounds, and little regularity or system seems to have been followed in their choice. In view of this and the expectation that observations on the polarization of fluorescence may give insight into the mechanism of the fluorescence phenomenon in general it was thought desirable to undertake investigations on solutions of some dyestuffs which have not so far been studied systematically and which represent different dyestuff groups. After preliminary tests on a large number of dyestuffs, Acridine Orange R, Safranine 6B, Thioflavine T and Aurophenine O were chosen as the dyestuffs which emitted fluorescent light of intensity sufficient for observation and reliable precision and also maintained their fluorescent characteristics constant over a fairly long period. This ensured that no decomposition was taking place in the course of observations. This paper contains our findings concerning the effects of viscosity and temperature of the medium on the degree of polarization of the fluorescent light emitted by these dyestuffs in solution when excited by linearly polarized monochromatic light.

§ 2. EXPERIMENTAL

A Philips 'Philora' 400-watt mercury arc lamp was used as the source of radiation. The wavelengths 5461 Å or 4358 Å was isolated by using the one or the other of the two filters recommended by Vaidya (1934). This monochromatic light, limited by a square aperture, was focused on the dyestuff solution contained in a rectangular glass cell with optically perfect sides after passing through a nicol which rendered it plane polarized in a vertical plane. The fluorescent light thus obtained was in the form of a rectangular patch and was practically parallel in the neighbourhood of the focus to which the observations were confined. For observing the effects at different temperatures the solution was kept in a small glass bulb in a water bath whose temperature could be maintained at any desired value.

---

* Now at the Victoria Jubilee Technical Institute, Bombay, 19.

Polarization measurements were made in a direction at right angles to the plane containing the direction of propagation and the direction of vibration of the incident light. The degree of polarization was measured by the well-known visual method of Cornu (Lotmar 1938, Krishnan 1939), and confirmation of the results was obtained by the photoelectric method (Ananthakrishnan 1934). When the degree of polarization was very small, measurements were made with a Savart plate and a pile of glass plates in the usual way (Wood 1943).

§ 3. RESULTS

(i) *The Effect of Viscosity on the Polarization*

Doubly distilled glycerine kept free from moisture was used as a solvent for the dyestuffs. The feeble scattered intensities by glycerine or glycerine–water mixtures were not found to have any appreciable effect on the polarization of the fluorescent light emitted by the dyestuff solutions. Also no fluorescence of glycerine or glycerine–water mixtures could be detected when they were excited by 5461 Å or 4358 Å lines. As the degree of polarization was far from unity for all the solutions, and the observations were confined to the neighbourhood of the focus of the incident light, where the rays were practically parallel, no corrections were necessary for the convergence of the incident rays (Krishnan 1925, Ramakrishna Rao 1927). The results of measurements of the degree of polarization of fluorescence of Safranine 6B are shown in fig. 1. In other cases results follow the same trend as illustrated by figs. 2 to 4. The viscosity values were calculated from the extensive measurements of Sheely (1932) by graphical interpolation.

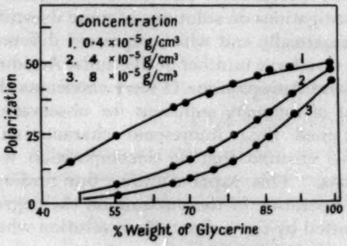

Fig. 1. Safranine 6B.

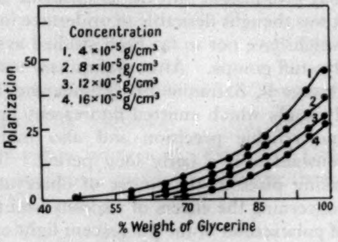

Fig. 2. Acridine Orange R.

(ii) *The Effect of Temperature on the Polarization*

The values of the degree of polarization for Acridine Orange R at different temperatures are recorded in fig. 5. The results in the case of other dyestuffs are given in figs. 6 to 8. They show that the degree of polarization decreases with temperature. But since the viscosity of the medium decreases with temperature and decreases in viscosity diminish the value of the polarization, it is necessary to know whether temperature alone influences the polarization

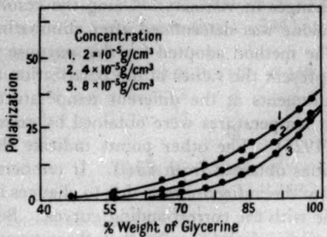

Fig. 3. Aurophenine O.

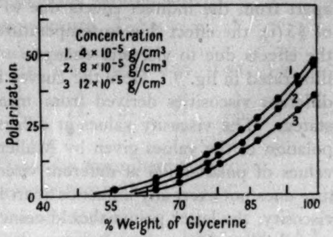

Fig. 4. Thioflavine T.

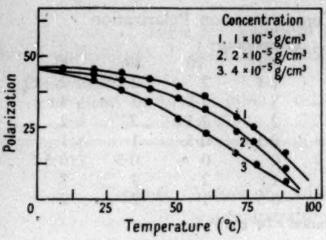

Fig. 5. Acridine Orange R.

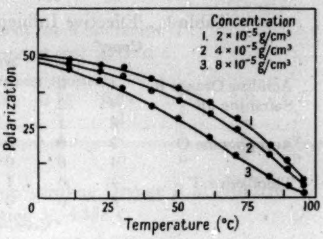

Fig. 6. Safranine 6B.

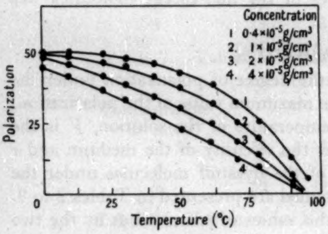

Fig. 7. Aurophenine O.

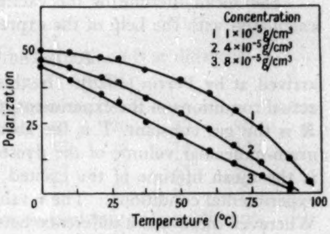

Fig. 8. Thioflavine T.

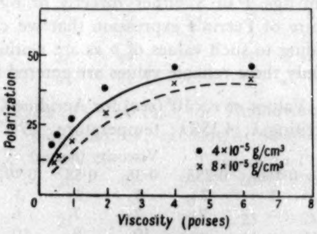

Fig. 9. Safranine 6B.

apart from the indirect effects due to changes in viscosity. Using the results of § 3 (i), the effect due to temperature alone was determined after eliminating the effects due to viscosity changes. The method adopted for this purpose is illustrated in fig. 9. Here the curves represent the values of the polarization at different viscosities derived from measurements at the different temperatures stated. The viscosity values at different temperatures were obtained by extrapolation of the values given by Muller (1925). The other points indicate the values of polarization at different viscosities obtained from § 3 (i). If temperature does not exert any influence apart from the indirect effects due to changes in viscosity, the latter points should coincide with the corresponding curves. But actually the temperature effect on polarization is slightly greater than the viscosity effect, although the viscosity is the same in both cases. The extent of the temperature effect for the various dyestuffs used is shown in table 1.

Table 1. Effective Influence of Temperature on Polarization

	Conc.*	Temperature (° c)						
		30	40	50	60	70	80	90
Acridine Orange R	4	0	0	1	1·5	2	2	2
Safranine 6B	4	2	3	3	3	3·5	3	3
	8	1	1	1	2	2·5	2	2
Aurophenine O	2	0	0	0	0·5	0·5	1	1
	4	0	0	0	0	0	0·5	0·5
Thioflavine T	4	0	1	1	1	2	3	3
	8	0	0	0·5	0·5	1	2	2

* Conc. = concentration × 10^5 g/cm^3.

(iii) *The Mean Lifetime of the Excited States of the Fluorescent Molecules*

The mean lifetime of the excited states of the fluorescent molecules was calculated with the help of the expression

$$p = p_0/[1 + (1 - \tfrac{1}{3}p_0)\boldsymbol{R}T\tau/V\eta]$$

arrived at by Perrin (1929). In this, p is the degree of polarization under the actual conditions of the experiment, p_0 is the maximum value of the polarization, $\boldsymbol{R}$ is the gas constant, T is the absolute temperature of the solution, V is the gram-molecular volume of the dyestuff, η is the viscosity of the medium and τ is the mean lifetime of the excited states of the dyestuff molecules under the experimental conditions. The τ-values obtained are presented in Tables 2 to 9. Wherever there was a difference between the values of p arrived at by the two methods, that of the photoelectric method was preferred for calculations as it is free from the personal element inherent in the visual method. The values of p_0 were obtained from figs. 1 to 8 either directly or by extrapolation. It is obvious from the nature of Perrin's expression that we can justifiably rely on values of τ corresponding to such values of p as are neither very near to p_0 nor very near to zero. Only these reliable values are entered in the tables.

Table 2. Values of $\tau \times 10^8$ (sec) for Acridine Orange R;
exciting λ: 4358 Å; temperature: 27·5° c

Concentration × 10^5 g/cm^3	Viscosity (poises) 0·117	0·160	0·235	0·36	0·58	0·99	1·83	3·9	6·2
4	3	3	3	3	3	3	3	3	3
8	–	–	7	7	7	6	7	6	6
12	–	–	–	10	9	10	10	10	10
16	–	–	–	–	13	13	13	13	13

Table 3. Values of $\tau \times 10^9$ (sec) for Safranine 6B; exciting λ: 5461 Å; temperature: 27·5° c

Concentration	Viscosity (poises)										
$\times 10^5$ g/cm^3	0·036	0·063	0·117	0·160	0·235	0·36	0·58	0·99	1·83	3·9	6·2
0·4	3	2	2	2	2	2	3	2	3	3	–
4	–	24	23	24	24	23	23	23	23	21	22
8	–	–	48	47	47	47	48	48	47	45	45

Table 4. Values of $\tau \times 10^8$ (sec) for Aurophenine O; exciting λ: 4358 Å; temperature: 27·5° c

Concentration	Viscosity (poises)								
$\times 10^5$ g/cm^3	0·117	0·160	0·235	0·36	0·58	0·99	1·83	3·9	6·2
2	5	5	5	4	5	4	5	5	5
4	–	–	10	9	9	8	10	8	9
8	–	–	–	–	20	18	18	18	18

Table 5. Values of $\tau \times 10^8$ (sec) for Thioflavine T; exciting λ: 4358 Å; temperature: 27·5° c

Concentration	Viscosity (poises)								
$\times 10^5$ g/cm^3	0·117	0·160	0·235	0·36	0·58	0·99	1·83	3·9	6·2
4	2	2	2	1	2	2	2	2	2
8	–	4	4	3	4	4	4	4	4
12	–	–	6	5	6	6	6	6	6

Table 6. Values of $\tau \times 10^9$ (sec) for Acridine Orange R at different temperatures; exciting λ: 4358 Å

Concentration	Temperature (°c)						
$\times 10^5$ g/cm^3	30	40	50	60	70	80	90
1	8	8	8	9	8	8	9
2	17	17	16	17	17	16	17
4	33	32	33	33	34	31	34

Table 7. Values of $\tau \times 10^9$ (sec) for Safranine 6B at different temperatures; exciting λ: 5461 Å

Concentration	Temperature (°c)						
$\times 10^5$ g/cm^3	30	40	50	60	70	80	90
2	13	14	12	12	12	14	14
4	27	28	26	24	24	24	30
8	50	49	52	49	49	53	56

Table 8. Values of $\tau \times 10^9$ (sec) for Aurophenine O at different temperatures; exciting λ: 4358 Å

Concentration	Temperature (°c)						
$\times 10^5$ g/cm^3	30	40	50	60	70	80	90
0·4	10	9	9	9	9	9	9
1	21	23	24	22	24	21	23
2	46	49	45	47	48	43	42
4	94	91	92	91	94	90	91

Table 9. Values of $\tau \times 10^9$ (sec) for Thioflavine T at different temperatures; exciting λ: 4358 Å

Concentration	Temperature (°c)						
$\times 10^5$ g/cm^3	30	40	50	60	70	80	90
1	5	5	6	5	6	6	6
4	21	22	22	23	21	23	23
8	45	44	46	44	44	44	49

Here mention must be made of the remarks of Pringsheim (1949) about the value of V in the equation of Perrin. According to him V is not the volume of the isolated dye molecule but that of the molecule with its solvation envelope, so that it differs in different solvents. But if the dissolved molecules retain the possibility of rotating within the sphere of the surrounding solvent molecules, one is justified in substituting the volume of the dye molecule for V in the above equation. In order to test this point in the case of dyestuffs used by us, we plotted a relation betwen $1/p$ and $1/\eta$, and this was found to be linear in every case. This can only mean that V is a constant, and it should represent the volume of the dye molecule as far as the cases studied here are concerned.

§ 4. DISCUSSION AND CONCLUSIONS

It is found that in all the cases studied the polarization increases with viscosity whatever the concentration of the dyestuff, and vanishes, or tends to vanish, at low viscosities. At high viscosities there is a tendency for the polarization to reach a maximum. This presumption is justified by the fact that values of p_0 extrapolated from the results of § 3 (i) are in agreement with those actually observed in § 3 (ii). The polarization also decreases with temperature and becomes, or tends to become, zero at high temperatures.

The vanishing of the polarization can be interpreted as complete isotropy of the fluorescent light, and hence all the directions of the oscillator are equally probable. The attainment of the maximum value p_0 means that the emitting molecule remains in its own orientation and does not undergo any rotation in the interval between absorption and emission of radiation. The extent to which temperature influences the polarization is given in § 3 (i). This influence is to be expected because, on the principle of the equipartition of kinetic energy, each degree of freedom of the molecule is associated with kinetic energy equal to $\frac{1}{2}\boldsymbol{R}T/N$. The higher the temperature the greater will be the rotational energy imparted, thus bringing about a state of isotropy as regards the resulting fluorescent light, and hence a decrease in polarization. It is, however, to be noted that the net effect due to temperature, where it exists, is much smaller than the effect due to changes in viscosity. Obviously, therefore, in the range observed, viscosity has a far greater influence than temperature on the rotational motions of the molecules.

The ultimate effective contribution of temperature alone to polarization seems to depend also on the concentration of the dyestuff as seen from the results obtained for Safranine 6B, where it is greater for the concentration 4×10^{-5} g/cm^3 than for the concentration 8×10^{-5} g/cm^3 for the same viscosity. Though this effect is not observed for all the cases studied, one could expect the observed dependence of it on concentration, for at lower concentrations of the dyestuff the probability of collisions with neighbouring molecules is much less, and thus there is greater freedom for the molecules to rotate. It may also be noticed that for the same concentration of two dyestuffs the effect due to temperature appears to be greater for the dyestuff with lower molecular weight. This can be verified from the negligible influence of temperature obtained for Aurophenine O (molecular weight 680) in comparison with that for Acridine Orange R (molecular weight 377), in which a measurable effect is observed at high temperatures. Similarly, Safranine 6B (molecular weight 364·5) and Thioflavine T (molecular weight 318·5), which are comparable in molecular weights to Acridine Orange R, exhibit quite a noticeable effect due to temperature. Hence the molecular rotations of heavier molecules are affected predominantly by viscosity, and temperature effect is almost negligible. The lighter the molecule the more appreciable becomes the effect of temperature.

The mean lifetime of excited states of the molecules remains practically constant at all viscosities and temperatures. To discuss this result, the relation $\tau_1/\tau_2=I_1/I_2$ (Pringsheim 1949), where I_1, τ_1, I_2, τ_2 are the fluorescence intensities and lifetimes under two different conditions, is helpful. The constancy of lifetime, on the basis of this expression, means that the intensity of the fluorescent light remains the same at all viscosities and temperatures employed in this investigation.

In a fluorescent dyestuff solution collisions are likely to occur not only between molecules of the dyestuff but also betwen the dyestuff molecules and the molecules of the solvent. Perrin (1930) has shown, however, that a dyestuff molecule activated by the absorption of light is practically unaffected by the presence of the solvent molecules irrespective of their number or the collisions they may cause, and that only collisions between dyestuff molecules are effective. Since the intensity of the fluorescent light depends on the number of molecules activated and de-activated in a given time, its constancy indicates that these numbers of activations and de-activations are not affected by changes in viscosity or temperature. One would expect that at lower viscosities or higher temperatures, when the translational energy of the molecules is likely to increase, the chances of collisions of an activated molecule with normal ones of the same kind will also increase and the probability of de-activation by emission of radiation will diminish, thus bringing about a slight decrease in intensity. Since, in our case, invariability of intensity follows from the constancy of mean lifetime, we have to conclude that either the chances of collisions are unaffected by viscosity or temperature changes or that the mean lifetime is so small compared with the mean time interval between two collisions or effective perturbations that the excited molecule re-emits the light before a transfer of energy into other channels can possibly take place. This is unlike the rotational energy of the molecules, which, mainly, are influenced by viscosity or temperature as shown by the observed dependence of the polarization on these factors.

It is evident from all the tables of § 3 that the concentration of the dyestuff plays a very significant role in the phenomenon of fluorescence as it affects, to a great extent, the polarization and mean lifetime of excited states of the fluorescent molecules. This aspect of the fluorescence mechanism will be examined in a later paper.

ACKNOWLEDGMENTS

One of the authors (N.R.) records his grateful thanks to the University of Bombay for the award of a Research Studentship which made this investigation possible. The authors are also indebted to Principal B. B. Deshpande of the Ramnarain Ruia College for the loan of a double image prism, to Mr. G. K. Mehta, the Research Assistant, for his helpful co-operation, and to Mr. N. Ganesan for translating papers in French into English.

REFERENCES

Ananthakrishnan, R., 1934, *Proc. Indian Acad. Sci.*, **1**, 201.
Choudhuri, K., 1944, *Indian J. Phys.*, **18**, 74.
Krishnan, K. S., 1925, *Phil. Mag.*, **50**, 697.
Krishnan, R. S., 1939, *Proc. Indian Acad. Sci.* A, **9**, 303.
Lotmar, W., 1938, *Helv. Chim. Acta*, **21**, 792.
Mitra, S. M., 1939, *Indian J. Phys.*, **13**, 349.
Muller, E., 1925, *Landolt–Bornstein Physikalische Chemische Tabellen* (Berlin: Springer).
Perrin, F., 1929, *Ann. Phys., Paris*, **12**, 169; 1930, *Chem. Rev.*, **7**, 231.
Pringsheim, P., 1949, *Fluorescence and Phosphorescence* (New York: Interscience).
Ramakrishna Rao, 1927, *Indian J. Phys.*, **2**, 61.
Sheely, M. L., 1932, *Industr. Engng. Chem.*, **24**, 1060.
Vaidya, B. K., 1934, *J. Univ. Bombay*, **3**, 141.
Wawilow, S. I., and Lewshin, W. L., 1923, *Z. Phys.*, **16** (ii), 135.
Weigert, F., 1921, *Verh. Dtsch. Phys. Ges.*, **23**, 100.
Wood, R. W., 1943, *Physical Optics*, 3rd Edition (London: Macmillan).

Optical Transmission of Certain Colloidal Solutions under Relaxation Conditions

By G. KLEIN[*]
Birkbeck College, London

Communicated by R. Fürth; MS. received 28th August 1951

ABSTRACT. Formulae are derived for the variation in time of transmission of light through dilute colloidal solutions of uniaxial particles which are initially orientated by an external electric or magnetic field from the instant the field is removed. Two cases are considered: (i) particles opaque and large compared with the wavelength of light, and (ii) metallic particles small compared with the wavelength.

§1. INTRODUCTION

Particles in colloidal solution, which are affected by a constant external field in such a manner that each particle is acted on by a couple, will, owing to their thermal motion, have orientations in accordance with a Boltzmann–Maxwell statistical equilibrium distribution. If the field is now suddenly removed, the particles are subject only to the random impacts from the medium molecules—they describe 'free' translational and rotational Brownian motion—and eventually all orientations are equally likely. In the interval, the transmission of light through the solution in any given direction will vary and depend at any instant only on the average orientation of the particles, assumed non-spherical. It is clear that if the initial concentration of the particles is uniform the translational Brownian motion may in this connection be disregarded.

The description of free rotational Brownian motion is mathematically equivalent to that of uniform diffusion of a representative point, or points, on the surface of a unit sphere for which, referred to fixed axes, the equation is

$$\frac{\partial f}{\partial t}=D\left\{\frac{1}{\sin\theta}\frac{\partial}{\partial\theta}\left(\sin\theta\frac{\partial f}{\partial\theta}\right)+\frac{1}{\sin^2\theta}\frac{\partial^2 f}{\partial\phi^2}\right\}, \qquad \ldots\ldots(1)$$

---

[*] Now at Université Libre, Brussels.

obtained by expressing the general diffusion equation in polar coordinates and taking the radial coordinate as constant. The solution of this equation for the particular initial Boltzmann distribution is required, and from it averages related to the orientations at any instant are to be calculated. What averages are taken to determine the transmission of light depends on the assumptions made as to how the light is lost: two distinct cases will be considered below.

The diffusion coefficient in equation (1) is to be taken as

$$D=kT/\beta. \qquad \ldots\ldots(2)$$

(Einstein 1906, Perrin 1925, 1926, 1934, 1936, Gans 1928) where k is Boltzmann's constant, T the absolute temperature of the medium, and $1/\beta$ is the rotational mobility of a particle about any line through its centre perpendicular to its axis, which will depend only on the shape and size of the particle and on the viscosity η of the medium. For instance, for a sphere of radius a under conditions when Stokes' law applies, $\beta=8\pi\eta a^3$, where one would take some particular diameter as axis; for a very flat, disc-like oblate spheroid, $\beta=(32/3)\eta b^3$, where b is the radius of its largest cross section. These values are special cases of the formulae for an ellipsoid of revolution given in Perrin's (1934) and Gans' (1928) papers.

The following treatment was prompted by an experimental investigation by Stott (1949). A particular relaxation problem of the kind considered here has been studied earlier by Elmore (1941).

.B
5
2

§ 2. SOLUTION OF THE DIFFUSION EQUATION

Using the variable

$$z=\cos\theta, \qquad \ldots\ldots(3)$$

the solution of equation (1) can be expressed in terms of tesseral harmonics,

$$f(z,\phi;\,t)=\frac{1}{4\pi}\sum_0^\infty A_nP_n(z)\exp\{-n(n+1)Dt\}$$

$$+\frac{1}{2\pi}\sum_1^\infty\exp\{-n(n+1)Dt\}\sum_1^n(A_{nm}\cos m\phi+B_{nm}\sin m\phi)P_n{}^m(z), \qquad \ldots(4)$$

where the constants depend only on the initial conditions:

$$A_n=(2n+1)\int_0^{2\pi}\int_{-1}^1 P_n(z)f(z,\phi;0)\,dz\,d\phi, \qquad \ldots\ldots(5)$$

$$A_{nm}+iB_{nm}=(2n+1)\frac{(n-m)!}{(n+m)!}\int_0^{2\pi}\int_{-1}^1 e^{im\phi}P_n{}^m(z)f(z,\phi;0)\,dz\,d\phi. \qquad \ldots\ldots(6)$$

Here $z=\cos\theta$ is the projection of unit length along the axis of a particle on a fixed direction OZ; ϕ is the angle between the plane containing the axis and the parallel to OZ through the centre of the particle and some fixed plane containing OZ; $f(z,\phi;t)$ is the probability per unit solid angle of the axis having at time t an orientation within a small solid angle $dz\,d\phi$ in the direction (θ,ϕ).

Since $f(z,\phi;t)$ is a probability distribution function,

$$1=\int_0^{2\pi}\int_{-1}^1 f(z,\phi;t)\,dz\,d\phi=A_0, \qquad \ldots\ldots(7)$$

and the average at any time t of a function $F(z,\phi)$ associated with the orientation of the axis is

$$\overline{F}=\int_0^{2\pi}\int_{-1}^1 F(z,\phi)f(z,\phi;t)\,dz\,d\phi. \qquad \ldots\ldots(8)$$

The averages of the simplest form are

$$\overline{P_n(\cos\theta)} = \frac{1}{2n+1} A_n \exp\{-n(n+1)Dt\}. \qquad \ldots\ldots(9)$$

When there is azimuthal symmetry about the direction parallel to OZ, the double sum in (4) and the constants (6) vanish; in such a case the distribution may be denoted by $f(z;t)$. The following initial conditions lead to distributions of this kind.

(i) Initial orientation *parallel* to a fixed direction. Taking the fixed direction as OZ, and measuring θ from it, $f(z;0)$ may be considered as a delta function vanishing except for $z=1$. Thus from (5), with (7),

$$A_n = (2n+1)P_n(1) = 2n+1. \qquad \ldots\ldots(10)$$

(ii) Initial orientation *perpendicular* to a fixed direction. Taking the fixed direction again as OZ, one finds similarly,

$$A_n = (2n+1)P_n(0), \qquad \ldots\ldots(11)$$

the constants vanishing for odd n.

(iii) Initial electric field, parallel to OZ, and polarized particles (or magnetic field and paramagnetic particles). Here

$$f(z;0) = \frac{\xi}{4\pi\sinh\xi} e^{\xi z}, \qquad \ldots\ldots(12)$$

$$A_n = \frac{2n+1}{2}\frac{\xi}{\sinh\xi}\int_{-1}^{1} e^{\xi z} P_n(z)\,dz \qquad \ldots\ldots(13)$$

$$= (2n+1)\frac{1}{\sinh\xi}(\tfrac{1}{2}\pi\xi)^{1/2} I_{n+\frac{1}{2}}(\xi), \qquad \ldots\ldots(14)$$

where the last function is a modified Bessel function of the first kind. In particular,

$$A_1 = 3(\coth\xi - \xi^{-1}), \qquad \ldots\ldots(15)$$

$$A_2 = 5\{1 - 3\xi^{-1}(\coth\xi - \xi^{-1})\}. \qquad \ldots\ldots(16)$$

From (15) and (9) follows

$$\overline{\cos\theta} = (\coth\xi - \xi^{-1})\, e^{-2Dt}. \qquad \ldots\ldots(17)$$

The distribution (12) was considered by Debye (1929) in the theory of the dispersion of the dielectric constant. Here it applies to a Brownian particle which has an electric moment μ along its axis and is at time $t=0$ released from a constant electric field F_0 along OZ; (12) is the original statistical equilibrium distribution with

$$\xi = \mu F_0/kT. \qquad \ldots\ldots(18)$$

Since the mobility of the medium molecules is very much larger than that of the Brownian particles, the relaxation time of the polarization of the medium (cf. eqn. (17) applied to medium molecules) will be very small compared with the intervals in which the distribution of orientations of the Brownian particles appreciably changes owing to the molecular impacts. Hence the particles may be considered 'free' and (1) holds practically as soon as the field is removed. The mutual electric influence of the Brownian particles themselves can be neglected if their number density is sufficiently small.

(iv) Initial magnetic field, parallel to OZ, and diamagnetic particles. Here

$$f(z\,;0)=(\alpha/4\pi E_{\alpha})\exp(-\alpha^2 z^2), \qquad \ldots\ldots(19)$$

where

$$E_{\alpha}=\int_0^{\alpha}\exp(-x^2)\,dx\,; \qquad \ldots\ldots(20)$$

$$A_{2r}=(4r+1)\frac{\alpha}{E_{\alpha}}\int_0^1 P_{2r}(z)\exp(-\alpha^2 z^2)\,dz, \qquad \ldots\ldots(21)$$

$$A_2=-\frac{5}{2}\left\{1-\frac{3}{2}\frac{1}{\alpha^2}+\frac{3}{2}\frac{\exp(-\alpha^2)}{\alpha E_{\alpha}}\right\}. \qquad \ldots\ldots(22)$$

All A_n of odd suffix vanish. This distribution arose in the experimental research by Stott (1949) on disc-shaped colloidal graphite particles which exhibit diamagnetism. (19) is the statistical equilibrium distribution under a constant magnetic field H_0 along OZ, and

$$\alpha^2=\tfrac{1}{2}(\chi_1-\chi_2)H_0^{\,2}V/kT \qquad \ldots\ldots(23)$$

where V is the volume of each particle, and $-\chi_1$, $-\chi_2$ are the susceptibilities normal to and in the plane of each disc, respectively.

For large original fields, cases (iii) and (iv) become cases (i) and (ii), respectively.

It may be noted in passing that since equation (1) has the same form as the equation of heat conduction in a uniform thin spherical shell, solution (4) also represents the temperature distribution for given initial conditions. Thus (10) and (11) correspond, respectively, to cases where an instantaneous point source of heat, and an instantaneous uniform line source of heat along a great circle are applied to the shell.

§ 3. SUSPENSIONS OF VERY LARGE PARTICLES

When the size of the particles is large compared with the wavelength of light, and they are considered opaque, it may be assumed that the diminution of light intensity will result only from the geometric shadow cast by each particle.

Let N be the number density per unit volume of the particles. Take the Z-axis in the direction of the light, and let I' be the intensity per unit area of the light entering the solution at $\zeta=0$—distances parallel to the Z-axis are here denoted by ζ to avoid confusion with (3). Let s be the area of the shadow cast by a particular particle on a plane perpendicular to the direction of the light. Consider the loss of intensity of light traversing a thin layer of the solution between ζ and $\zeta+d\zeta$, sufficiently thin to ensure that no particle in this layer is within the shadow of any other particle in the same layer. Hence, if $I_t(\zeta)$ is the light intensity at ζ at time t,

$$I_t(\zeta+d\zeta)\simeq(1-N\,d\zeta\,\bar{s}_t-c\,d\zeta)\,I_t(\zeta), \qquad \ldots\ldots(24)$$

where the last term accounts for the absorption in the medium (owing to the dilution assumed independent of the presence of the particles), and the average projected area $\bar{s}_t$ does not depend on ζ. Passing to the limit and integrating, the intensity of light having traversed distance l of the solution is therefore given by (cf. the Lambert–Beer law)

$$\ln I_t/I'=-Nl\bar{s}_t-cl. \qquad \ldots\ldots(25)$$

After a long time, when the effect of the initial distribution has died down, the final intensity will similarly depend on the mean projected area when all orientations of the particles are equally likely, hence

$$\ln I_t/I_{\infty}=-Nl(\bar{s}_t-\bar{s}_{\infty}). \qquad \ldots\ldots(26)$$

This relation, into which the absorption of the medium does not enter, is the most suitable for the present purpose.

Let the particles be ellipsoids of revolution of eccentricity ϵ. From the geometry of the ellipse it is easily shown that the shadow, defined above, when the axis of the particle makes an angle $\cos^{-1} z$ with the direction of light, is

$$s = a\,|(1+\kappa z^2)^{1/2}|, \qquad \ldots\ldots(27)$$

where a is the area of a section of the spheroid containing the axis, and

$$\kappa = \epsilon^2/(1-\epsilon^2) \quad \text{for an oblate spheroid,} \qquad \ldots\ldots(28)$$

$$\kappa = -\epsilon^2 \quad \text{for a prolate spheroid.} \qquad \ldots\ldots(29)$$

The distribution of the orientations of the axes, eqn. (4), referred to the direction of the light as Z-axis, will in general not be azimuthally symmetric, but in forming the average of (27) at time t in accordance with (8), the terms containing the trigonometric functions and those in the Legendre polynomials of odd order will make no contribution, so that

$$\bar{s}_t = a\sum_{r=0}^{\infty} J_{2r} A_{2r} \exp\{-2r(2r+1)Dt\}, \qquad \ldots\ldots(30)$$

where

$$J_{2r} = \int_0^1 (1+\kappa z^2)^{1/2} P_{2r}(z)\,dz. \qquad \ldots\ldots(31)$$

Hence the required variation of light intensity is given by

$$\ln I_t/I_\infty = -Nla\sum_{r=1}^{\infty} J_{2r} A_{2r} \exp\{-2r(2r+1)Dt\}. \qquad \ldots\ldots(32)$$

Very soon the first term in the sum will predominate so that, apart from the exceptional cases discussed below,

$$\frac{d}{dt}\ln(\pm \ln I_t/I_\infty) \simeq -6kT/\beta, \qquad \ldots\ldots(33)$$

the sign depending on that of the first term in (32), that is, on whether I_t is greater or less than I_∞. Thus curves of $\ln(\pm \ln I_t/I_\infty)$ will asymptotically approach lines of downward slope $6kT/\beta$.

For particles of a more general axially symmetrical shape the same method will lead to a relation of the same form as (32), with a now as a factor depending only on the size of the particles and the J_{2r} as numerical coefficients determined only by their shape; relation (33) will again follow.

The initial distribution will in most practical cases be azimuthally symmetric with respect to some fixed direction, OZ′, say. Referred to OZ′, it will then be completely characterized by constants A_n' only, cf. (5). Let the direction of light, OZ, make an angle α with OZ′. By application of the addition theorem for Legendre polynomials it can be shown that

$$A_n = A_n' P_n(\cos\alpha). \qquad \ldots\ldots(34)$$

Hence the intensity of light transmitted in the direction making an angle α with the direction of symmetry of the original distribution—that is, that of the original field—is given by (32) as

$$\ln I_t/I_\infty = -Nla\sum_{1}^{\infty} J_{2r} A_{2r}' P_{2r}(\cos\alpha) \exp\{-2r(2r+1)Dt\}, \qquad \ldots\ldots(35)$$

and (33) follows as before.

The shape coefficients J_{2r} are easily found in the following special cases:

(i) Nearly spherical particles, where $\kappa \simeq \pm\epsilon^2$ is small, so that the root in (31) may be expanded up to the first power in κ only: it is easily found that

$$J_2 = \pm(2/15)\epsilon^2, \qquad \ldots\ldots(36)$$

and all J_{2r} of higher suffix vanish. Thus only the first terms in (32) or (35) survive and (33) will hold very approximately even for small times.

(ii) Rod-like spheroidal particles, $\kappa \sim -1$ (see Appendix):

$$J_{2r} = -\frac{\pi}{2}\frac{1}{(2r-1)(2r+2)}\{P_{2r}(0)\}^2, \qquad \ldots\ldots(37)$$

$$J_2 = -\pi/32. \qquad \ldots\ldots(38)$$

(iii) Disc-like spheroidal particles, $\kappa \simeq -\infty$: here the notation is unsuitable and it is best to write $aJ_{2r} = a'J_{2r}'$, where $a' = \pi b^2$ is the area of largest cross section, so that

$$s = a'|z|, \qquad \ldots\ldots(39)$$

$$J_{2r}' = \int_0^1 zP_{2r}(z)\,dz = -\frac{1}{(2r-1)(2r+2)}P_{2r}(0), \qquad \ldots\ldots(40)$$

$$J_2' = 1/8. \qquad \ldots\ldots(41)$$

This case, together with (19)–(22) applies to Stott's (1949) relaxation experiment on the assumption that the effect of diffraction is negligible. For a strong original field, taking the limiting case (11) instead of (21),

$$\ln I_t/I_\infty = Nla'\sum_1^\infty \frac{4r+1}{(2r-1)(2r+2)}\{P_{2r}(0)\}^2 P_{2r}(\cos\alpha)\exp\{-2r(2r+1)Dt\}. \quad ..(42)$$

For the angle $\alpha = 0$, taking now into account the original field to a first approximation, from (22), as soon as the first term in (35) predominates,

$$\ln\ln I_t/I_\infty = -6(kT/\beta)t + \ln\{5Nla'(1-3/2\alpha^2)/16\}. \qquad \ldots\ldots(43)$$

The experimentally useful relation (33) will hold only when the first terms in the sums (32) or (35) do not vanish. It will break down in the following cases, considering only (35): for an exceptional initial distribution for which $A_2' = 0$; for particles of exceptional shape for which $J_2 = 0$; and when the light is in an exceptional direction of angle α_1 relative to the direction of symmetry, where $P_2(\cos\alpha_1) = 0$, that is,

$$\alpha_1 = \pm\cos^{-1}(1/\sqrt{3}). \qquad \ldots\ldots(44)$$

In, or near, these very special cases, the relation in place of (33) will in general be

$$\frac{d}{dt}\ln(\pm\ln I_t/I_\infty) \simeq -20kT/\beta. \qquad \ldots\ldots(45)$$

For the verification of (33) the best experimental conditions should obtain when $P_2(\cos\alpha)$ has its largest numerical value, that is, for $\alpha = 0$. Considering the variation of (35) with the direction of the incident light, it is clear that there will be distinct angular regions in which $I_t < I_\infty$ and $I_t > I_\infty$, respectively, separated by a cone of critical angle α_c which varies in time in accordance with

$$\sum_1^\infty J_{2r}A_{2r}'P_{2r}(\cos\alpha_c)\exp\{-2r(2r+1)Dt\} = 0, \qquad \ldots\ldots(46)$$

and (44) is thus the limiting value of this critical angle. In the case of (42), the initial critical angle can be shown to be 45°.

§4. SUSPENSIONS OF SMALL METALLIC PARTICLES

Another limiting case will now be considered: the particles are assumed metallic and small so that the electric field inside them due to the light is quasi-static; on the other hand, they are assumed sufficiently large, so that the decrease in optical transmission is almost wholly due to their absorption of the electromagnetic waves, a volume phenomenon, and not to their scattering of the waves, a surface phenomenon. The method and notation is based on that of Gans (1912). Gans treated the absorption of random orientated particles: in the present relaxation problem a non-uniform distribution of orientations is assumed initially, azimuthally symmetric about some fixed direction, tending with time to uniformity, cf. (4), (34).

Let $\mathbf{E}$ be an external electric field. Let $\mathbf{a}$ be the unit vector along the axis of a particular particle, then the electric moment $\mathbf{F}$ induced in the particle is

$$\mathbf{F}=\mathbf{G}\,.\,\mathbf{E}, \qquad \ldots\ldots(47)$$

where $\mathbf{G}$ is a tensor, diagonal if referred to the axis of the uniaxial particle as one coordinate axis, that is,

$$\mathbf{G}=\mathbf{U}g'+\mathbf{aa}(g-g'); \qquad \ldots\ldots(48)$$

here $\mathbf{U}$ is the unit tensor, and the complex quantities g and g' depend on the shape of the particle, its volume, the real dielectric constant of the medium, and on the complex dielectric constant of the particle; their values for spheroidal particles are given by Gans (1912). Now let light fall in a certain direction, to which $\mathbf{E}$ is perpendicular,

$$\mathbf{E}=\mathbf{u}E_0, \quad \text{say}, \qquad \ldots\ldots(49)$$

where $\mathbf{u}$ is a unit vector, and the numerical quantity E_0 contains the amplitude and phase. Hence the component of the induced electric moment in the particle in the direction $\mathbf{u}$ is

$$\mathbf{u}\,.\,\mathbf{F}=(\mathbf{u}\,.\,\mathbf{G}\,.\,\mathbf{u})\,E_0. \qquad \ldots\ldots(50)$$

Considering now all the particles of the solution, it can be shown (cf. Gans 1912, eqn. 17) that the absorption per unit length k of the formula $I=I'\exp(-kl)$, is

$$k=\frac{2\pi}{\lambda'}\,\frac{4\pi N}{{m_0}^2}\,\mathscr{I}\{-\overline{(\mathbf{u}\,.\,\mathbf{G}\,.\,\mathbf{u})}\}, \qquad \ldots\ldots(51)$$

where λ' is the wavelength in the medium, N is the number of particles per unit volume, ${m_0}^2$ is the real dielectric constant of the medium, and the average is to be taken over all orientations of the axes at the instant considered. With (48) the absorption per unit length at time t is therefore

$$k_t=\frac{2\pi}{\lambda'}\,\frac{4\pi N}{{m_0}^2}\,\mathscr{I}\{-g'-\overline{(\mathbf{u}\,.\,\mathbf{a})^2}_t(g-g')\}. \qquad \ldots\ldots(52)$$

With reference to some fixed axes, let

$$\mathbf{a}=\mathbf{u}_x\sin\theta\cos\phi+\mathbf{u}_y\sin\theta\sin\phi+\mathbf{u}_z\cos\theta, \qquad \ldots\ldots(53)$$

and let light fall in the direction $\mathbf{u}_z$ of the Z-axis, so that

$$\mathbf{u}=\mathbf{u}_x\cos\phi'+\mathbf{u}_y\sin\phi', \qquad \ldots\ldots(54)$$

where ϕ' assumes all values between 0° and 360°. Hence for (52) the average needed is

$$\overline{(\mathbf{u}\,.\,\mathbf{a})^2}=\overline{\sin^2\theta\cos^2(\phi-\phi')} \qquad \ldots\ldots(55)$$

$$=\tfrac{1}{3}-\tfrac{1}{15}A_2'P_2(\cos\alpha)\,\mathrm{e}^{-6Dt}, \qquad \ldots\ldots(56)$$

using (8) and (34). Substituting into (52), only the difference

$$k_t - k_\infty = \frac{2\pi}{\lambda'}\frac{4\pi N}{m_0^2}\{\mathscr{I}(g-g')\}\tfrac{1}{15}A_2'P_2(\cos\alpha)\,\mathrm{e}^{-6Dt} \qquad \ldots\ldots(57)$$

is required here. With the suffix notation of the previous section it therefore follows that

$$\ln I_t/I_\infty = -l\frac{2\pi}{\lambda'}\frac{4\pi N}{m_0^2}\{\mathscr{I}(g-g')\}\tfrac{1}{15}A_2'P_2(\cos\alpha)\,\mathrm{e}^{-6Dt}, \qquad \ldots\ldots(58)$$

and hence, in this case, accurately,

$$\frac{d}{dt}\ln(\pm\ln I_t/I_\infty) = -6kT/\beta. \qquad \ldots\ldots(59)$$

The theory can be extended to the consideration of the —in general polarized— light re-emitted by the particles under relaxation conditions. As a basis for further study of similar relaxation problems the following papers will be found useful: Mie (1908), Gans (1920), Möglich (1927), and Oster (1948).

§ 5. CONCLUSION

Although more detailed results have been given, the main purpose of this paper is to draw attention to the relation

$$\frac{d}{dt}\ln(\pm\ln I_t/I_\infty) \simeq -6kT/\beta \qquad \ldots\ldots(60)$$

as an important Brownian motion formula. It has been derived here only on two special assumptions concerning the loss of light but inspection of (4) and general considerations suggest that the quantity on the left of (60) can, after a short time, depend only on the exponent of the second term of (4). The relation (60) is thus of considerable generality.

A modification of the method may have application to the theory of liquid crystals: formula (60) as it stands would apply also to small crystals freely suspended in a medium and released from a magnetic field when monochromatic polarized light is transmitted. The nature of liquid crystals is however not described by such a simple model; the 'particles' in this case are not 'free' but under mutual influence, and they are not crystals but only aligned molecules (cf. Symposium on Liquid Crystals 1931, Fürth 1937).

APPENDIX

In (37) use has been mde of

$$\int_{-1}^{1}(1-z^2)^{1/2}P_n(z)\,dz = -\frac{1}{(n-1)(n+2)}\int_{-1}^{1}(1-z^2)^{-1/2}P_n(z)\,dz$$

$$= -\frac{1}{(n-1)(n+2)}\pi\{P_n(0)\}^2.$$

The last equation follows from Copson (1944, p. 310, ex. 17).

Other relations used involving Legendre polynomials can be derived from the well-known recurrence relations and from Legendre's equation.

For reference it may be noted that

$$P_{2r}(0) = (-1)^r\frac{(2r)!}{2^{2r}(r!)^2}, \qquad P_2(z) = \tfrac{1}{2}(3z^2-1).$$

.B
5
2

ACKNOWLEDGMENT

The author is indebted to Dr. R. Fürth, of Birkbeck College, for suggesting the present problem, for discussion of its treatment, and for the constant interest shown in his work in general.

REFERENCES

COPSON, E. T., 1944, *Functions of a Complex Variable* (Oxford : University Press), p. 310.
DEBYE, P., 1929, *Polar Molecules* (New York : Chemical Catalog Co.).
EINSTEIN, A., 1906, *Ann. Phys., Lpz.*, **19**, 371.
ELMORE, W. C., 1941, *Phys. Rev.*, **60**, 593.
FÜRTH, R., 1937, *Ann. Phys., Lpz.*, **30**, 388.
GANS, R., 1912, *Ann. Phys., Lpz.*, **37**, 881; 1920, *Ibid.*, **62**, 331; 1928, *Ibid.*, **86**, 628.
MIE, G., 1908, *Ann. Phys., Lpz.*, **24**, 377.
MÖGLICH, F., 1927, *Ann. Phys., Lpz.*, **83**, 609.
OSTER, G., 1948, *Chem. Rev.*, **43**, 319.
PERRIN, F., 1925, *C.R. Acad. Sci., Paris*, **181**, 514; 1926, *J. Phys. Radium*, **7**, 390; 1934, *Ibid.*, **5**, 497; 1936, *Ibid.*, **7**, 1.
STOTT, F. D., 1949, *Proc. Phys. Soc.* B, **62**, 418.
Symposium on Liquid Crystals, 1931, *Z. Kristallogr.*, **79**.

An Interferometric Method of Studying Local Variations in the Refractive Indices of a Solid

BY R. C. FAUST
British Rayon Research Association, Manchester

Communicated by H. G. Howell; *MS. received* 11*th May* 1951

ABSTRACT. Many small transparent solids possess local variations in their refractive indices that cannot be detected by the standard immersion methods. This difficulty has been overcome by placing the immersed solid between the two parallel, metal-coated plates of an interferometer illuminated at normal incidence by a parallel beam of white light. The immersion liquid is so chosen that its dispersion curve intersects that of the solid at some wavelength within the visible spectrum. An image of the immersed specimen is then projected on to the slit of a spectrometer, whereupon one can observe coloured fringes of equal chromatic order (channelled spectra). These fringes generally suffer a displacement on crossing from the liquid to the liquid–solid region of the interferometer; this displacement does, however, vanish at that wavelength at which the refractive index of the liquid equals that of the solid. The method is equally applicable to both isotropic and birefringent specimens, the index measurements under favourable conditions being accurate to within ±0·0001.

The paper is illustrated by several examples, particular reference being made to the possibility of studying the skin effect in rayon fibres.

§1. INTRODUCTION

THE measurement of the refractive indices of small transparent solids plays an important role in many fields of research, and the worker may choose one of several standard procedures. Common to all these methods is the fact that the solid, viewed under a microscope, is immersed in a liquid the refractive index of which is altered until the presence of the specimen can no longer be detected. The index of the liquid, which can be measured on a suitable refractometer, will then be equal to that of the solid under the given experimental conditions. The means by which the index of the liquid may be changed relative to that of the solid fall into three classes: (i) the composition of the immersion medium may be altered, either by using a series of liquids, the measured refractive index of each differing slightly from that of the preceding member, or by mixing liquids on a cavity slide as was practised by Fisher (1931) and Jelley (1934); (ii) the wavelength of the incident light may be varied so as to take advantage of the difference between the dispersions of the liquid and of the solid (Posnjak and Merwin 1922); (iii) the temperature of the liquid–solid system may be changed, thereby relying on the fact that the refractive index of a liquid displays a much greater dependence on temperature than does that of a solid (Gaubert 1923). These basic ideas can be used jointly as, for example, in the combined temperature and wavelength variation method (Winchell and Emmons 1926, Emmons 1928, 1929).

The immersed specimen may be illuminated in one of two ways, the merits of which have been discussed by Saylor (1935). In the first method, that of central illumination, a stopped-down condenser restricts the light to a narrow axial pencil. If the liquid and solid indices differ, defocusing of the microscope will give rise to a Fresnel diffraction pattern at the edges of the specimen, this pattern often being observed as the familiar Becke line (Faust 1951). The second method involves the use of stops so placed that in the absence of the specimen the field of view is uniformly but dimly illuminated. If the specimen is now inserted its edges will stand out against the background provided that the refractivity of the solid differs from that of the surrounding medium. The actual image appearance will depend upon the amount of diffracted light cut off by the stops (Zernike 1942, Wolter 1950); in the Schlieren method the diffracted light on one side of the direct beam is removed, but when using oblique dark ground illumination the direct light is also stopped.

Although these methods are capable of detecting small differences between the indices of the solid and the ambient liquid, the image bears little resemblance to the object structure, variations in intensity only revealing those parts of the specimen where the index or the thickness changes abruptly. In certain fields, particularly that of high polymers, one might handle specimens with continuously varying refractive indices. To this class belong samples which have been cut from plastic sheets, thereby undergoing distortion at the edges, extruded textile fibres in which the degree of molecular alignment and, therefore, the birefringence alter radially, native fibres possessing a wall or scaly outer structure, and also specimens into which a liquid is diffusing. It was in order to observe such index variations that the present work was undertaken.

Köhler and Loos (1941) have suggested that phase contrast microscopy be used for refractive index determinations, but it is unlikely that this would overcome the peculiar difficulty of observing continuous index variations. If an isolated solid specimen is immersed in a liquid, some of the diffracted light, as well as the direct light, will be influenced by the phase strip in the rear focal plane of the objective. As a result the image intensity will vary across the field of view in a manner not readily related to the properties of the solid and the liquid. If, for example, a solid of constant thickness and refractive index were immersed in a liquid film of constant depth, the ideal image would be of uniform intensity over the purely liquid region and of uniform but different intensity over the area containing the solid; equality of the liquid and solid indices would naturally cause the abrupt intensity change at the liquid–solid boundary to vanish. In practice, however, the image often deviates markedly from this ideal form (Wolter 1950).

Interference microscopy has been used on several occasions to detect changes in the refractive index and the concentration of the solution surrounding a growing crystal (Berg 1938, Bunn 1949, Humphreys-Owen 1949). It has also been used by Merton (1947) and by Ambrose (1948) in order to reveal variations in either the thickness or the index of thin specimens, the method described by Ambrose having recently been employed in an examination of the penetration of liquids into stretched cellulose acetate sheets (Robinson 1950, Crank and Robinson 1951). In these experiments a displacement of the fringe pattern is due to an alteration in the optical thickness of the material between the interferometer plates, that is, by changes in either the thickness or the index of the material. If, therefore, a solid is immersed in a liquid between the plates of an interferometer, any point-to-point variations in the properties of the solid specimen cannot generally be ascertained unless the changes in the specimen thickness are already known. If, however, the immersion liquid and the solid are of the same refractive index, the fringe displacement should disappear whatever thickness the specimen might have. The purpose of this paper is thus to describe a means whereby the absolute refractive index can be measured at any point of a thin solid specimen of irregular and unknown thickness.

§ 2. THEORY OF IMAGE FORMATION

Two optical flats, the inner surfaces of which are coated with semi-transparent highly reflecting metallic films, are arranged parallel to each other, the intervening gap containing the thin specimen S surrounded by a liquid of suitable refractive index (fig. 1). This interferometer is illuminated at normal incidence by a parallel beam of monochromatic light and viewed under a microscope. The formation of the primary image can best be appreciated if the specimen is regarded as a simple phase grating of step-like nature.

In the absence of the optical flats F_1 and F_2 the incident parallel beam is split into an infinite number of diffracted beams which form 'spectra' of order 0, 1 and $-1, \ldots . M$ and $-M \ldots .$, in the rear focal plane of the objective. If all these beams are collected, the resultant disturbance in the conjugate plane S′ represents the object structure in both amplitude and phase; the image is therefore of uniform intensity, and detail within the object remains undetected. (In practice, however, the ideally postulated conditions are not fully satisfied, and the edges of the rulings of the grating appear as narrow dark lines on a uniformly bright background.)

The presence of the optical flats produces an optical multilayer system, the liquid–solid interfaces acting as partially reflecting surfaces. If, however, the refractive indices of the liquid and the solid are almost equal, these interfaces will possess very small reflection coefficients and therefore will be of no significance. The interferometer, bounded on either side by a highly reflecting surface, thus degenerates into a single layer of uniform geometrical thickness but of variable optical thickness. After transmission through F_1 the incident beam falls upon S, where it is divided into an infinite number of diffracted beams, all of which are partly transmitted and partly reflected at F_2. Each reflected component traverses S in the opposite direction and is in turn divided into a series of diffracted beams; these are then reflected at F_1, whereupon the cycle begins again. As a result of this repeated diffraction the phase and amplitude of every one of the original diffracted waves is affected to a different degree but, because of the parallelism of F_1 and F_2, the diffraction angles remain unchanged and the separation of the new spectra in the rear focal plane of the objective is no different from that obtained in the absence of the flats. The periodic changes in the optical thickness of the interferometer gap are therefore observed in the image plane S′ as intensity variations of the correct periodicity. The greatest attainable intensity variation that can be produced by a given alteration in the optical thickness will increase as the reflectivity of the interferometer flats is enhanced (Tolansky 1948). If the optical flats are parallel and close together, and if the interferometer is illuminated at normal incidence, the image fidelity is high, that is, a given image intensity corresponds to a definite optical thickness. The intensity distribution in the image of the phase grating is therefore similar to the full curve in the upper part of fig. 1.

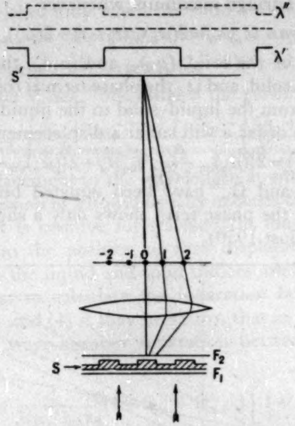

Fig. 1. Image formation in interference microscopy. The to-and-fro motion of the light between the flats is not shown.

The image intensity is greatest when the optical thickness of the interferometer is a multiple of the wavelength of the incident radiation. Each point of the interferometer is therefore imaged more intensely by certain wavelengths than by others; for example, the full and dotted curves in the upper part of fig. 1 portray the intensity distributions in the plane S′ for two different wavelengths λ′ and λ″. This wavelength dependence can be studied by using a white light source and projecting the image on to the slit of a spectrometer, whereupon one will observe a series of coloured interference fringes, the sharpness of which is critically controlled by the reflectivity of the interferometer plates. These are a general form of channelled spectra to which Tolansky (1948) has given the name 'fringes of equal chromatic order'. From them the refractive index of the solid specimen can be determined in the manner to be described.

Although these general conclusions have been reached by considering a grating-like object, they are equally applicable to specimens with aperiodic structures.

§ 3. THE FRINGE PATTERN

The wavelengths at which fringe maxima appear are determined by the optical thickness of the interferometer gap. In that part of the interferometer filled by the liquid alone a maximum fringe intensity is produced by those vacuum wavelengths λ_n' which satisfy the equation

$$(n-\Omega_n')\lambda_n'=2(\mu_n')_{\mathrm{liq}}t_g, \qquad \ldots\ldots(1)$$

in which n is a variable integer, t_g the geometrical thickness of the interferometer gap, $(\mu_n')_{\mathrm{liq}}$ the appropriate refractive index of the liquid, and Ω_n' the sum of the reflection phase changes occurring at the two metal films expressed as a fraction of the wavelength. When the refractive indices of the solid and the liquid differ but slightly, that region of the interferometer containing both substances is effectively reduced to a single optical layer and light of vacuum wavelength λ_n leads to a fringe maximum whenever

$$(n-\Omega_n)\lambda_n=2(\mu_n)_{\mathrm{liq}}(t_g-t)+2(\mu_n)_{\mathrm{sol}}t. \qquad \ldots\ldots(2)$$

Here t is the thickness of the solid, $(\mu_n)_{\mathrm{liq}}$ and $(\mu_n)_{\mathrm{sol}}$ the appropriate refractive indices of the liquid and solid, and Ω_n the phase term at this particular wavelength. Hence, upon crossing from the liquid–solid to the liquid region of the interferometer, a fringe of given order n will suffer a displacement $(\lambda_n-\lambda_n')$ given by

$$(n-\Omega_n')(\lambda_n-\lambda_n')=2\{(\mu_n)_{\mathrm{liq}}-(\mu_n')_{\mathrm{liq}}\}t_g+2\{(\mu_n)_{\mathrm{sol}}-(\mu_n)_{\mathrm{liq}}\}t. \qquad \ldots\ldots(3)$$

In this expression Ω_n and Ω_n' have been equated because for many highly reflecting metallic films the phase term shows only a slight wavelength dependence (Rouard 1937, Faust 1950).

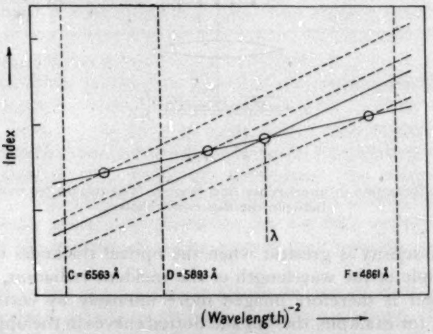

Fig. 2. The dispersion curve of a solid as obtained from the dispersion curves of four immersion liquids.

It is assumed that the refractive indices of the liquid and the solid are identical at a wavelength λ and that the simple Cauchy dispersion formula, which relates the index to the inverse square of the wavelength, is applicable to both substances (fig. 2). The change in the refractive index of the liquid occasioned by an alteration of wavelength is, therefore,

$$(\mu_n)_{\mathrm{liq}}-(\mu_n')_{\mathrm{liq}}=-k(\pi)_{\mathrm{liq}}(\lambda_n-\lambda_n')(\lambda_n+\lambda_n')/(\lambda_n\lambda_n')^2, \qquad \ldots\ldots(4)$$

in which k is a constant whose value is $5{\cdot}23\times10^7$ when the wavelengths are expressed in Å. π_{liq} denotes the wavelength dispersion of the liquid between the

F and C lines of hydrogen; π_{sol} will be used for the dispersion of the solid. One now obtains from eqns. (1), (3) and (4) the new relationship

$$\frac{\Lambda_n}{\lambda_n'}(1+B)=\frac{\{(\mu_n)_{\mathrm{sol}}-(\mu_n)_{\mathrm{liq}}\}}{(\mu_n')_{\mathrm{liq}}}\frac{t}{t_{\mathrm{g}}}. \qquad \ldots\ldots(5)$$

for the wavelength difference $\Lambda_n=(\lambda_n-\lambda_n')$. Because Λ_n is generally small, B can be expressed as $2k\pi_{\mathrm{liq}}/\{(\mu_n)_{\mathrm{liq}}\lambda_n^2\}$ and its magnitude can be gauged from table 1, where the values 1·6 and 0·025 have been ascribed to the index and the dispersion of the liquid.

Table 1

Wavelength (Å)	6500	6000	5500	5000	4500	4000
B	0·037	0·044	0·052	0·062	0·079	0·098

It is evident from eqn. (5) that, whatever the thickness of the solid specimen, the fringe displacement vanishes only when the solid and liquid indices agree, that is, at the wavelength λ. The difference in indices at any wavelength λ_n is

$$(\mu_n)_{\mathrm{sol}}-(\mu_n)_{\mathrm{liq}}=-k(\pi_{\mathrm{sol}}-\pi_{\mathrm{liq}})(\lambda_n-\lambda)(\lambda_n+\lambda)/(\lambda_n\lambda)^2. \qquad \ldots\ldots(6)$$

Hence, remembering that $\lambda_n\simeq\lambda_n'$ one obtains the general expression

$$\Lambda_n=\frac{k}{1+B}\frac{(\pi_{\mathrm{liq}}-\pi_{\mathrm{sol}})}{(\mu_n)_{\mathrm{liq}}}\frac{t}{t_{\mathrm{g}}}\frac{(\lambda_n-\lambda)(\lambda_n+\lambda)}{\lambda_n\lambda^2} \qquad \ldots\ldots(7)$$

relating the fringe displacement to the wavelength at which the observations are made. Since the dispersion of a liquid usually exceeds that of a solid of the same index, the displacement is positive for wavelengths longer than λ and negative for shorter ones. From the position of zero displacement can be found the wavelength λ for which the liquid and solid indices are identical.

It is also of interest to calculate the separation between adjacent fringes. By combining eqns. (1) and (4) it may be shown that in the purely liquid part of the interferometer the wave-number separation between two fringes of order n and $n+1$ is

$$\nu_{n+1}'-\nu_n'=\frac{\lambda_n'-\lambda_{n+1}'}{\lambda_n'\lambda_{n+1}'}=\frac{1}{2(\mu_n')_{\mathrm{liq}}t_{\mathrm{g}}}(1+\Omega_n'-\Omega_{n+1}')\left[1+\frac{k\pi_{\mathrm{liq}}}{(\mu_n')_{\mathrm{liq}}}\frac{(\lambda_n'+\lambda_{n+1}')}{\lambda_n'\lambda_{n+1}'^2}\right]^{-1}. \qquad \ldots\ldots(8)$$

The term containing the dispersion of the liquid is of almost the same magnitude as the quantity B, which, as seen from table 1, gains in significance as the blue end of the spectrum is approached. As already mentioned, the wavelength variation of the reflection phase term is usually slight. For example, an examination of evaporated silver films of high reflectivity has shown that the difference $\Omega_n'-\Omega_{n+1}'$ between the phase term at $\lambda_n'=6300$ Å, and that at $\lambda_{n+1}'=4300$ Å is approximately $-0{\cdot}1$. In the studies to be described, the wavelength separation between the fringes rarely exceeds 100 Å, and the presence of the phase term in eqn. (8) is therefore of little importance in comparison with that term containing the dispersion of the liquid. It is thus evident that the wave-number separation between neighbouring fringes has an approximate value of $1/2(\mu_n')_{\mathrm{liq}}t_{\mathrm{g}}$, but that the exact value decreases as one moves towards the blue. On the other hand, the wavelength separation between fringes is almost directly proportional to $\lambda_n'\lambda_{n+1}'$, and is therefore much larger in the red than in the blue.

If the thickness of the solid specimen is the same as that of the interferometer gap, the wave-number separation of the fringes in the region occupied by the solid is given again by eqn. (8), but the primes are naturally dropped and the index and dispersion of the liquid are replaced by those of the solid. Although the indices of the liquid and the solid differ but little, the dispersion of the liquid is generally much greater than that of the solid. As a consequence, the fringe separation is slightly greater in the solid than in the liquid region of the interferometer. Furthermore, the fringe displacement that occurs upon crossing from one region of the interferometer to the other would clearly vanish at the wavelength λ. Hence the displacement $\Lambda_n = (\lambda_n - \lambda_n')$ will be positive if the wavelength of observation exceeds λ and negative if it is shorter, these conclusions being in accordance with those reached earlier.

§4. EXPERIMENTAL PROCEDURE

By stirring together two non-volatile, miscible liquids a stable mixture can be obtained which has a refractive index close to that of the thin solid specimen under study. This rough matching of the indices is tested by the central illumination method referred to in the Introduction; if a monochromator is used to vary the wavelength of the incident radiation one may find an approximate value for the wavelength λ at which the liquid and solid indices are the same. The specimen, with a little of this liquid, is now inserted between the two optical flats of the interferometer; the inner surface of each glass flat is coated with an evaporated silver film possessing a reflection coefficient of 80% or more, the actual value depending upon the magnification to be employed. The flats are illuminated at normal incidence by a parallel beam of monochromatic light and the sensitive controls of the jig in which they are mounted are adjusted until the inner surfaces of the flats are parallel and the interferometer gap is as small as the specimen will allow; the field of view is then covered by a single interference band. The monochromatic light source is now replaced by a carbon arc and an image of the specimen is cast on to the slit of a spectrometer using an apochromatic objective of suitable power. To attain relatively high magnifications the objective should be combined with a projection eyepiece. If it is necessary to employ an objective of focal length less than 16 mm, the small working distance makes it essential to replace the optical flat between the specimen and the objective by a silvered glass coverslip. At such magnifications it is generally possible to discover a small area of the coverslip which approaches an optical plane to a satisfactory degree.

In the present studies a Hilger constant deviation spectrometer has been used to observe the fringes of equal chromatic order. It is naturally fortuitous for a fringe to occur at that wavelength λ corresponding to the intersection of the dispersion curves of the liquid and solid. No undisplaced fringe may therefore exist, but from the observed displacements it is possible to find by interpolation that wavelength for which a fringe, if formed, would be undeviated. The refractive index of the liquid at the sodium D lines and its dispersion between the C and F lines of hydrogen are measured with an Abbe refractometer, after which the dispersion curve of the liquid is constructed and the index of the solid determined for the wavelength λ. The composition of the liquid is now altered slightly and the refractive index of the solid found for a new wavelength. In this manner the dispersion curve of the solid is constructed (fig. 2).

The examples in the following sections will illustrate the scope and accuracy of the method.

§ 5. CHANGES IN SPECIMEN THICKNESS

The fringe pattern reveals any variations in the optical thickness of the interferometer which might occur along the line section selected by the spectrometer slit. It is assumed that the gap thickness t_g and the index of the specimen are constant along this line, but that the specimen thickness t is irregular. Eqn. (7) shows that whatever the specimen thickness there is no fringe displacement when the solid and liquid indices agree at wavelength λ. At any other wavelength λ_n there exists a displacement which is related to the specimen thickness by the approximate expression

$$\Lambda_n = \lambda_n - \lambda_n' = Ct(\lambda_n^2 - \lambda^2)/\lambda_n, \qquad \ldots\ldots(9)$$

in which λ_n' is constant for a given fringe. Since the constant C is positive, the displacement is positive for wavelengths longer than λ and negative for shorter ones, its magnitude increasing with the remoteness of the fringe wavelength from λ. As Λ_n is substantially smaller than $\lambda_n - \lambda$, the displacement of a given fringe is almost proportional to the specimen thickness.

(i) *A Glass Film*

If the specimen is of uniform thickness, the fringes are everywhere perpendicular to the wavelength axis, an abrupt displacement generally occurring at the specimen edge. Such a pattern, obtained by immersing a glass film (0·025 mm thick) in a mixture of ethyl salicylate and butyl stearate, is presented in fig. 3 (Plate), the glass being in the upper part of the photograph. An apparently undisplaced fringe occurred at $\lambda_n = 5058$ Å, the fringes on either side suffering slight displacements in opposite directions. As the spacing between fringes was 30 Å the wavelength at which the solid and liquid indices agreed was $\lambda = 5058 \pm 15$ Å. The index of the solid at 5058 Å was then determined from the measured refractive index and dispersion of the liquid ($(\mu_D)_{\text{liq}} = 1{\cdot}5061$ and $\pi_{\text{liq}} = 0{\cdot}0181$), the wavelength uncertainty of ± 15 Å leading to an error in the index of $\pm 0{\cdot}0001$. (A discussion on the accuracy of the method is reserved for a later section.) The procedure was repeated with other liquids, whereupon the dispersion curve of the glass was drawn and the values $(\mu_D)_{\text{sol}} = 1{\cdot}5111$ and $\pi_{\text{sol}} = 0{\cdot}0090$ obtained.

If the film were not plane, but suffered from 'wrinkling' (Tolansky 1948), no irregularities would be noticeable in the fringe pattern because of the close matching of the liquid and solid indices. This advantage would, however, be lost if a strongly anisotropic film were examined; such wrinkling would probably lead to fringe distortion, due to the fact that the inclination of the optic axes to the direction of incidence would then vary slightly from one part of the specimen to another.

(ii) *A Glass Fibre*

An isotropic cylindrical glass fibre of 0·038 mm diameter has also been examined. The interferometer was rotated on the microscope stage until the fibre axis was perpendicular to the spectrometer slit, that is, until the slit was parallel to the cylinder radius. The variation of the specimen thickness along the slit was therefore $t = 2(r^2 - y^2)^{1/2}$, where r is the fibre radius and y the distance from the axis. Since the spectrometer dispersion could be regarded as linear over the small wavelength range covered by a fringe of given order n, the displaced portion of the fringe took the form of half an ellipse with its centre on the fibre axis at the wavelength λ_n' (fig. 4, Plate). The wavelength λ, at which the solid and liquid indices were identical, lay between 5052 and 5028 Å; the maximum error was therefore ±12 Å, corresponding to an error in the index of ±0·0001 at the wavelength 5040 Å ($(\mu_D)_{\text{liq}}=1{\cdot}5082$, $\pi_{\text{liq}}=0{\cdot}0182$, $(\mu_D)_{\text{sol}}=1{\cdot}5135$ and $\pi_{\text{sol}}=0{\cdot}0086$).

§ 6. BIREFRINGENT SPECIMENS

If the direction of incidence of the radiation does not coincide with an optic axis of a birefringent solid, either uniaxial or biaxial, the light will be divided into two beams traversing the specimen with different velocities. A fringe-doubling will therefore be observed in that part of the interferometer in which the specimen is situated, the two fringe patterns, corresponding to the two refractive indices of the solid, being plane polarized in mutually perpendicular directions. By using a number of immersion liquids the value of each refractive index component may be determined at several different wavelengths. The birefringence at any wavelength can then be obtained by plotting the two dispersion curves.

(i) *Mica*

A mica flake 0·009 mm thick was chosen as an example of an optically anisotropic substance. When it was immersed in a suitable liquid and placed between the interferometer plates with the cleavage plane normal to the microscope axis, the birefringent doubling (Tolansky 1948) was immediately observed (fig. 5, Plate). As the birefringence was small, it was possible to find on the one plate two wavelengths, one for each refractive index component, at which the fringe displacement vanished. They were $\lambda^{\gamma}=4904\pm30$ Å and $\lambda^{\beta}=5240\pm33$ Å, the longer wavelength corresponding to the lower refractive index. These maximum wavelength errors led to an uncertainty of ±0·0004 in the individual values of the indices at these two wavelengths. The optical properties of the liquid were $(\mu_D)_{\text{liq}}=1{\cdot}5885$ and $\pi_{\text{liq}}=0{\cdot}0264$, whilst those for the mica were $\mu^{\gamma}{}_D=1{\cdot}5998$, $\pi^{\gamma}=0{\cdot}0092$ and $\mu^{\beta}{}_D=1{\cdot}5951$, $\pi^{\beta}=0{\cdot}0090$. The birefringence was sensibly constant throughout the visible spectrum with a value of 0·0047 ± 0·0002.

When the fringe pattern in fig. 5 was photographed, the interferometer was formed from two pieces of good quality glass instead of from optical flats, thereby illustrating the high accuracy attainable with relatively inexpensive equipment. Due to the thinness of the specimen, a smaller interferometer gap was possible than that used for the first two photographs. Hence, in accordance with eqn. (8), the fringes in fig. 5 were more widely separated than those in figs. 3 and 4. This equation also leads one to expect the wavelength separation of the fringes to be greater in the red than in the blue, but, as seen from the photographs, the linear separation increases as the blue is approached, this being caused by the nature of the dispersion curve of the prism spectrograph.

If it is remembered that the indices of the solid and the liquid differ by little, it may be demonstrated that a small birefringence $(\Delta\mu_n)_{\text{sol}}$ and the associated fringe doubling $\Delta\lambda_n$ are connected by the approximate equation

$$\frac{\Delta\lambda_n}{\lambda_n}\left\{1+\frac{2k}{(\mu_n)_{\text{sol}}\lambda_n^{2}}\left[\pi_{\text{liq}}-\frac{t}{t_g}(\pi_{\text{liq}}-\pi_{\text{sol}})\right]\right\}=\frac{(\Delta\mu_n)_{\text{sol}}}{(\mu_n)_{\text{sol}}}\frac{t}{t_g}. \qquad \ldots\ldots(10)$$

As the ratio t/t_g is generally unknown, this expression cannot yield a direct measurement of $\Delta\mu_n$. However, by assuming that $t=t_g$ one can use the relationship $(\Delta\mu_n/\mu_n)_{\text{sol}}=\Delta\lambda_n/\lambda_n$ in order to find the minimum birefringence which could lead to the observed doubling. (This neglects the small correction factor $2k\pi_{\mathrm{sol}}/(\mu_n)_{\mathrm{sol}}\lambda_n^2$, cf. table 1.) In fig. 5, for example, the doubling at 5000 Å is but 9 Å, leading to a minimum birefringence of about 0·003. The true value being 0·0047, it is clear that the ratio t/t_g is approximately 0·6.

(ii) *A Nylon Fibre*

When the specimen is of irregular thickness the two overlapping fringe patterns often lead to confusion, and it is therefore advisable to insert a polarizer in the incident light beam in order to eliminate each pattern in turn. A nylon fibre that had not been subjected to delustring was examined in this manner. Like the majority of textile fibres, this nylon sample behaved as a positive uniaxial medium, the refractive index being greatest for light vibrating parallel to the fibre axis and least for light vibrating perpendicular to the axis. The fibre was laid between the interferometer plates and the microscope stage rotated till the fibre axis was perpendicular to the direction of the spectrometer slit. Using a suitable immersion liquid ($(\mu_D)_{\mathrm{liq}}=1{\cdot}5361$ and $\pi_{\mathrm{liq}}=0{\cdot}0212$), the fringe patterns were photographed for light vibrating parallel to and perpendicular to the fibre axis (figs. 6 (*a*) and 6 (*b*), Plate). It was observed that the fringes were undisplaced in the immediate neighbourhood of the two wavelengths $\lambda_{\parallel}=5060$ Å and $\lambda_{\perp}=5940$ Å, the shorter wavelength naturally corresponding to the higher refractive index. Below 5060 Å both the indices of the fibre were less than that of the liquid and the fringes were therefore curved in the same sense in the two photographs. Between 5060 Å and 5940 Å the index of the liquid was intermediate between the two values for the fibre and the fringe curvatures were opposed. Finally, when the wavelength was above 5940 Å, both the indices of the solid were greater than that of the liquid, and the fringe curvatures were again in the same sense; they were, however, reversed with respect to those seen at wavelengths shorter than 5060 Å.

In fig. 6 (*a*) no fringe can be strictly described as straight, the correct interpretation of this observation being that the refractive index $\mu_{\parallel}$ of the fibre varied slightly in a radial direction. An analysis of the fringe pattern in accordance with the considerations of § 7 has shown that this index variation did not exceed ± 0·0003. The smaller index $\mu_{\perp}$ changed even less. The average optical properties of the fibre were $\mu_{D\parallel}=1{\cdot}5414$, $\mu_{D\perp}=1{\cdot}5373$, $\pi_{\parallel}=0{\cdot}0110$ and $\pi_{\perp}=0{\cdot}0104$.

Because of the large diameter of the nylon fibre (0·08 mm or about 24 denier) the fringes were separated by only 12 Å in the blue–green and 18 Å in the red. From this it can be concluded that specimens with an optical thickness much in excess of 0·15 mm cannot be satisfactorily studied in this fashion since it would then be difficult to resolve adjacent fringes.

§ 7. VARIATIONS IN THE INDICES OF THE SPECIMEN

An interesting situation arises when the optical properties of the solid specimen are not uniform but vary from point to point. It is convenient to divide such changes in the properties into two groups. In the first are classed those variations which cannot be studied, namely, those occurring in a direction parallel to the optical axis of the microscope. If the refractive index of the solid at any point along this axis is μ_t, then a mean index μ may be defined by

$$\int_0^t \mu_t\,dt=\mu t, \qquad \ldots\ldots(11)$$

the ($)_{\text{sol}}$ notation being henceforth omitted. In the previous examples it was this mean quantity that was measured; any variations that it might suffer in directions perpendicular to the microscope axis fall into the second group and are revealed by the form of the observed fringe pattern.

(i) *Cellulose Acetate Sheet*

When a small square was cut from an isotropic sheet of cellulose acetate containing 10% butyl phthalate as plasticizer, the edges were distorted and the refractive index measurements obtained from the central illumination method differed from the interferometric determinations made on the undisturbed material ($\mu_D = 1{\cdot}4925$ and $\pi_{\text{sol}} = 0{\cdot}0102$). The distortion caused by the cutting process led to the observation of a slight birefringent doubling at many points along the edges of the specimen. In fig. 7 (Plate), which shows the sheet at the top, no evidence of such anisotropy is to be seen, but the marked fringe displacement towards the red clearly indicates that the mean index at the edge was greater than that of the sheet itself, the largest index difference $d\mu$ being found at the point at which the wavelength of a given fringe was greatest. The value of $d\mu$ has been ascertained in three different ways: (i) At 4910 ± 30 Å the indices of the sheet and the liquid were identical, the greatest fringe displacement at the edge then being 18 Å. Assuming that $t = t_g$, eqn. (5) was used to calculate the minimum index difference which could lead to this displacement, namely $d\mu = 0{\cdot}006$. (ii) Equality between the indices of the liquid and the edge was not attained until the wavelength was well below 4000 Å, in which region no fringes were recorded on the photographic plate. However, if it is considered that the Cauchy dispersion formula still holds outside the visible spectrum, then one may regard eqn. (9) as valid and $(\lambda_n - \lambda_n')\lambda_n$ can be plotted against λ_n^2 to produce a straight line whose intercept on the abscissa corresponds to the wavelength at which the indices of the liquid and the sheet edge agree. Here λ_n is the maximum fringe wavelength observed at the edge and λ_n' is the fringe wavelength in the liquid region. In this manner (fig. 8) the value $\lambda = 3\,600$ Å was discovered. By making

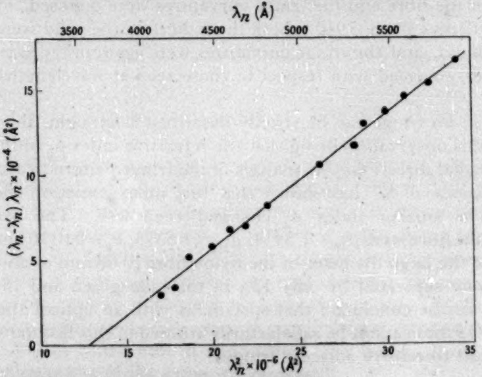

Fig. 8. Extrapolation in order to find the wavelength λ at which the index of the liquid equalled that of the sheet edge.

the reasonable assumption that the dispersion of the edge was little different from that of the undeformed sheet, it was possible to find the index of the edge at 4910 Å, whereupon the figure $d\mu \simeq 0{\cdot}009$ was obtained. (iii) Finally, the composition of the immersion liquid was so chosen that the refractive index was the same as that of the edge at some wavelength within the visible spectrum. The index of the edge at 4910 Å was then calculated, yielding the result $d\mu = 0{\cdot}008$.

(ii) *Viscose Rayon Fibre*

The introduction of special staining techniques has shown that many viscose rayon fibres consist of a skin surrounding a core of different properties (fig. 9 (*a*)). The nature of the structural difference between these two zones has not yet been satisfactorily settled, and it is of interest to make brief reference to several optical experiments which have been undertaken with a view to elucidating this matter. Wuhrmann (1945) has claimed that the superficial optical properties of the fibre are measured by the central illumination (Becke line) method and that the birefringence of the skin is therefore readily ascertainable. After preparing a longitudinal section (fig. 9 (*c*)), he used a compensator to determine the ratio of the birefringence of the skin to that of the core, and was thus able to calculate the core birefringence without knowing the thickness of the prepared section. The absolute refractive indices of the core, which are of importance in providing information about the core density, were not, however, found. Preston and Narasimhan (1949) have followed Wuhrman in believing that the Becke line procedure measures the properties of the skin, but they have determined the absolute indices of the core by means of the fibre refractometer (Freeman and Preston 1943, Preston and Bhat 1948), thereby avoiding any damage to the fibres. A completely different method has been adopted by Hermans (1950), who has used a difficult chemical technique (Elöd and Fröhlich 1948) in order to strip the fibre, the optical properties of the skin and the core then being determined separately by means of the Becke line. Unfortunately the objection may be raised that the fibre structure is influenced by the chemical treatment received.

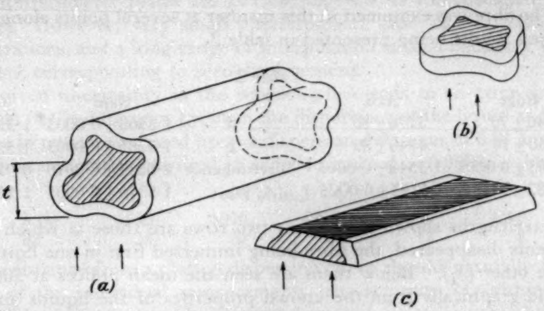

Fig. 9. Skin and core structure of a viscose rayon fibre: (*a*) a fibre length, (*b*) a transverse section and (*c*) a longitudinal section.

In view of the uncertainty of the present position it is believed that the new interference experiments described in this paper provide a valuable approach to the study of the skin effect. As in the previous examples, the fibre is laid between the interferometer plates and the microscope stage rotated until the fibre axis is perpendicular to the length of the spectrometer slit. If it is assumed that the optical properties are uniform within the two zones denoted as skin and core, but that an abrupt change occurs at the interface, then the mean index $\mu_{\parallel}$ for light vibrating parallel to the fibre axis is expressed by

$$\mu_{\parallel}t = \mu_{\parallel c}t_c + \mu_{\parallel s}t_s, \qquad \ldots\ldots(12)$$

an analogous statement holding for vibrations perpendicular to the axis. The overall fibre thickness t consists of two parts, t_c representing the thickness of the core and t_s the total thickness of the skin. At the edges of the fibre $t_s = t$ and the mean indices which are measured are those of the skin alone; at the centre of the fibre, however, contributions are provided by both the skin and the core, and a knowledge of the ratio t_c/t_s is required before the properties of the core itself may be deduced.

The birefringence of a viscose fibre (Courtaulds' 'Fibro' rayon staple, 18 denier or 0·05 mm) was large enough to demand that two different liquids be used, one for light vibrations parallel to the axis (fig. 10(*a*), Plate), the other for vibrations perpendicular to the axis (fig. 10(*b*), Plate). The radial variations in the mean indices were revealed by the fact that no fringe was straight, the mean index $\mu_{\parallel}$ clearly being greater at the fibre edge than on the axis, the reverse being true for $\mu_{\perp}$. The fibre was examined in this manner at several points along its length, the averaged results being presented in table 2.

Table 2

	Edge	Axis		Skin	Core
$\lambda_{\parallel}$ (Å)	4940 ± 70	5170 ± 80	$\parallel$	1·5563 ± 0·0005	1·5538 ± 0·0010
$\lambda_{\perp}$ (Å)	4960 ± 70	4740 ± 80	$\perp$	1·5282 ± 0·0005	1·5304 ± 0·0010
$\mu_{\parallel}$	1·5563 ± 0·0005	1·5548 ± 0·0005	Birefringence	0·0281 ± 0·0010	0·0234 ± 0·0020
$\mu_{\perp}$	1·5282 ± 0·0005	1·5295 ± 0·0005	μ_{iso}	1·5376 ± 0·0005	1·5382 ± 0·0010

The wavelengths shown in the first two rows are those at which the fringe displacements disappeared, the fibre being immersed first in one liquid ($\lambda_{\parallel}$) and then in the other ($\lambda_{\perp}$). Below them are seen the mean indices at 5000 Å, these being found graphically from the known properties of the liquids and the dispersion of the fibre. (It was assumed that the dispersion was the same at all parts of the fibre, its magnitude being determined by the more rapid central illumination method.) The mean indices at the edge are a direct measure of the properties of the skin, but those of the core must be calculated from eqn. (12); for this purpose it was estimated from the fringe patterns that the skin thickness was about one fifth of the fibre diameter, that is, on the axis $t_c/t_s = 3/2$. From these calculated values (rows $\parallel$ and $\perp$) is is evident that the birefringence of the skin is greater than that of the core; it is therefore considered that the skin possesses the higher degree of molecular orientation, this conclusion being in general agreement with the work of others in this field. For a given substance the density d may be related to the refractive index by the empirical formula of Gladstone and Dale; when applied to a fibre with radial symmetry the relationship assumes the form (Hermans 1949)

$$\left.\begin{aligned}(\mu_{\text{iso}} - 1)/d &= \text{constant}.\\ \mu_{\text{iso}} &= \tfrac{1}{3}(\mu_{\parallel} + 2\mu_{\perp}).\end{aligned}\right\} \qquad \ldots\ldots(13)$$

The quantity μ_{iso} was calculated for both the skin and the core; as the two values agreed within the experimental errors, the densities and the percentage of crystalline material are presumably very similar in the two zones.

The immersion liquids used were mixtures of butyl stearate and tricresyl phosphate, these being unlikely to penetrate into the fibre (Hermans 1949). In fig. 10 (*a*) there is an indication that the extreme edges of the fibre are of nearly the same mean index as that on the axis, but the significance of this feature, which was not observed on other photographs taken with this fibre, is unknown. Unfortunately, the thickness t at the fibre edges is only a small fraction of the interferometer gap thickness, and the sensitivity of measurement is not as high as on the fibre axis. A possible solution to this difficulty might lie in the careful preparation of fibre sections. Transverse sections (fig. 9 (*b*)) are the easiest to make, but they only permit one to study the properties for light vibrating in radial directions, whereas longitudinal sections (fig. 9 (*c*)) allow one to utilize both radial and axial vibrations.

§ 8. ACCURACY AND LIMITATIONS

The various factors influencing the accuracy and the scope of the method are:

(i) Any specimen of a thickness less than about 0·1 mm can be studied, the fringe displacement at a given wavelength being independent of the thickness provided that the interferometer plates are as close together as the specimen will allow (cf. eqn. 7). However, very small interferometer gaps lead to relatively large fringe separations, and a long range of interpolation is then necessary to find the wavelength λ corresponding to zero displacement.

(ii) A given uncertainty in the wavelength λ leads to an error $d\mu$ which is proportional to the difference between the dispersions of the liquid and the solid. The figures in table 3 are based upon a dispersion difference of 0·01 and show the wavelength uncertainties required in order to make $d\mu = 0{\cdot}0001$. The error in the indices obtained from a plotted dispersion curve should naturally be smaller than that of the individual measurements, an accuracy of within ±0·0001 being possible under favourable circumstances.

Table 3

λ (Å)	6500	6000	5500	5000	4500
$d\lambda$	25	20	16	12	8

(iii) A small interferometer gap ensures that the image faithfully portrays the structure of the specimen.

(iv) An objective with a focal length as short as 8 mm can be used successfully, but the restriction of the light to an axial parallel beam prohibits the utilization of the full aperture.

(v) Any irregularities in the surfaces of the interferometer plates will lead to their own fringe displacements.

(vi) The fringes formed by a prism spectrograph are not straight, but suffer from a slight astigmatic curvature.

ACKNOWLEDGMENTS

The writer has been greatly helped by Mr. B. J. Corr, who made the evaporated silver films, did much of the photographic processing, and prepared many of the immersion liquids.

This work forms part of the fundamental research programme undertaken by the British Rayon Research Association.

.B
5
2

REFERENCES

AMBROSE, E. J., 1948, *J. Sci. Instrum.*, **25**, 134.
BERG, W. F., 1938, *Proc. Roy. Soc.* A, **164**, 79.
BUNN, C. W., 1949, *Discussions of the Faraday Society*, No. 5, 132.
CRANK, J., and ROBINSON, C., 1951, *Proc. Roy. Soc.* A, **204**, 549.
ELÖD, E., and FRÖHLICH, H. G., 1948, *Text. Res. J.*, **18**, 487.
EMMONS, R. C., 1928, *Amer. Min.*, **13**, 504; 1929, *Ibid.*, **14**, 414, 482.
FAUST, R. C., 1950, *Phil. Mag.*, **41**, 1238; 1951, *Proc. Phys. Soc.* B, **64**, 105.
FISHER, D. J., 1931, *Amer. Min.*, **16**, 550.
FREEMAN, K., and PRESTON, J. M., 1943, *J. Text. Inst.*, **34**, T19.
GAUBERT, P., 1923, *Bull. Soc. Franç. Min.*, **45**, 89.
HERMANS, P. H., 1949, *Physics and Chemistry of Cellulose Fibres* (New York : Elsevier); 1950, *Text. Res. J.*, **20**, 553.
HUMPHREYS-OWEN, S. P. F., 1949, *Proc. Roy. Soc.* A, **197**, 218.
JELLEY, E. E., 1934, *J. Roy. Micr. Soc.*, **54**, 234.
KÖHLER, A., and LOOS, W., 1941, *Naturwissenschaften*, **29**, 49.
MERTON, T., 1947, *Proc. Roy. Soc.* A, **189**, 309; A, **191**, 1.
POSNJAK, E., and MERWIN, H. E., 1922, *J. Amer. Chem. Soc.*, **44**, 1970.
PRESTON, J. M., and BHAT, R. V., 1948, *J. Text. Inst.*, **39**, T211.
PRESTON, J. M., and NARASIMHAN, K. J., 1949, *J. Text. Inst.*, **40**, T327.
ROBINSON, C., 1950, *Proc. Roy. Soc.* A, **204**, 339.
ROUARD, P., 1937, *Ann. Phys., Paris*, **7**, 291.
SAYLOR, C. P., 1935, *J. Res. Nat. Bur. Stand., Wash.*, **15**, 277.
TOLANSKY, S., 1948, *Multiple Beam Interferometry* (Oxford : Clarendon Press).
WINCHELL, A. N., and EMMONS, R. C., 1926, *Amer. Min.*, **11**, 115.
WOLTER, H., 1950, *Ann. Phys., Lpz.*, **7**, 33, 147.
WUHRMANN, K., 1945, *Helv. Chim. Acta*, **28**, 666.
ZERNIKE, F., 1942, *Physica*, **9**, 686, 974.

Optical Properties of Tellurium in the Infra-Red

BY T. S. MOSS

Telecommunications Research Establishment, Great Malvern, Worcs.

MS. received 4th June 1951

ABSTRACT. The refractive index and absorption constant of tellurium layers have been measured in the near infra-red. The refractive index has been measured over the wavelength range 3 μ to 11 μ. The value extrapolated to long wavelengths is found to be 4·8; this is much higher than any other known refractive index. Absorption measurements were made for wavelengths 1 μ to 3 μ : the absorption constant is $2{\cdot}2\times10^5$ cm^{-1} at 1·0 μ, falling rapidly with increasing wavelength. Transmission measurements on bulk specimens are possible at wavelengths greater than 3·3 μ.

§ 1. INTRODUCTION

For calculation of the semiconducting properties of tellurium it is desirable to know the dielectric constant at optical frequencies. It is also interesting to compare the absorption spectrum with the spectral distribution of photoconductivity. Previous measurements of refractive index have been confined to the visible or ultra-violet regions of the spectrum, and have been made by reflection methods which tend to give results characteristic of the surface rather than of the tellurium itself (Van Dyke 1922, Miller 1925). Rough transmission measurements on films of unknown thickness have been made by Rutter (1930), Pfund (1933) and Soezima (1949).

§ 2. EXPERIMENTAL DETAILS

The measurements to be described were carried out on films of 'Specpure' tellurium evaporated in a high vacuum.

The refractive index was determined by measurement of interference fringes. Reflection fringes were used in order to increase the ratio of maxima to minima, and to make measurements with backing plates possible at longer wavelengths. The plates used were discs of artificial sapphire which give good transmission only as far as 6μ, but for which the reflection is low except for wavelengths between 11μ and 13μ. Using a rock-salt monochromator and thermopile detector fringes could be plotted for wavelengths up to 14μ. For wavelengths less than 3μ, increasing absorption in films 1μ to 6μ in thickness rendered the fringes insignificant.

The absorption constant was determined by measurement of transmission, using films of various thicknesses down to $0{\cdot}26\mu$. The measurements covered the range 1μ to 3μ, a lithium fluoride monochromator being used for this region because of its greater dispersion. As the absorption decreased rapidly with increasing wavelength, scatter in the spectrometer tended to give spuriously high transmission readings. This effect was minimized by using as the detector a lead sulphide cell, which is sensitive only to wavelengths less than 3μ. This detector determined the long wavelength limit of the measurements.

The value of the thickness was found by weighing the films. The nominal density of tellurium is 6·25 gm/cm^3, but the value for an evaporated film is inevitably somewhat lower. A measurement by Brattain and Briggs (1949) on a germanium film showed that the density was only 1% less than the bulk density. However, the long wavelength value of refractive index obtained by these workers is 7% greater than the precise value obtained by Briggs (1950), and it would seem probable that the major source of error was the determination of film thicknesses by weighing. Hence for germanium the density of films can probably be taken as 3% less than the bulk density, with an error of $\pm 3\%$. By analogy the specific gravity of tellurium films will be taken as $6{\cdot}1 \pm 3\%$.

§ 3. EXPERIMENTAL RESULTS

(i) *Refractive Index*

The curve of fig. 1 shows a typical set of interference fringes.

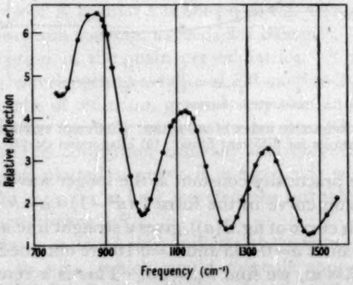

Fig. 1. Interference fringes for a tellurium film.

The frequencies f of the reflection minima are given by $2nd\cos\theta = N/f$ where d is the film thickness, n the refractive index, N the order of the fringe, and θ is the angle between the normal and the direction of a ray inside the film. All the measurements were carried out near normal incidence so that $\cos\theta = 1$. (It may be noted that with such a high refractive index, even an angle of incidence of 30° would reduce $\cos\theta$ by only $\frac{1}{2}\%$.) Hence $2nd = N/f_1 = (N+1)/f_2 = 1/(f_2 - f_1)$.

Now $f_2 - f_1$ is the fringe separation, which from fig. 1 has the average value 237 cm^{-1} in the non-dispersive region. Hence $2nd = 42\,\mu$. More accurate values of $2nd$ may now be obtained by inserting the relevant integral values of N. The results thus obtained are given in table 1.

Table 1

N	$f(\text{cm}^{-1})$	λ (microns)	$2nd$	n
3	~770	~13	~39	—
4	1004	9·97	39·8	4·97
5	1245	8·03	40·1	5·01
6	1477	6·77	40·6	5·08

Note : The minimum near 770 cm^{-1} is still in the region of high reflectivity from the sapphire, and is thus only approximate.

The thickness of the above film was $4{\cdot}0\,\mu$. This is the value used in calculating n.

The main error in the results lies in the determination of the thickness, due to uncertainties in the value of the density, as discussed previously. There is relatively little error in the determination of values of $2nd$. Hence, to plot a representative dispersion curve, the values of refractive index in the $10\,\mu$ region have been averaged, and all the results then normalized to this average value by correction of the measured value of d. The composite curve thus obtained is shown as fig. 2 (a). It may be seen that there is high dispersion at $3\,\mu$, but that the index has become practically constant at the longer wavelengths.

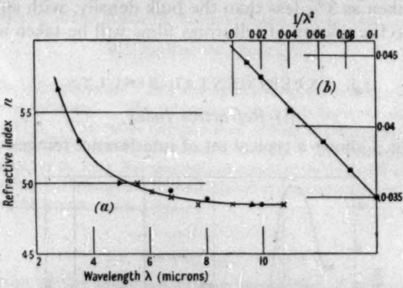

Fig. 2. (a) Refractive index of tellurium. Different symbols represent results for different films. (b) Dispersion curve.

Plotting a dispersion curve in the form $1/(n^2 - 1) = a - b/\lambda^2$ (using the values taken from the smooth curve of fig. 2 (a)), gives a straight line as shown by fig. 2 (b). From the graph the values $a = 0{\cdot}045$ and $b = 0{\cdot}10$ are obtained.

Extrapolating to $\lambda = \infty$, we find $n_\infty = 4{\cdot}8$. This is a remarkably high value of refractive index (considering that it is for the non-dispersive region) and is much higher than any other known refractive index. Assuming the density of the film to be within ±3% of the value used in the calculations, this value of n_∞ should be in error by less than ±5%.

(ii) *Absorption Constant*

The absorption A is defined by the relation

$$A=\frac{\text{Incident radiation}}{\text{Transmitted radiation}}=e^{Kd}$$

where K is the absorption constant in cm^{-1}. Measurement of the incident and transmitted energies thus gives K directly, if the thickness d is known. Some correction must be applied for reflection losses at the tellurium–air–sapphire interfaces. It was not convenient to measure these individually, but they may be estimated from the Fresnel formula $R=[(n_1-n_2)/(n_1+n_2)]^2$. Hence for air–sapphire, with $n=1{\cdot}7$, $R_1=7{\cdot}5\%$; for air–tellurium, with $n\simeq 5{\cdot}5$, $R_2=48\%$; for sapphire–tellurium, $R_3=28\%$. It may be remarked that the full formula for reflection involves the absorption index $nk=nK\lambda/4\pi$. At $3\,\mu$ (using the value of absorption constant quoted later in the paper), $nk=0{\cdot}6$, and inclusion of this term only increases the reflection coefficient by $\frac{1}{2}\%$. At $2\,\mu$ the reflection coefficient would be about 6%, with negligible effect on the calculated absorption constant. At $1\,\mu$ it is estimated that nk might be as high as 4 or 5. With the higher value the reflection loss would be increased 1·5 : 1. As the measured absorption at $1\,\mu$ was approximately 1000 : 1 for the thinnest film used, the correction would still have little effect on the absorption constant.

From the product $(1-R_1)(1-R_2)(1-R_3)$ we see that the three reflections represent a total loss of 3 : 1. In view of possible errors in this value and other possible insertion losses, only measured absorptions of 10 : 1 or more were considered satisfactory for the calculation of K.

For films greater than $1\,\mu$ in thickness, d was determined by weighing as before. For very thin films the value was determined relative to a thicker film, utilizing the absorption equation in the form $(1/d_1)\log A_1=(1/d_2)\log A_2$. Thus a graph of $\log A_1$ against $\log A_2$ for various wavelengths (using values of absorption corrected for reflection losses) should give the thickness ratio d_1/d_2. Such a graph is shown in fig. 3, where the ratio is 1·5 : 1. In this manner thicknesses down to $0{\cdot}26\,\mu$ were determined.

The composite curve of K against λ is shown in fig. 4 (curve A). It will be seen that at $1\,\mu$ the absorption constant exceeds $2\times10^5\ \text{cm}^{-1}$. Such a high value must be due to absorption in the main crystal lattice. The absorption falls rapidly with increasing wavelength to a value of $10^4\ \text{cm}^{-1}$ at $2{\cdot}5\,\mu$.

Experiments with slabs of tellurium ground very thin and polished, showed transmission measurements on bulk samples to be possible. At the longest wavelength used, $12\,\mu$, the absorption constant was only 130 cm^{-1}. Results of bulk measurements are plotted as curve B in fig. 4. It will be seen that the absorption is practically constant at long wavelengths but that it rises rapidly as the wavelength is reduced below $3{\cdot}5\,\mu$.

Measurements on bulk material thus indicate the presence of an absorption edge in the region $3\,\mu$ to $3{\cdot}5\,\mu$, which would coincide approximately with the 'threshold' wavelength of the photoconductive effect for tellurium (Moss 1951).

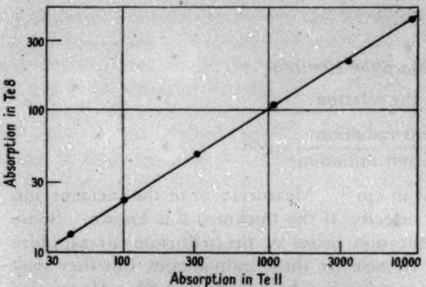

Fig. 3. Relative absorptions in two tellurium films designated Te 8 and Te 11.

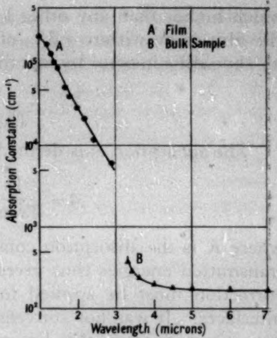

Fig. 4. Absorption constant for tellurium.

§ 4. CONCLUSIONS

The refractive index of tellurium has been measured in the near infra-red. The value of the index at long wavelengths is found to be $n_\infty = 4{\cdot}8$. This value is much higher than any other known refractive index.

The absorption constant has been measured between $1\,\mu$ and $3\,\mu$. The high values found (greater than 2×10^5 cm^{-1} at $1\,\mu$) show that the absorption must be in the main crystal lattice. The two sets of measurements are generally in agreement in that the dispersion becomes small where the absorption is small.

The above value of absorption constant at $1\,\mu$ gives an extinction coefficient slightly greater than that found by Van Dyke (1922) at $0{\cdot}6\,\mu$. These two absorption measurements thus indicate that the main part of the absorption band lies between 0·6 and $1{\cdot}0\,\mu$. The refractive index should therefore increase rapidly with wavelength in this region. Thus the values of refractive index found by Van Dyke for the visible region ($n = 2{\cdot}5$ to 3) are not necessarily incompatible with the present results.

Measurements on bulk tellurium indicate the presence of an absorption edge in the region $3\,\mu$ to $3{\cdot}5\,\mu$.

ACKNOWLEDGMENTS

The above work was carried out at the department of Colloid Science, University of Cambridge. Acknowledgment is due to the Chief Scientist, Ministry of Supply, and to the Controller, H.M. Stationery Office, for permission to publish this paper.

REFERENCES

Brattain, W. H., and Briggs, H. B., 1949, *Phys. Rev.*, **75**, 1705.
Briggs, H. B., 1950, *Phys. Rev.*, **77**, 287.
Miller, R. F., 1925, *J. Opt. Soc. Amer.*, **10**, 621.
Moss, T. S., 1951, *Proc. Phys. Soc.* A, **64**, 590.
Pfund, A. H., 1933, *J. Opt. Soc. Amer.*, **23**, 375.
Rutter, E., 1930, *Z. Phys.*, **60**, 1.
Soezima, Y., 1949, *J. Sci. Res. Inst., Tokyo*, **44**, 68.
Van Dyke, G. D., 1922, *J. Opt. Soc. Amer.*, **6**, 917.

The Diffraction of X-Rays by Distorted-Crystal Aggregates III: Remarks on the Interpretation of the Fourier Coefficients

By J. N. EASTABROOK and A. J. C. WILSON
Viriamu Jones Laboratory, University College, Cardiff, Wales

MS. received 11*th September* 1951

ABSTRACT. The line profile of the *h*th order reflection from a set of lattice planes is known to be given by a Fourier series with coefficients $A(h, m)=N(m)J(h, m)$. The function $N(m)$ depends on the particle shapes and sizes, and $J(h, m)$ depends on the state of strain. Neither can be completely determined from the experimental Fourier coefficients for a single value of h. They have, however, different behaviours for small m, and $A(h, m)$ has an unambiguous interpretation in this region only: its initial slope gives the mean particle thickness, and its initial curvature sets a lower limit to the mean-square strain. The practical value of this interpretation is subject to two limitations: (i) the initial shape of the $A(h, m)$ curve depends on the 'tail' of the line profile, (ii) if the crystals are large enough to contain several regions of compression and extension, probability theory shows that $J(m)$ is likely to be approximately proportional to $\exp\{-\text{const.}\,|m|\}$ for m large. Extrapolation to small m could then tend to give fictitiously small values for both particle size and strain.

The problem of obtaining the greatest possible amount of information from observed line profiles of all orders is discussed. Usually only a few orders can be measured, and the information obtainable is less, but in three special cases the Fourier coefficients of two lines can yield all information obtainable from the full set.

§ 1. INTRODUCTION

It has been shown that under certain general conditions the function broadening the lines of the powder pattern of an aggregate of imperfect crystals is given by a Fourier series with coefficients (Wilson 1942, 1943, 1949 b, Stokes and Wilson 1942, 1944 b)

$$A(m)=N(m)J(m). \qquad \ldots\ldots(1)$$

Here $J(m)$ is the average value of the product FF^* of the complex structure factors of a pair of cells separated by m interplanar spacings, and $N(m)$ is the number of such pairs in the crystals (formerly written $V(m)/U$). In most of the work cited above, the Fourier series was replaced as soon as possible by a Fourier integral, more easily evaluated and a sufficient approximation in the problems being considered, but Averbach and Warren (1949, Warren and Averbach 1950) have found it preferable to retain the series in the interpretation of their experiments on cold-worked metals, and Bertaut (1949, 1950) has used the series coefficients in his discussion of particle-size broadening. The coefficients are evaluated naturally, at any rate within a scale factor, in the course of Stokes' (1948) method of separating the instrumental and significant broadenings in measured line profiles.

The present paper attempts to extend Warren and Averbach's discussion of the inferences that may legitimately be made from an experimental set of coefficients for an aggregate of crystals that may be both small and distorted.

Other forms of imperfection, for example mistakes, are not considered, and it is assumed that extinction can be neglected or allowed for. It is found that (unless an elaborate process suggested by Warren and Averbach can be carried out) the only portion of the curve of $A(m)$ against m with an immediate physical interpretation is that for m small. The initial slope is proportional to the reciprocal of the mean thickness of the crystals, and the initial curvature gives a lower limit to the mean-square strain. In practice there are certain difficulties. First, the details of this portion of the $A(m)$ curve depend on the 'tails' of the lines, and as these are not easy to measure accurately, the interpretable part of the curve is likely to be subject to considerable experimental error. Secondly, if a crystal contains regions of compression and extension, it is probable that $J(m)$ approximates to $FF^* \exp\{-\text{const.}\,|m|\}$ for large m, so that an attempt to extrapolate to $m=0$ in order to obtain the initial values is likely to give a fictitiously large negative slope and a fictitiously small curvature, interpreted as too small particle sizes and strains. It may be preferable, therefore, to develop methods based directly on the line profile, rather than on the values of $A(m)$ deduced from it.

§ 2. RELATIONS BETWEEN THE LINE PROFILE AND THE SERIES COEFFICIENTS

It is convenient to begin by reviewing the relation between the series coefficients and the line profile. The sample irradiated is assumed to be large enough for each size and shape of crystal to be present in all orientations; as Bertaut has shown, it is not necessary to assume that all crystals are of the same size and shape, though the interpretation of $N(m)$ is less obvious if this is not so. Let the a axis be chosen perpendicular to the reflecting planes, and suppose that the reflection $h00$ is being investigated. Then the line profile is given by

$$I(h,s)=K\sum_{m=-\infty}^{+\infty} N(m)J(h,m)\exp\{2\pi ism\}, \qquad \ldots\ldots(2)$$

where s is $[\lambda/(2a\sin\theta)-h]$, K is a proportionality constant involving some slowly varying functions of θ, $N(m)$ is the number of pairs of cells in the sample separated by m interplanar spacings, and $J(h,m)$ is the mean value, for the $h00$ reflection, of FF^* for pairs of cells separated by m interplanar spacings. The meaning of s is not immediately obvious from the statement above; it expresses the angle at which the intensity is being evaluated as a fraction of the distance $1/a$ between successive $h00$ points in the reciprocal lattice. The function $I(h,s)$ is a measurable quantity, and hence it is possible to determine $N(m)J(m)$ by Fourier analysis. Replacing m by n in eqn. (2), multiplying by $\exp\{-2\pi ims\}$ and integrating from $-\frac{1}{2}$ to $+\frac{1}{2}$ with respect to s gives

$$N(m)J(h,m)=K^{-1}\int_{-1/2}^{1/2} I(h,s)\exp\{-2\pi ims\}\,ds. \qquad \ldots\ldots(3)$$

§ 3. RELATION OF THE FOURIER COEFFICIENTS TO THE STRAIN

3. 1 *General Relations*

If $F(h)$ is the structure amplitude of a cell of the undistorted crystal, and aX_m is the relative displacement of a pair of cells separated by m interplanar spacings,

$$FF^*=F(h)F^*(h)\exp\{2\pi ihX_m\} \qquad \ldots\ldots(4)$$

and

$$J(h,m)=|F(h)|^2\langle\exp\{2\pi ihX_m\}\rangle, \qquad \ldots\ldots(5)$$

where angular brackets indicate 'the average value of'. Let $X_m = me(m)$, where $e(m)$ is the average strain between the two cells, and let $P(m, e)$ be the proportion of cells m planes apart for which the average strain is e. Then

$$J(h,m) = |F(h)|^2 \int_{-\infty}^{\infty} P(m,e)\exp\{2\pi ihme\}\,de \qquad \ldots\ldots(6)$$

and

$$A(h,m) = N(m)J(h,m) = |F(h)|^2\, N(m) \int_{-\infty}^{\infty} P(m,e)\exp\{2\pi ihme\}\,de. \qquad \ldots\ldots(7)$$

If $A(h, m)$ were known as a continuous function of h it would be possible to find $N(m)P(m, e)$ by inversion of this Fourier transform. In the nature of things, however, $A(h, m)$ is measurable only for integral values of h, and the function that it is possible to find is

$$N(m)Q(m,e) = |m| \sum_{h=-\infty}^{\infty} A(h,m)\,|F(h)|^{-2}\exp\{-2\pi imeh\}. \qquad \ldots\ldots(8)$$

The relation between $Q(m, e)$ and $P(m, e)$ is (see next paragraph)

$$Q(m,e) = \sum_{n=-\infty}^{\infty} P(m, e+n/|m|). \qquad \ldots\ldots(9)$$

Since ordinary materials will not support elastic strains greater than 1 or 2%, the terms of the series having $n \neq 0$ are negligible for small m, so that the distinction between $Q(m, e)$ and $P(m, e)$ is important only for large m. Eqns. (8) and (9) form a generalization of the result of Warren and Averbach (1950, eqn. 15), and the evaluation of $N(m)Q(m, e)$ for all orientations of the reflecting planes would provide all the information obtainable from Debye–Scherrer lines without some hypothesis regarding the nature of the distortion. It cannot, in practice, be carried out completely, as the coefficients $A(0, m)$ are not determinable in the same way as the others, and for h large the reflections are no longer distinct from one another. There are, however, three special cases in which a knowledge of $A(h, m)$ for only two values of h suffices to determine both $N(m)$ and $Q(m, e)$. Two of these are recognizable by inspection of the $A(h, m)$ curves, but there seems to be no easy way of recognizing the third. These cases are further considered in §§ 3.2–3.4.

The relation, eqn. (9), between $P(m, e)$ and $Q(m, e)$ may be verified as follows. From eqn. (7)

$$\begin{aligned} A(h,m) &= |F(h)|^2\, N(m) \int_{-\infty}^{\infty} P(m,e)\exp\{2\pi ihme\}\,de \\ &= |F(h)|^2\, N(m) \sum_{n=-\infty}^{\infty} \int_{n/|m|-1/2|m|}^{n/|m|+1/2|m|} P(m,e)\exp\{2\pi ihme\}\,de \\ &= |F(h)|^2\, N(m) \sum_{n=-\infty}^{\infty} \int_{-1/2|m|}^{1/2|m|} P(m,\eta+n/|m|)\exp\{2\pi ihm\eta\}\,d\eta \qquad \ldots(10) \end{aligned}$$

on replacing e by $\eta + n/|m|$. Thus $A(h, m)\,|F(h)|^{-2}$ is the hth coefficient in a Fourier series for

$$|m|^{-1} N(m) \sum_{n=-\infty}^{\infty} P(m, \eta + n/|m|),$$

and comparison with eqn. (8) defining $Q(m, e)$ shows that eqn. (9) is the relation between $P(m, e)$ and $Q(m, e)$.

3.2. *No Strain*

When there is no strain $J(h, m)$ is constant, and

$$A(h,m) = |F(h)|^2 N(m). \qquad \ldots\ldots(11)$$

The curves of $A(h, m)$ against m have thus the same shape and breadth for every order, a condition recognizable by inspection of the curves for two values of h, and $N(m)$ is obtained immediately.

This case may be further analysed by the method developed by Bertaut (1949, 1950). If $p(n)$ is the number of columns of cells of length n in the sample, N is the total number of cells in the sample, and M is the average column length, then it has been shown that

$$\left(\frac{\partial N(m)}{\partial |m|}\right)_{|m|=0} = -\frac{N}{M}, \qquad \ldots\ldots(12) \qquad\qquad \frac{\partial^2 N(m)}{\partial |m|^2} = p(|m|). \qquad \ldots\ldots(13)$$

Thus the mean column length (or mean thickness of a crystal expressed in interplanar spacings) is the negative reciprocal of the initial slope of the $N(m)$ curve, and the second derivative of $N(m)$ gives the number of columns in the sample of length m.

3.3. *Strain Distribution independent of m; Crystals large*

If the crystals making up the sample are large, the variation of $N(m)$ can be neglected, and if also $P(m, e)$ is independent of m, the Fourier coefficients become

$$A(h,m) = NJ(h,m) = N|F(h)|^2 \int_{-\infty}^{\infty} P(e) \exp\{2\pi i h m e\}\, de, \qquad \ldots\ldots(14)$$

and the curves of $A(h, m)$ against m have the same shape for every order, depending essentially only on the product hm. Their breadths thus decrease as h^{-1}. The line profile is

$$\begin{aligned} I(h,s) &= KN|F(h)|^2 \sum_m \int_{-\infty}^{\infty} P(e) \exp\{2\pi i m(he+s)\}\, de \\ &= KNh^{-1}|F(h)|^2 P(-s/h). \qquad \ldots\ldots(15) \end{aligned}$$

The line profile is thus, within a factor, the strain distribution function, and its breadth is directly proportional to the order of reflection. This is the result obtained by Stokes and Wilson (1944 a). (More strictly, $P(-s/h)$ should be replaced by a series depending on $n/|h|$, as that in eqn. (9) depends on $n/|m|$, but the additional terms will ordinarily be negligible.)

Some examples of $P(m, e)$ independent of m are as follows. (So far it has not been possible either to extend the list or to show that it is exhaustive.) (i) Strain constant within each crystal, $P(e)$ for different crystals arbitrary. (ii) Local strain varying linearly and $P(e)$ constant within each crystal, $P(e)$ for different crystals arbitrary. (iii) Local strain varying exponentially and $P(e)$ proportional to e^{-1} within each crystal, $P(e)$ for different crystals arbitrary. (iv) The Cauchy strain distribution discussed in § 4.2. The first of these is essentially that assumed by Brindley (1940). Strain variation of the second type is found in the bent lamella (Wilson 1949 a), though with a thin lamella the variation of $N(m)$ cannot be neglected. The third type does not appear to correspond to any physically plausible situation.

3.4. *Strain Distribution independent of m; Crystals small*

If the strain distribution is independent of m, but the crystals are small, it is possible to obtain $N(m)$ and $J(m)$ from the Fourier coefficients of two lines, but there is no obvious way of deciding by inspection whether the assumptions are fulfilled or not. Probably this could be established by the analysis of three lines taken in pairs. As in § 3.3, $J(h, m)$ is a function of hm only, and, for example,

$$A(1, m) = N(m)J(m),\quad A(2, m) = N(m)J(2m),\quad A(1, 2m) = N(2m)J(2m), \quad \ldots\ldots(16)$$

$$J(2m) = \frac{A(2, m)}{A(1, m)}J(m), \qquad N(2m) = \frac{A(1, 2m)}{A(2, m)}N(m); \quad \ldots\ldots(17)$$

from a knowledge of $N(m)$ or $J(m)$ for any value of m other than zero it would be possible to build up the $N(m)$ and $J(m)$ curves step by step.

Alternatively, the coefficients of power series for $N(m)$ and $J(m)$ can be found in terms of those for $A(h, m)$. Let $A, A_1', A_1'' \ldots$ and $A, A_2', A_2'' \ldots$ represent the values of $A(1, m), A'(1, m), A''(1, m), \ldots$ and $A(2, m), A'(2, m), A''(2, m), \ldots$ for $m = 0$ and similarly for $N(m), J(m)$. Then

$$A + mA_1' + \tfrac{1}{2}m^2A_1'' + \ldots = (N + mN' + \tfrac{1}{2}m^2N'' + \ldots)(J + mJ' + \tfrac{1}{2}m^2J'' + \ldots),$$

$$NJ = A, \quad N'J + J'N = A_1', \quad N''J + 2N'J' + J''N = A_1'', \ \ldots \quad \ldots\ldots(18)$$

$$A + mA_2' + \tfrac{1}{2}m^2A_2'' = (N + mN' + \tfrac{1}{2}m^2N'' + \ldots)(J + 2mJ' + 2m^2J'' + \ldots),$$

$$NJ = A, \quad N'J + 2J'N = A_2', \quad N''J + 4N'J' + 4J''N = A_2'', \quad \ldots\ldots(19)$$

$$N' = N(2A_1' - A_2')/A, \quad N'' = \tfrac{1}{3}N[A(4A_1'' - A_2'') - 4(2A_1' - A_2')(A_2' - A_1')]/A^2,$$

$$J' = J(A_2' - A_1')/A, \quad J'' = \tfrac{1}{3}J[A(A_2'' - A_1'') - 2(2A_1' - A_2')(A_2' - A_1')]/A^2. \quad \ldots\ldots(20)$$

The higher coefficients become rapidly more complex. This case may be of some importance as it corresponds to Heyn intergranular stresses coexistent with small particle size.

3.5. *General Case; m small*

In general only the part of the $A(m)$ curve near the origin has a ready physical interpretation. The function $N(m)$ can always be expanded as a power series in m:

$$N(m) = N - N\,|m|\,M^{-1} + \tfrac{1}{2}\,|m|^2\,p(0) + \tfrac{1}{6}\,|m|^3\,p'(0) + \ldots, \quad \ldots\ldots(21)$$

where $p(n)$ is the function introduced in § 3.2. From the meaning of $p(n)$ it follows that $p(0)$, interpreted as the limit of $P(n)$ as n goes to zero, is non-negative. For a number of simple crystal shapes $N(m)$ is a cubic in m, and all terms except those written are zero (Wilson 1949 b, p. 42). From eqn. (5),

$$\begin{aligned} J(h, m) &= |F(h)|^2\,\langle \exp\{2\pi i h X_m\}\rangle \\ &= |F(h)|^2\,[1 + 2\pi i h\langle X_m\rangle - 2\pi^2h^2\langle X_m^2\rangle + \ldots]. \end{aligned} \quad \ldots\ldots(22)$$

The mean value of X_m is near zero, and could in any case be made zero by proper choice of the value of a. The mean value of X_m^2, however, is finite, and can be expressed in terms of the strain and its gradients at the position of the first cell of the pair:

$$X_m = em + \tfrac{1}{2}e'm^2 + \ldots \quad \ldots\ldots(23)$$

(Here e is the actual local strain, not the average value over m interplanar spaces, as elsewhere.) Then

$$\langle X_m^2\rangle = \langle e^2\rangle m^2 + \text{terms in } m^3 \text{ and higher}, \quad \ldots\ldots(24)$$

and

$$N^{-1}\,|F(h)|^{-2}\,A(h, m) = 1 - |m|\,M^{-1} - \{2\pi^2h^2\langle e^2\rangle - \tfrac{1}{2}N^{-1}p(0)\}m^2 + \ldots. \quad \ldots\ldots(25)$$

Thus if $m^{-1}\{1 - A(h, m)/A(h, 0)\}$ is plotted as a function of m, the intercept for $m = 0$ should give M^{-1}, where M is the average thickness of the crystals expressed in interplanar distances. The initial slope of the curve should be $2\pi^2h^2\langle e^2\rangle-\frac{1}{2}N^{-1}p(0)$, and this ~~sets~~ a lower limit to the mean-square local strain. For some crystal shapes $p(0)$ is zero, and probably it would not be large in any case, so that the lower limit would be close to the true value. However, the term in $p(0)$ is independent of h, so that measurement of two orders of the same reflection would make it possible to separate the two terms.

3.6. *The Bent Lamella*

The bent lamella appears to be the only model of a distorted crystal which has been worked out in detail, and it is perhaps of some interest to verify that the leading terms in the expansion of $A(h, m)$ are those to be expected from the results of the previous paragraph. From eqn. (4) (Wilson 1949 a)

$$N^{-1}\,|\,F(h)\,|^{-2}\,A(m,h)=(BTh\,|\,m\,|)^{-1}\sin\{Bh(T-a\,|\,pm\,|)\,|\,m\,|\},\qquad\ldots\ldots(26)$$

$$=1-a\,|\,pm\,|/T-\tfrac{1}{8}B^2h^2T^2\,|\,m\,|^2+\ldots,\qquad\ldots\ldots(27)$$

where T is the thickness of the lamella, $B=\pi\,|\,q^2-\alpha p^2\,|/R$, R is the radius of curvature, p and q are direction cosines of the reflecting plane relative to axes perpendicular to the lamella and tangent to it in the plane of bending, and α is a sort of Poisson's ratio. The mean column length is $M=T/|\,p\,|\,a$, in agreement with the reciprocal of the coefficient of $|\,m\,|$, and $p(0)=0$. The strain components are

$$e_{11}=-\alpha x/R,\qquad e_{22}=x/R,\qquad e_{12}=0,\qquad\ldots\ldots(28)$$

so that the local strain is

$$e=p^2e_{11}+q^2e_{22}=(q^2-\alpha p^2)x/R=B\pi^{-1}x,\qquad\ldots\ldots(29)$$

$$\langle e^2\rangle=\frac{B^2}{\pi^2T}\int_{-T/2}^{+T/2}x^2\,dx=\frac{B^2T^2}{12\pi^2},\qquad\ldots\ldots(30)$$

and $2\pi^2h^2\langle e^2\rangle=\frac{1}{6}B^2h^2T^2$, in agreement with the coefficient of $|\,m\,|^2$ in eqn. (27).

§ 4. SOME REMARKS ON DISTRIBUTION FUNCTIONS

4.1 *Characteristic Function for large m*

In § 3.5 it was shown that for small m

$$J(h,m)=|\,F(h)\,|^2\,[1-2\pi^2h^2\langle e^2\rangle m^2+\ldots].\qquad\ldots\ldots(31)$$

In general

$$|\,F(h)\,|^{-2}J(h,m)=\int_{-\infty}^{\infty}P(m,X)\exp\{2\pi ihX\}\,dX,\qquad\ldots\ldots(32)$$

where $P(m,X)$ is the probability of there being a relative displacement aX of two cells m interplanar spacings apart. In this section it is convenient to consider displacements rather than mean strains; the present $P(m,X)$ is related to the $P(m,e)$ used in § 3 by the equation $mP(m,X)=P(m,e)$. We now seek to examine the behaviour of $J(h,m)$ for large m, on the assumption that the strain passes through positive and negative cycles in each crystal. The displacements of neighbouring planes are highly correlated, being practically the local value of the strain multiplied by the distance between them, but the displacements of widely separated planes will be more or less independent if the assumption stated above is fulfilled. The actual displacements are additive; if $X_m=u_{j+m}-u_j$, and if $0<k<m$,

$$u_{j+m}-u_j=(u_{j+m}-u_{j+k})+(u_{j+k}-u_j),\qquad\ldots\ldots(33)$$

and if the displacements $(u_{j+m}-u_{j+k})$ and $(u_{j+k}-u_j)$ are independent,

$$P(m,X)=\int_{-\infty}^{\infty}P(k,x)P(m-k,X-x)\,dx.\qquad\ldots\ldots(34)$$

This 'folding' operation is equivalent to multiplication of the ***characteristic functions*** (Fourier transforms, cf. Cramér 1946, pp. 188–192) of the probability distributions, so that if $\psi(m,t)$ is the characteristic function of $P(m,X)$

$$\psi(m,t)=\psi(k,t)\,\psi(m-k,t). \qquad \ldots\ldots(35)$$

This functional equation has the solution

$$\psi(m,t)=\exp\{-mf(t)\}, \qquad \ldots\ldots(36)$$

where $f(t)$ is a function of t limited only by the general restrictions on characteristic functions.

4.2 *Cauchy and Gaussian Distributions*

The various distribution functions consistent with the assumption above are then obtained from

$$P(m,X)=\int_{-\infty}^{\infty}\exp\{-mf(t)-2\pi iXt\}\,dt \qquad \ldots\ldots(37)$$

by giving $f(t)$ suitable values. The simplest is $f(t)=\alpha\,|t|$, which gives the distribution ('Cauchy' in X)

$$P(m,X)=\frac{2\alpha|m|}{\alpha^2m^2+4\pi^2X^2}, \qquad \ldots\ldots(38)$$

with α as an adjustable parameter. The next simplest is $f(t)=\alpha t^2$, giving the distribution (Gaussian in X)

$$P(m,X)=\left(\frac{\pi}{\alpha\,|\,m\,|}\right)^{1/2}\exp\left(-\frac{\pi^2X^2}{\alpha\,|m|}\right). \qquad \ldots\ldots(39)$$

Powers higher than t^2 do not satisfy the conditions for characteristic functions, but clearly it is possible to manufacture many more distributions by suitable choices of $f(t)$, for example $\log(1+\alpha t^2)$.

4.3 *Mean-Square Displacements*

The mean value of X^2 is easily found from the properties of distribution functions. From Cramér (1946, p. 186), the variance of X from its mean value 0 is minus twice the coefficient of t^2 in the expansion of $\log\psi(t)$ in powers of t. This coefficient is readily seen to be $-\frac{1}{2}mf''(0)$, so that

$$\langle X^2\rangle = mf''(0). \qquad \ldots\ldots(40)$$

The mean-square displacement of planes with a considerable separation thus increases linearly with their distance apart. (For planes close together the mean-square displacement increases as the square of the distance, as found in eqn. (24).) For $f(t)=\alpha t^2$ eqn. (40) gives $\langle X^2\rangle=2\alpha m$, which is readily verified from eqn. (39). For $f(t)=\alpha\,|\,t\,|$, $f''(0)=\infty$, which is in accord with the properties of the Cauchy distribution.

4.4 *Line Profiles*

The values of $J(h,m)$ are obtained by applying eqn. (32) to the various values of $P(m,X)$, but fortunately the properties of Fourier transforms make it possible to avoid the labour of individual calculations. From (32) and (37)

$$\begin{aligned}|\,F(h)\,|^{-2}J(h,m)&=\int_{-\infty}^{\infty}\int_{-\infty}^{\infty}\exp\{-mf(t)-2\pi iXt+2\pi ihX\}\,dX\,dt\\&=\exp\{-\,|\,m\,|f(h)\}. \qquad \ldots\ldots(41)\end{aligned}$$

Thus any distribution consistent with eqn. (34) gives a Laplacian dependence of $J(h, m)$ or m. The line profile, in the absence of instrumental broadening and appreciable particle-size effect, would be (eqn. (2))

$$\begin{aligned}(KN)^{-1}\,|F(h)|^{-2}\,I(h,s) &= \sum_{m=-\infty}^{\infty} \exp\{-|m|f(h)+2\pi ism\}\\ &= \frac{\sinh f(h)}{\cosh f(h)-\cos 2\pi s}, \qquad \ldots\ldots(42)\\ &= \frac{2f(h)}{f^2(h)+4\pi^2 s^2} \qquad \ldots\ldots(43)\end{aligned}$$

if s and $f(h)$ are small. The line profile is thus of the Cauchy type for small s.

The Cauchy line profile is possibly a better approximation to those observed than the Gaussian form frequently used (for example, by Shull 1946). The Cauchy form was considered by Jones (1938), and claimed suitable by Bradley (1947) and Wood and Rachinger (1949). It has the property that integral breadths are simply additive, and thus has been assumed by Hall (1949) in his analysis of line breadths.

(The fact that Stokes and Wilson (1944 a) obtained Gaussian line profiles from a Gaussian strain distribution is only at first sight in conflict with the results of §§ 4.2 and 4.4. By a different approach they assumed, in effect, that $P(m, X)$ was proportional to $\exp\{-\alpha X^2/m^2\}$, which differs from eqn. (39) through an extra factor of m^{-1} in the exponent. It was designed to be approximately correct for m small.)

§ 5. PRACTICAL DETERMINATION OF FOURIER COEFFICIENTS FROM LINE PROFILES

It has been seen that the most easily interpretable features of an $A(h, m)$ curve are its slope and curvature near the origin. Unfortunately this part of the curve is most affected by the non-inclusion of the extremities of the diffraction line. From eqn. (3)

$$A(h,m) = K^{-1}\int_{-1/2}^{+1/2} I(h,s)\exp\{-2\pi ims\}\,ds, \qquad \ldots\ldots(44)$$

but in practice it is not possible to include the whole range of integration indicated. This is partly due to the interference of other lines, and partly to the difficulty of distinguishing the tail of the line from the background. For the broad lines produced by samples containing distorted crystals the limitation of the range of integration may be serious.

Suppose that the range of integration that it is practicable to use is $-1/2z$ to $+1/2z$. Then only the exponential terms with $|m|$ greater than z will pass through a complete cycle within the range of integration, and it seems improbable that the numerical values found for $A(h, m)$ for $|m|$ less than z will have any physical significance. This means, in particular, that the initial slope and curvature must be estimated from the part of the curve extending from $m=0$ to $m \sim 3z$, and if z is large the average values over this region may deviate considerably from the true initial values. In general, any detail of the $A(h, m)$ curves covering a range of m less than z will be of doubtful physical significance. (Line profiles determined by the method of Stokes (1948) do not have a particularly dubious region near the peak, as the method involves a double Fourier transformation, and shifts the doubtful part back into the tail of the line.)

A related reason for distrusting the range $|m|<z$ is the effect of an error in estimating the background level. The effect of this is to add or subtract a peak of height proportional to z^{-2} and width of the order of z, with a consequent uncertainty in the initial slope.

From the arguments put forward in § 4 it seems probable that $J(m)$ for large m approximates to $|F(h)|^2 \exp\{-\text{const.}\,|m|\}$. The true value of $J(m)$ for m small has no term linear in m, but from the form of $J(m)$ for large m it is likely that extrapolation backwards would give too big an initial slope and too small an initial curvature, thus exaggerating the apparent particle-size broadening and reducing the apparent strain broadening. Pending an investigation sufficiently thorough to make the direct application of eqn. (8) possible, therefore, the values of particle size and strain obtained from the Fourier coefficients should be received with some caution.

ACKNOWLEDGMENTS

We are grateful to Professor J. L. B. Cooper for some helpful discussions on Fourier transforms, and to Professor B. E. Warren for access to an unpublished manuscript. The work forms part of an investigation of imperfect structures for which grants have been received from the British Iron and Steel Research Association and the Royal Society. A brief account was given at the Second International Congress of Crystallography, Stockholm, 1951.

REFERENCES

AVERBACH, B. L., and WARREN, B. E., 1949, *J. Appl. Phys.*, **20,** 885.

BERTAUT, F., 1949, *C. R. Acad. Sci., Paris*, **228,** 187, 492, 1597; 1950, *Acta Crystallogr.*, **3,** 14.

BRADLEY, A. J., 1947, *J. Sci. Instrum.*, **24,** 266.

BRINDLEY, G. W., 1940, *Proc. Phys. Soc.*, **52,** 117.

CRAMÉR, H., 1946, *Mathematical Methods of Statistics* (Princeton : University Press).

HALL, W. H., 1949, *Proc. Phys. Soc.* A, **62,** 741.

JONES, F. W., 1938, *Proc. Roy. Soc.* A, **166,** 16.

SHULL, C. G., 1946, *Phys. Rev.*, **70,** 679.

STOKES, A. R., 1948, *Proc. Phys. Soc.*, **61,** 382.

STOKES, A. R., and WILSON, A. J. C., 1942, *Proc. Camb. Phil. Soc.*, **38,** 313; 1944 a, *Proc. Phys. Soc.*, **56,** 174; 1944 b, *Proc. Camb. Phil. Soc.*, **40,** 197.

WARREN, B. E., and AVERBACH, B. L., 1950, *J. Appl. Phys.*, **21,** 595.

WILSON, A. J. C., 1942, *Proc. Roy. Soc.* A, **180,** 277; 1943, *Ibid.*, **181,** 360; 1949 a, *Acta Crystallogr.*, **2,** 220; 1949 b, *X-Ray Optics* (London : Methuen).

WOOD, W. A., and RACHINGER, W. A., 1949, *J. Inst. Metals*, **75,** 571.

A New Determination of the Luminance Factor of Magnesium Oxide

By J. S. PRESTON and G. W. GORDON-SMITH
National Physical Laboratory, Teddington, Middlesex

Communication from the National Physical Laboratory; *MS. received* 2nd *August* 1951

ABSTRACT. A simple, direct, and absolute method of reflectometry is described, avoiding the use of the inverse square law, and overcoming several of the drawbacks of the selenium photovoltaic cell which is used for the measurements. These advantages are secured through the use of calibrated apertures and certain integrating properties of the cell. The result obtained for the luminance factor for white light of an MgO smoked layer 1 mm thick was 1·01 for normal incidence and 45° view.

§ 1. INTRODUCTION

A SURFACE of magnesium oxide, made by depositing the smoke from burning magnesium ribbon, has long been used as a standard of luminance* factor for white light. The accepted value of the luminance factor for normal incidence and 45° viewing angle is 1·00. The luminance at this angle happens conveniently to be closely the same as that of a non-absorbing diffuser under the same illumination obeying Lambert's law. This accepted value is, however, based chiefly on measurements that are more or less indirect, depending on the use of an integrating sphere (e.g. Preston 1929–30), or on the integration of a family of polar curves of luminance (Taylor 1937). The principle of the direct absolute method is the comparison of the luminous intensity of a known area of the reflecting surface with that of the source. Large intensity ratios have then to be measured, and it may be difficult to eliminate or assess errors with certainty. For instance, the distance of the source from the surface or photometer may have to be varied over a large range. There may then be some uncertainty in the use of the inverse square law due to stray light, unevenness in the radiation field of the lamp, or difficulty in ascertaining precisely the light-centre of the filament within the bulb. With a photocell, if the two readings differ too much, significant corrections may have to be determined and made, because of non-linearity of the cell characteristic.

The present note describes a method in which a selenium photovoltaic cell is used. The two readings taken with it are arranged to be equal, and variation of the source distance is avoided by the use of apertures of widely differing but known areas.

§ 2. THE METHOD

The first reading was taken with the apparatus shown in fig. 1.

Close in front of a gas-filled projector lamp is a fixed screen with a square hole a little bigger than the square occupied by the filament. This confines the source to a definite small size. At a fixed distance *a* from the light-centre of the lamp is a plate in which is a small circular aperture X, carefully cut and of diameter about one millimetre. Behind this is placed the circular photovoltaic cell, of 45 mm nominal outside diameter, where the pinhole image of the lamp just falls entirely within the sensitive area. At any shorter distance from X the cell will receive the same quantity of light, and will give the same reading, assuming for

---

* The internationally agreed definition of *luminance factor* is given in *C.I.E. Compte Rendu*, 1948, page 18. This factor has in the past frequently been called ' apparent reflection factor '.

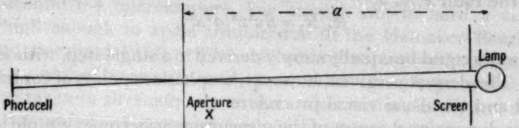

Fig. 1.

the moment that its sensitivity is independent of how a given amount of light is distributed on it. Then if R_1 is this reading, k a sensitivity constant, ϕ_1 the luminous flux on the cell, I the intensity of the source, and X the area of the aperture,

$$kR_1 = \phi_1 = IX/a^2, \qquad \ldots\ldots(1)$$

if, as was the case, the aperture and source are both small compared with the distance between them.

The arrangement for the second reading is shown in fig. 2.

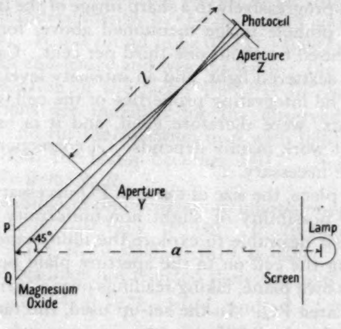

Fig. 2.

The aperture plate X is removed and replaced by the magnesium oxide surface located in the same plane as the aperture by a suitable jig. The distance a thus remains unchanged. The photocell is now placed to view the surface at 45° through another larger aperture Y. The sensitive area of the cell is defined by an aperture Z close against it and exposing a circular area extending nearly, but not quite, to the contact-ring. The distance l between Y and Z is fixed and known. From the point of view of the cell, then, the oxide surface is indistinguishable from a disc having the same luminance but coincident in position and size with the aperture Y. The distance of the cell–aperture system from the surface does not matter, so long as the luminance over the area PQ from which light reaches the cell does not vary significantly. Then, if R_2 is the cell reading, ϕ_2

the luminous flux on the cell, Y, Z the areas of the apertures, *d* the diameter of a sphere passing through their perimeters, *B* the luminance of the oxide and β its luminance factor,

$$kR_2 = \phi_2 = BYZ/d^2 = \beta IYZ/\pi a^2 d^2. \qquad \ldots\ldots(2)$$

Combining (1) and (2), $R_2/R_1 = \beta YZ/\pi d^2 X$, or expressing the areas X, Y, Z in terms of the radii x, y, z,

$$R_2/R_1 = \beta y^2 z^2/d^2 x^2. \qquad \ldots\ldots(3)$$

This formula could be equally simply derived in a single step, without reference to I and a. The derivation given, however, emphasizes points of contrast between this method and the usual visual procedure.

Thus, the dimensional aspect of the measurement becomes simple and precise, and consists in measuring the areas or radii of three circular apertures, and the distance between two of them, from which *d* can also be found. Also, by suitable choice of these, R_2/R_1 can be as near unity as may be desired. It now remains to examine certain assumptions.

(i) First, there is the question of the constancy of *k* with variation in distribution of a given quantity of light on the cell. It was not found difficult to select a cell whose sensitivity was constant, to within about one-third per cent, when a weak, uniform spot of light 3 mm in diameter was used to explore the sensitive area. This cell was then illuminated by a lamp and lens, so that when close to the lens it received a disc of light nearly filling it, while, as the cell was moved away from the lens, the disc changed progressively to a sharp image of the lamp filament of about the same size as the pinhole image mentioned above, formed by aperture X. The cell reading increased by about one-third per cent. Care was taken to use a lens giving very little scattered light, and an intensity level similar to that of the main experiment. The integrating properties of the cell, over its surface, for a constant luminous flux, were therefore good, and it is on this point that the interest of the present work mainly depends. A correction of about 0·3% was, however, shown to be necessary.

(ii) In the second place, the size of the area PQ necessary to give the required cell reading, and the possibility of slight non-uniformity in polar distribution from the lamp, made it desirable to explore the illumination within PQ. This was done by clamping the cell on to the aperture plate behind aperture X and moving X about in its own plane, taking readings over a 'grid' of positions within the roughly elliptical area PQ. In the set-up used, the ratio of average to axial illumination was found to be 0·995.

(iii) In the third place, the light reaching the cell from the oxide surface was not all scattered at 45°, but was embraced within a finite range of angles. This range cannot be reduced to zero without reducing the light on the cell to zero also. It was, however, kept quite small enough for no uncertainty to arise from the (small) variation of luminance of the surface with angle of view.

(iv) Finally, an implicit assumption is that the spectral quality of the light is unchanged by reflection from the oxide, so that the result is not influenced by the spectral response of the cell. This is justified by previous work on the whiteness of the oxide and by a recent absolute determination at the National Physical Laboratory, an account of which is being published.

The magnesium oxide surface was prepared upon a silver-plated copper disc, from the smoke of burning magnesium ribbon cleaned with fine glass paper.

The coating was 1·1 mm in thickness, was dense and free from any fluffy spots, and smooth except for the slight undulation inevitable in a coating of this thickness.

The practical procedure was as follows. The lamp was a 100 v 250 w tubular projector lamp, run at a colour temperature of about 2852° K (Illuminant A) with precise manual control of voltage. The photocell was used in a Campbell–Freeth, or zero-resistance, circuit (Campbell and Freeth 1934). The output chosen was around 0·4 microampere, low enough not to need a very intense source, but high enough to avoid trouble due to the Hamaker–Beezhold effect (Hamaker and Beezhold 1934). The cell was never exposed, in the course of observations, to higher intensities, and was at other times kept in total darkness. Readings were taken in alternate sets of three observations of R_1 and three of R_2. In each set the periods of exposure and of obscuration (for zero check) were timed, and were of one minute duration. The first reading of each set was discarded. Aperture X was cleaned under a microscope before use, and inspected afterwards. Screening precautions were meticulous, especially with the oxide surface in position and scattering much light.

§ 3. MEASUREMENTS AND RESULTS

The diameters of apertures Y and Z were measured directly on a measuring microscope and gave mean values for the radii of $y = 19{\cdot}06$ mm and $z = 16{\cdot}83$ mm. These apertures were known to be almost circular. Though the diameter of the small aperture X, measured as the distance between parallel tangents, was uniform to a high accuracy, the aperture was not known to be truly circular. Its area was therefore measured independently by the method of counting squares under sufficient magnification. It was found to be $0{\cdot}7121 \pm 0{\cdot}003$ mm². The distance l was set by means of an end-gauge and was 665·0 mm; the corresponding value of d is 666·0 mm; the value of the factor y^2z^2/d^2x^2 in eqn. (3) was therefore 1·025. When corrections are included for the observed non-uniformity of illumination over PQ, and for the variation in k with light distribution on the cell, as referred to earlier, the factor becomes 1·017. Inserting this value in equation (3) we have $\beta = 0{\cdot}983 R_2/R_1$.

The experimental readings of photocurrent in microamperes were R_1 (0·3840), 0·3835, 0·3835; R_2 (0·3947), 0·3953, 0·3952; R_1 (0·3814), 0·3825, 0·3825; R_2 (0·3941), 0·3935, 0·3938; R_1 (0·3806), 0·3819, 0·3820.

The mean values of readings not rejected therefore give

$$R_2/R_1 = 0{\cdot}3945/0{\cdot}3827 = 1{\cdot}031 \quad \text{and} \quad \beta = 1{\cdot}014.$$

A second series of observations was made using another aperture X of area $0{\cdot}8725 \pm 0{\cdot}003$ mm², and with $l = 616{\cdot}2$ mm. The precision was equally good, and the result was $\beta = 1{\cdot}008$. The photoelectric readings show a steady downward drift, almost linear with time, and probably due to the effect of change in temperature of the measuring apparatus and cell. The precision of reading would seem, however, to be within about ± 0·1%, while the difference between the two values of luminance factor, of 0·6%, is not more than the sum of the possible errors in the areas of the two small apertures used. It therefore seems reasonable to take, as the final result of this determination of the luminance factor, for normal incidence and 45° view, of a smoked magnesium oxide surface, the value $1{\cdot}01 \pm 0{\cdot}003$. This is about one half per cent higher than the value given in the previous indirect determination by one of us (Preston 1929–30), when the oxide coating was probably rather thinner than the present one.

ACKNOWLEDGMENTS

Acknowledgment is made of the help of Mr. L. O. C. Johnson who advised on, and undertook measurements of the apertures used in this investigation. The work described in this paper formed part of the programme of general research of the National Physical Laboratory, and the paper is published by permission of the Director of the Laboratory.

REFERENCES

Campbell, N. R., and Freeth, M. K., 1934, *J. Sci. Instrum.*, **11**, 125.
Hamaker, H. C., and Beezhold, W. F., 1934, *Physica*, **1**, 119.
Preston, J. S., 1929–30, *Trans. Opt. Soc.*, **31**, 15.
Taylor, A. K., 1937, *Proc. Phys. Soc.*, **49**, 105.

LETTERS TO THE EDITOR

A Note on some Proposed Equations of State for the Expansion of Rigid Porous Solids on the Adsorption of Gases and Vapours

It has been shown in the case of charcoal and coal by Bangham and his associates (Bangham 1934, Bangham and Fakhoury 1930, Bangham, Fakhoury and Mohamed 1934, Bangham and Maggs 1943, Bangham and Razouk 1938) that upon the reduction of the free surface energy by the adsorption of gases and vapours, as calculated from the Gibbs adsorption isotherm (Bangham 1937), the solid increases in size by amounts of the order of 0·5% in one dimension.

The experimental results show that, within the limits of accuracy of the experiments, the equation $x=\lambda F$ is obeyed where x is the percentage linear expansion of the solid due to a change in the free surface energy per unit area F, λ being a constant. For the purposes of this note, the equation is rewritten $x=-\theta\, dF'$ as F is essentially a decrease in free surface energy and x is an increase in dimensions. Here F' is the free surface energy per unit area. Bangham and Maggs (1943) related λ to the Young's modulus E of the solid by considering it as one long thin rod, such that the specific surface of the rod was equal to that of the solid, the decrease in free surface energy being assumed to act as a tangential stress tending to increase the length of the rod. It is found that $E=100\Sigma\rho/\lambda$ where Σ is the specific surface in cm^2/g and ρ the density.

As Meehan, the discoverer of this effect, pointed out (1927), for an isotropic substance the expansion due to adsorption is also isotropic. It would seem that a better model of the processes taking place would be obtained by relating the expansion constants to the bulk modulus rather than the Young's modulus, as in the measurement of the former the solid expands or contracts equally in all directions for an isotropic solid while in the measurement of the latter, for the same solid, an expansion in one direction is accompanied by contractions in the other two.

For an aggregate of lightly sintered spheres, the properties of the aggregate can be considered an additive function of the spheres making up the whole. This view is confirmed by the work of Shuttleworth and Mackenzie (1949) who show that the most probable mechanism of sintering is that with increase of temperature and decrease of rigidity of the solid, the surface tension forces cause the solid to flow. Thus the 'neck' holding sintered spheres together will have the elastic properties of the material of the sphere.

From this model, for a small change in dimensions and treating the surface tension γ of the sphere as exerting a pressure $2\gamma/r$ where r is the radius of the sphere, we find that the bulk modulus, $K=200\Sigma\rho/9\theta$.

It will be seen that both in the case of the Young's modulus and the bulk modulus calculation, changes in free surface energy have been equated to changes in surface tension.

As Shuttleworth (1950) points out, because the surface tension and free surface energy of a one component liquid are numerically equal, the two terms have tended to become confused, and are often regarded as identical. That this is incorrect in the case of solids was originally pointed out by Gibbs (1928) in 1876. In the special case of the reduction of the free surface energy by reversible physical adsorption, that is where the molecules have no fixed points of attachment, it has been shown by Bangham (1937) that the free surface energy lowering and surface tension lowering are equal, and can be identified as a surface pressure.

Thermodynamic equations. A thermodynamic relationship between the lowering of the free surface energy of a rigid porous solid can be derived as follows.

Consider the equations :

$$x = -\theta \, dF', \qquad \ldots\ldots (1)$$

$$K = 200\Sigma\rho/9\theta. \qquad \ldots\ldots (2)$$

Now $-\theta \, dF' = 100 \, dl/l = 100 \, dV/3V$ (isotropic solid), thus assuming that eqn. (1) is correct for the isothermal conditions under which it was derived, $-\theta = (100/3V)(\partial V/\partial F')_T$, where dF' is the decrease in free surface energy per unit area. The decrease in total free surface energy is given by $dF = dF'A = dF'\Sigma\rho V$, where A is the area of the solid. Hence

$$-\theta = \frac{100}{3}\Sigma\rho\left(\frac{\partial V}{\partial F}\right)_T; \qquad \left(\frac{\partial F}{\partial V}\right)_T = -\frac{3}{2}K.$$

By the use of general thermodynamical relations of the form $dF = (\partial F/\partial P)_V \, dP + (\partial F/\partial V)_P dV$ it is easily found that

$$\left(\frac{\partial F}{\partial P}\right)_T = \frac{3}{2}V, \qquad \left(\frac{\partial F}{\partial V}\right)_P = -\frac{3}{2}K - \frac{S}{V\alpha},$$

$$\left(\frac{dF}{\partial T}\right)_P = -\frac{3}{2}KV\alpha - S, \qquad \left(\frac{\partial F}{\partial P}\right)_V = -\frac{S}{K\alpha},$$

where the cubical coefficient of thermal expansion $\alpha = V^{-1}(\partial V/\partial T)_P$, and the bulk modulus $K = -V(\partial P/\partial V)_T$; S is the entropy and P the pressure.

It is proposed to undertake experimental work to verify these equations.

Thanks are due to Dr. J. H. Schulman, and to Dr. A. R. Miller of the Cavendish Laboratory, for helpful discussions, and to the Consolidated Zinc Corporation for a maintenance grant.

Department of Colloid Science,
The University, Cambridge.
D. J. C. Yates.

19th November 1951.

Bangham, D. H., 1934, *Proc. Roy. Soc.* A, **147**, 175; 1937, *Trans. Faraday Soc.*, **33**, 805.
Bangham, D. H., and Fakhoury, N., 1930, *Proc. Roy. Soc.* A, **130**, 81.
Bangham, D. H., Fakhoury, N., and Mohamed, A. F., 1934, *Proc. Roy. Soc.* A, **147**, 152.
Bangham, D. H., and Maggs, F. A. P., 1943, *Conference on the Ultra-fine Structure of Coals and Cokes*, 118 (London : British Coal Utilization Research Association Committee).
Bangham, D. H., and Razouk, R. I., 1938, *Proc. Roy. Soc.* A, **166**, 572.
Gibbs, J. W., 1928, *Collected Works*, **1**, 315 (London : Longmans, Green).
Meehan, F., 1927, *Proc. Roy. Soc.* A, **115**, 199.
Shuttleworth, R., 1950, *Proc. Phys. Soc.* A, **63**, 444.
Shuttleworth, R., and Mackenzie, J. K., 1949, *Proc. Phys. Soc.* B, **62**, 833.

REVIEWS OF BOOKS

The High Pressure Mercury Vapour Discharge, by W. Elenbaas. Pp. xii + 173. (Amsterdam: North-Holland Publishing Co., 1951.) fl. 14.50.

This is the second volume of the series on Selected Topics in Modern Physics which is edited by de Boer, Brinkman and Casimir. Here a treatise of the positive column in mercury vapour is presented which is valid only within a range of pressures and temperatures in which thermal excitation and ionization are operative. During the last fifteen years the author has contributed about thirty papers on this subject and a greater part of the book is based on them.

Starting with historical notes an introduction into the mechanism of the positive column is given. Itis shown that when the pressure rises above about 10 mm of mercury the positive column contracts, while the temperature at the axis (but not at the wall) rises rapidly to a constant value. For example, in lamps working at 1 atmosphere and containing 1 to 100 mg of mercury per cm length of column, a gas temperature of 5000 to 7000°K is obtained at the axis when the input is about 30 w/cm.

The radiation emitted by the positive column, and the potential gradient are discussed as well as the various measurements of gas temperature and pressure and how they compare with theory. Only a small difference exists between electron and gas temperature supporting the assumption of a thermal equilibrium. By balancing input and losses the differential equation of the temperature distribution is derived, but a solution is only possible by numerical integration. Other chapters contain the similarity relations, the aerodynamics of the discharge (it can be shown that laminar and turbulent flow are both possible) and the effect of an external magnetic field or a rotation of the tube. A short chapter deals with very bright lamps and a larger one with the properties of the spectrum emitted.

The difficulties of translation from Dutch into English have, on the whole, been overcome, except for a few unusual expressions which do not, however, make the book less readable. The monograph is a comprehensive account of the various problems associated with mercury lamps and should be of interest to physicists, engineers and designers of lamps alike.

A. VON ENGEL.

The Hardness of Metals, by D. Tabor. Pp. ix + 175. (Oxford: Clarendon Press, 1951.) 15*s*.

This attractive little book has been written round several recent papers by the author on the interpretation of hardness in terms of the elastic and plastic properties of the specimen. Techniques and instrumentation are touched on only indirectly.

The most thoroughly treated aspects of a hardness test are those that depend solely on the elasticity of the specimen and indenter. Hertz and others showed a long time ago that it is possible to calculate closely the area of contact between an indenter and a specimen when both are stressed below their elastic limits. Dr. Tabor summarizes the Hertz theory for a spherical indenter and discusses critically its range of validity, making the valuable point that a comparatively small load causes local plastic yielding in the specimen or, if this is exceptionally hard, in the indenter itself. Experiments by Dr. Tabor show that the Hertz theory also satisfactorily describes the elastic recovery when the load is removed.

However, hardness measurements are generally made at loads for which the specimen is plastically distorted throughout a considerable zone near the indented surface, and for this the mathematical theory is far less developed. Despite this handicap, Dr. Tabor succeeds in presenting a clear overall qualitative picture. On the one hand, appeal is made to most (though not all) of the available theoretical resources (such as the calculations by Prandtl and others for non-hardening solids indented by a wedge or flat die), and, on the other hand, to empirical results from his own tests on metals with various work-hardening capacities. This union permits a derivation of the Meyer law and the familiar relation between hardness number and ultimate tensile ' strength '. The available results from the mathematical theory of plasticity are applied with understanding, while the empirical approach is generally used with discretion, save perhaps that ingenuity is pressed too far when a rough equality is seen between the ' mean ' strain around an indentation and the actual strain at its edge.

There is an excellent chapter on the dynamic hardness test, the various phenomena and contributing factors being clearly distinguished. It is difficult, however, to see the relevance of the final chapter. This deals with the contact between asperities of microscopic size, and, while interesting in itself, has only a remote connection with hardness measurement. For a wider view of the engineering and metallurgical significance of hardness, it would have been better to discuss such practically important topics as the influence of specimen size, the strain distribution below an indenter, the hardness of single crystals and anisotropic metals such as cold-drawn wires. R. HILL.

Die elektromagnetische Schirmung in der Fernmelde- und Hochfrequenztechnik, by H. KADEN. Pp. viii + 274. 1st Edition. (Berlin: Springer-Verlag, 1950.) DM. 38.

Dr. Kaden's book represents a most laudable attempt to develop the subject of electromagnetic shielding (or screening) from a rule-of-thumb technique into an exact science. One may ask whether such a step is necessary as in most cases shielding requirements need only be estimated to an order of magnitude, and a generous safety factor will be available to look after details.

However, Dr. Kaden shows that there are a variety of problems where economy and other considerations impose severe limitations. In such cases exact solutions of the shielding problem are needed.

Exact analysis of the shielding problem leads to solutions of Maxwell's equations with difficult and peculiar boundary conditions. Kaden's book is, therefore, heavily mathematical in nature: Bessel functions are in frequent use, so is conformal transformation; even elliptic integrals, hypergeometric series, Fourier integrals and matrices occur.

The appeal of the book is thus severely limited to those who are interested in critical and accurate shielding and who, at the same time, possess considerable mathematical interest and ability. Those who belong to this category will find Kaden's work a valuable textbook and reference book, giving a thorough survey of the field. O. BUNEMAN.

The Earth's Magnetism, by S. CHAPMAN. Pp. xi + 127. 2nd Edition. (Methuen's Monographs on Physical Subjects.) (London: Methuen, 1951.) 6*s*.

So many students of Physics are taught what are meant by the magnetic elements, so many learn how they are measured, to some slight degree of accuracy at least, and learn to recite the precautions which must be taken to avoid the more serious errors in their measurement. But, unfortunately, few ever seem to concern themselves in any way with the fact that enormous quantities of experimental data have been and are being accumulated and that very interesting deductions can be made from these data.

Professor Chapman's little book represents a very worthy attempt to remedy this state of affairs, and practically every physicist should find some enjoyment in reading it. Some of the magnetic diagrams it contains are, of course, well known, but others are not, and Chapman's penetrating analysis of the several kinds of solar, lunar and magnetic storm disturbances, together with the outline of the new knowledge to which such analysis leads, is heartily commended to all interested in the physical phenomena of the world around them.

L. F. BATES.

Advances in Electronics, Vol. II, edited by L. MARTON. Pp. x + 378. (New York Academic Press, 1950.) $7.60.

This second volume more than fulfils the promises of the first. The Editor and his Board must be congratulated on the selection of the material and for the choice of the authors. The articles fall more or less into two classes. Some, like the articles on cathodoluminescence or on the dielectric breakdown, are suitable as first introductions for the nonspecialist to vast specialized fields of research. Others, like the article on field plotting and ray tracing, aim at encyclopaedic completeness. All of them mean an immense saving of labour for those who want to bring their general knowledge up to date, and for those who want to engage in specialized research. Now that the flow of the German *Handbuch* has ceased—probably for ever, as their editor would have to contemplate perhaps 100 volumes instead of the 40 volumes of Geiger–Scheel—we shall have to rely on this type of publication for putting on record, and keeping up to date the state of progress in physics. It is to be hoped that sooner or later an international editorial board will do for the whole of physics what Dr. Marton and his Board have done and are doing for electronics. *En passant* one must note with satisfaction that the *Advances* will be a powerful agency for giving back its proper and original meaning to the term ' Electronics ', as it appeared for the first time in the title of the *Jahrbuch der Radioaktivität und Elektronik*, which was in danger of being annexed by what should be called ' applications of electronic devices '.

In this volume only the first article, by Hilary Moss, on Cathode Ray Tube Progress and Manufacture, and perhaps Gunnar Hok's short but very clear introduction to the Microwave Magnetron, belong to electronic engineering, the others are chapters of electronic physics, pure and applied. P. Grivet has very successfully undertaken the difficult task of writing a comprehensive account on the whole theory of electron lenses in 50 pages. G. Liebmann gives, for the first time, a complete review of all field-plotting and ray-tracing methods, with 129 references, for which he deserves the thanks of all the workers to whom he has saved long hours of search in libraries, not to mention the hundreds of hours which they might waste by using inadequate numerical methods. The four articles by G. F. J. Garlick on Cathodoluminescence, by H. Fröhlich and J. H. Simpson on the Intrinsic Dielectric Breakdown of Solids, by G. T. Rado on Ferromagnetic Phenomena at Microwave Frequencies and by D. K. Coles on Microwave Spectroscopy are equally competent introductions to four new and important fields of electron physics.

There is nothing that could be criticized or ' regretted ' in this book, except that as it is printed in the U.S. only a limited quota will be available in this country. D. GABOR.

Advanced Dynamics, by E. HOWARD SMART. Vol. I, pp. xi+419; Vol. II. pp. xi+420. (London: Macmillan, 1951.) 40*s*. each volume.

The two volumes of the work under review embody the substance of lectures given by the late Mr. E. Howard Smart, sometime Head of the Department of Mathematics at Birkbeck College, and they are obviously the work of a man of wide and varied experience as a teacher and examiner. One of the most useful features of the work is the range and number of examples which are solved in detail to illustrate general principles and theorems; these examples form a substantial proportion of the text and they make the work very valuable to a student who is forced to grapple with the difficulties of dynamics without much help from a teacher or supervisor. The two volumes could, for example, be recommended without hesitation to a physicist who feels his lack of knowledge of the subject, and who is, at the same time, forced to remedy this state of affairs by his own unaided efforts.

The scope of the work may be judged from the headings of the chapters. Volume I: Introductory, Fundamental dynamical principles, Rectilinear motion of a particle, Accelerations parallel to rectangular axes, Radial and transversal accelerations (central forces), Free motion under the law of inverse square, Constrained motion in two dimensions, Motion in a resisting medium, Motion of a chain in two dimensions, Motion of a particle in three dimensions; Volume II: Moments and products of inertia, Plane kinematics, D'Alembert's principle and the equations of motion, Two-dimensional motion of a rigid body (finite forces), Two-dimensional motion of a rigid body (impulsive forces), Dimensions and dynamical similarity, Motion in three dimensions, Lagrange's equations, Motion under no forces, Motion of a top or gyrostat, Hamilton's equations: general theorems on impulses, etc., Theory of small oscillations.

The work is obviously written from the standpoint of a mathematician and mainly, one suspects, with an eye on the syllabus of certain specific examinations. For a physicist, one result of these restrictions is a weakness in the treatment of those parts of the subject where physics and applied mathematics meet, and by way of illustration one may quote the disappointing chapter in Volume II on Dimensions and dynamical similarity. A second result is the omission of certain topics which are important to physicists; for example, whilst there is an exhaustive treatment of the small oscillations of a conservative system about a configuration of equilibrium, there is no mention of oscillations of finite amplitude or of non-linear oscillations.

On opening these books one is immediately struck by the absence of Clarendon type, due to the fact that the subject is treated almost entirely by resolution into Cartesian components, vector methods being ignored. This is not the place to marshal the case for and against the vector treatment of dynamics ; it is sufficient to record that this work offers neither apology nor explanation for omitting the use of vector methods, and, as a physicist, the reviewer is not unsympathetic to this standpoint, if it were only because vector equations have to be translated into Cartesian language before thay can be used in experimental physics. R. M. D.

Fundamentals of Acoustics, by L. E. KINSLER and A. R. FREY. Pp. vii + 516. (New York: Wiley and Sons; London: Chapman and Hall, 1950.) 48*s*.

This book consists essentially of two parts. In the first the mathematical basis of the subject is developed with considerable reference to the analogues of acoustical problems in alternating current theory. The large number of numerical questions appended to each chapter are very useful for the student. The whole of this part covers all that he is likely to need if he is content to study acoustics as though it bore little relation to hydrodynamics and, among other things, is willing to accept the introduction of velocity potential into the wave equations without explanation.

In the second part a series of more or less distinct chapters deals with the practical applications to such fields as loudspeaker and microphone design, architectural and underwater acoustics, the last a subject which does not receive its due attention in many books on sound.

On the other hand, a number of important applications which would not be covered by a predominantly ' electro-mechanical ' approach, such as fluid vibrations, vortex sounds and shock waves are regrettably—in the mind of the reviewer—omitted altogether. Nor is there any reference to musical acoustics, except a brief and surprising excursion into the theory of the kettledrum.

The nomenclature does not in all respects conform to the accepted international standards.

In spite of these limitations the book is to be recommended. It treats the subject in an interesting way, the mathematics is clear and the production excellent. E. G. R

Dielectric Breakdown of Solids, by S. WHITEHEAD. (Monographs on the Physics and Chemistry of Materials.) Pp. xv + 271. (Oxford : Clarendon Press, 1951.) 25*s*.

About twenty years ago Dr. Whitehead published his first treatise on dielectric breakdown. Since that time so much progress has been made both experimentally, under the leadership of Von Hippel and of the author and his colleagues, and theoretically, mainly by Von Hippel and Fröhlich, that the author has now produced an entirely new book on the subject.

Dielectric breakdown is a phenomenon of great practical importance and it has great theoretical interest. There are at least three distinct types : intrinsic breakdown takes place almost instantaneously if the electric field reaches a level at which an electronic equilibrium is no longer possible; thermal breakdown is due to the heat developed in the dielectric as Joule heat or by dielectric losses; and discharges outside the dielectric or in small cavities inside can weaken it chemically or thermally to the point of breakdown. It is the burden of Dr. Whitehead's book to set out these types, to show and to illustrate how the dielectric strength in its different aspects is measured, to summarize the results obtained and to explain the theoretical background and the detailed theories and finally to assess the importance of the different aspects of breakdown and the future trends of practice and research. In addition a discussion is given of the variation with time of dielectric strength due to diffusion and slow chemical processes.

This task is even more formidable than it may appear at first sight. The author tries to reduce to a compass of about 250 pages the contents of about 200 original papers, the scope of which includes subtle experimenting and fundamental theoretical analyses of electronic processes in dielectrics; and as original papers are, these days, usually already condensed almost beyond the limit of comprehensibility, the book makes very heavy demands on the reader's acumen. Details concerning experimental arrangements are scanty and the reader needs a great deal of imagination to get an idea how measurements are actually made and how the results given in diagrams are obtained. Even the plates showing photographs of faulty dielectrics are barely explained. The mathematical theories are given an appreciable portion of the space available; but the story is so involved that only readers with a good knowledge of the original literature may be able to follow.

The book will be warmly welcomed by those specially interested in dielectric breakdown as a clearly laid out summary of the subject written from a very high level. It is further an important book of reference for scientists interested in electronic processes in solids. It will give the reader readily an idea of the state of the subject, to the extent to which a much shorter review article could. But it will yield its full contents only to those who are prepared for a great deal of additional study. W. E.

CONTENTS FOR SECTION A

PAGE
Editorial 1
Dr. H. G. Wolfhard and Dr. W. G. Parker. A Spectroscopic Investigation into the Structure of Diffusion Flames 2
Dr. A. G. Gaydon and Dr. H. G. Wolfhard. The Spectrum-Line Reversal Method of Measuring Flame Temperature 19
Mr. I. C. Cheeseman. The Structure of the Long Wave Absorption Edge of Insulating Crystals 25
Dr. D. W. Pashley. Oriented Deposits on Crystalline Substrates 33
Dr. O. Theimer. On the Relations between the Photo-Elastic Properties and the Raman Effect in Crystals 38
Mr. C. G. Kuper and Dr. D. H. Trevena. The Effect of Dissolved Gases on the Tensile Strength of Liquids 46
Dr. P. J. Price. Classical Theory of Compressibility 54
Mr. K. Phillips. The Experimental Determination of the Spectrum of a Betatron 57
Mr. E. G. Muirhead, Mr. B. M. Spicer and Mr. H. Lichtblau. The Angular Distribution of Synchrotron Target Radiation 59
Dr. F. A. El-Bedewi. Angular Distribution of Elastically Scattered Deuterons and Disintegration Protons from the Bombardment of Beryllium by 7·7 MeV Deuterons 64
Letters to the Editor:
  Mr. S. K. Ghosh, Mr. G. M. D. B. Jones and Dr. J. G. Wilson. Ionization in Oxygen by μ-Mesons 68
  Dr. Kurt E. Shuler. On Vibrational Transition Probabilities in Electronic Transitions 70
  Dr. R. F. Barrow, Dr. A. R. Downie and Mr. R. K. Laird. The Spectrum of NS 70
  Dr. P. G. Klemens. On θ Values in the Resistance of Metals 71
  Mr. F. R. Barclay, Mr. W. Galbraith and Mr. W. J. Whitehouse. Neutrons from the Spontaneous Fission of Thorium 73
  Dr. U. W. Arndt and Dr. D. P. Riley. Comparison of Geiger and Proportional Counters for Intensity Measurements in X-ray Diffraction . 74
Reviews of Books 75
Contents for Section B 78
Abstracts for Section B 78

ABSTRACTS FOR SECTION A

A Spectroscopic Investigation into the Structure of Diffusion Flames, by H. G. Wolfhard and W. G. Parker.

ABSTRACT. Ammonia–oxygen, ethylene–oxygen and other diffusion flames were examined spectroscopically using the flat flame technique described in a previous paper. Each flame is shown to consist of a main reaction zone where the temperature is a maximum. The emission from this zone is thermal and the component gases are in chemical equilibrium. On either side of the main reaction zone there is a region with a steep temperature gradient which constitutes a pre-heating zone. Fuels such as hydrocarbons or ammonia and oxidizers such as nitric oxide undergo chemical change in these pre-heating zones. On the fuel side the change is principally a thermal decomposition because the main reaction zone presents a barrier to oxygen penetration. Thus carbon formation in hydrocarbon diffusion flames is essentially a pyrolytic process. The application and value of absorption spectroscopy are discussed and quantitative measurements of the concentrations of molecular oxygen and OH radicals are recorded which could not have been otherwise obtained. These results and a number of qualitative observations clearly show that diffusion flames with oxygen at atmospheric pressure have the structure predicted for a flame in which diffusion is the rate determining process. A number of differences are described between the characteristics of diffusion and pre-mixed gas or Bunsen flames.

.B
55
52

The Spectrum-Line Reversal Method of Measuring Flame Temperature, by A. G. Gaydon and H. G. Wolfhard.

ABSTRACT. Processes of electronic excitation in flames are briefly discussed, and it is shown that if there is lack of equilibrium the reversal temperature may be closer to the effective vibrational temperature of the surrounding molecules than to the mean translational temperature. The lack of radiative equilibrium in all flames will cause measured temperatures to be too low; for a flame with air at 2000° K using Na the error will be between 3·3° and 1·6° at 1 atm and more at lower pressure. For hot flames, above 2700° K, the OH band may be used for reversal measurements; it appears to give satisfactory results and has some advantages over the use of sodium.

The Structure of the Long Wave Absorption Edge of Insulating Crystals, by I. C. Cheeseman.

ABSTRACT. A general process, by which light can be absorbed in insulators at frequencies less than the frequency corresponding to the energy gap, is considered. Using an Einstein model with a constant energy gap, calculation of such a process is made by means of the method of intermediate states. The results are tested for the case of cadmium sulphide, and agreement with experimental results is found to be good when allowance is made for mathematical approximations made in the calculations.

Oriented Deposits on Crystalline Substrates, by D. W. Pashley.

ABSTRACT. Layers of silver and thallium halides have been evaporated, *in vacuo*, on to cleavage surfaces of rocksalt, potassium bromide, magnesium oxide and mica, at various substrate temperatures. These layers have been studied by means of electron diffraction. Examples of both high and low inter-atomic misfits between the substrate and the oriented overgrowth are found. In the case of silver chloride on potassium bromide, a chemical reaction occurred between the substrate and the deposit. Thallium chloride crystallized in an abnormal rocksalt type structure on potassium bromide, but had its normal caesium chloride type structure on the other substrates used.

On the Relations between the Photo-Elastic Properties and the Raman Effect in Crystals, by O. Theimer.

ABSTRACT. General relations are derived between Pockel's elasto-optical constants and the polarizability derivatives $\alpha_{\varrho\sigma,\mu}\begin{pmatrix} l \\ kk' \end{pmatrix}$ used in Born's theory of the Raman effect in crystals. Numerical data are given for the case of diamond. Using these relations a formula is derived for the intensity of the Brillouin components of crystals in terms of the elasto-optical constants. This formula avoids the simplifications implied in an earlier expression due to Leontowitsch and Mandelstamm.

The Effect of Dissolved Gases on the Tensile Strength of Liquids, by C. G. Kuper and D. H. Trevena.

ABSTRACT. A theoretical investigation is made of the amount by which a dissolved gas should reduce the tensile strength of a liquid. The tensile strength is assumed proportional to the surface energy of a vapour nucleus, which is further assumed to have the form of a product of a function of its radius and a function of the dissolved gas concentration. The surface tension of a one-component system is expressed in terms of the van der Waals constants (developing Fowler's theory) and the treatment is extended to a two-component system on the basis of Wall and Stent's theory of van der Waals binary mixtures. The conclusion is reached that the reduction in the tensile strength of water caused by saturating it with air at a pressure of one atmosphere is less than $\frac{1}{2}\%$.

Classical Theory of Compressibility, by P. J. Price.

ABSTRACT. By extending Green's treatment of the classical virial theorem, a formula for the bulk modulus of an assembly of atoms, when classical physics applies, is derived. This formula involves the binary and ternary distribution functions.

The Experimental Determination of the Spectrum of a Betatron, by K. Phillips.

ABSTRACT. By measuring the energy of photo-protons from deuterium the x-ray spectrum of a betatron, of maximum energy 20 Mev, has been deduced. A small difference between the experimental determination and the theoretical curve in the 10 Mev region is found.

The Angular Distribution of Synchrotron Target Radiation, by E. G. Muirhead, B. M. Spicer and H. Lichtblau.

ABSTRACT. Some measurements on the angular distribution of thin target radiation produced in a synchrotron are reported using ionization chambers to measure the x-ray intensity. Quantitative agreement has been obtained with the bremsstrahlung–multiple scattering theories of Schiff and Lawson for the case of a platinum target in the range of electron energies of 10–14 Mev.

Angular Distribution of Elastically Scattered Deuterons and Disintegration Protons from the Bombardment of Beryllium by 7·7 MeV Deuterons, by F. A. El-Bedewi.

ABSTRACT. The deuteron beam from the Liverpool 37 in. cyclotron was used to bombard a thin beryllium foil in a vacuum chamber. The photographic plate method was employed in detecting the charged particles emitted from the reaction. The angular distribution of the elastically scattered deuterons shows a secondary maximum at 65°. Angular distributions of the two longest range proton groups are compared with the recent theories of the angular distributions of the (d, p) and (d, n) reactions. The results indicate that both the ground state and first excited state of the residual nucleus ^{10}Be have even parity and spin either 0, 1, 2 or 3.

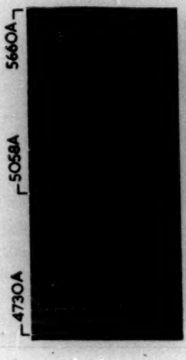

Fig. 3 (×18)

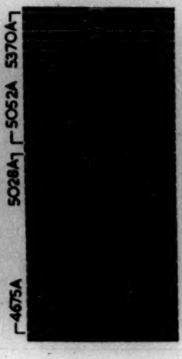

Fig. 4 (×75)

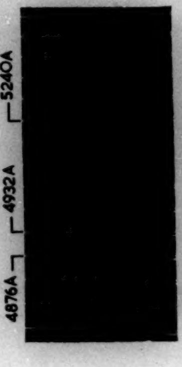

Fig. 5 (×18)

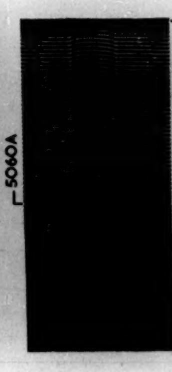

Fig. 6 (*a*) (×90)

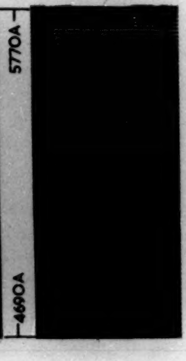

Fig. 6 (*b*) (×90)

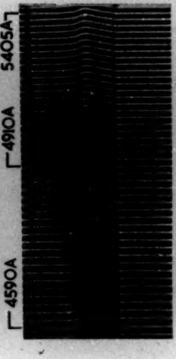

Fig. 7 (×300)

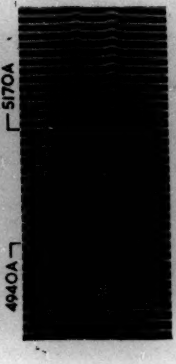

Fig. 10 (*a*) (×210)

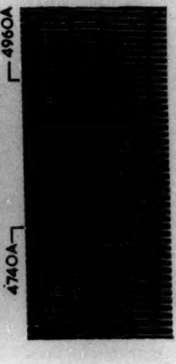

Fig. 10 (*b*) (×210)